

Title: Implications of the cosmic ray anomalies on DM particles

Date: Jun 18, 2009 02:00 PM

URL: <http://pirsa.org/09060062>

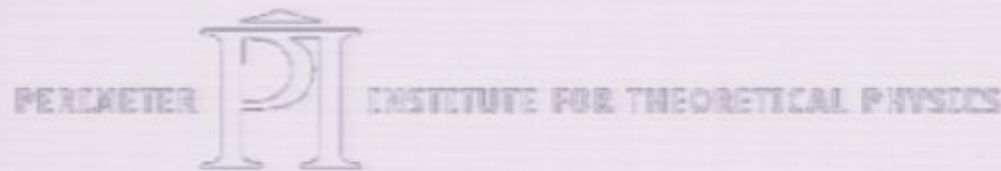
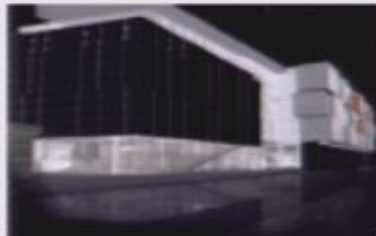
Abstract: The particle physics community is bubbling with excitement since the recent discovery in the cosmic radiation of a positron and electron excess at high energy. This may be the first indirect hint that dark matter particles wander in the halo of the Milky Way. However, these species do not seem to have the expected properties. I will review the various pieces of that puzzle and present a status report of the current developments in that fast moving field.

# Implications of the cosmic ray anomaly on DM particles

Pierre Salati – Université de Savoie & LAPTH

## Outline

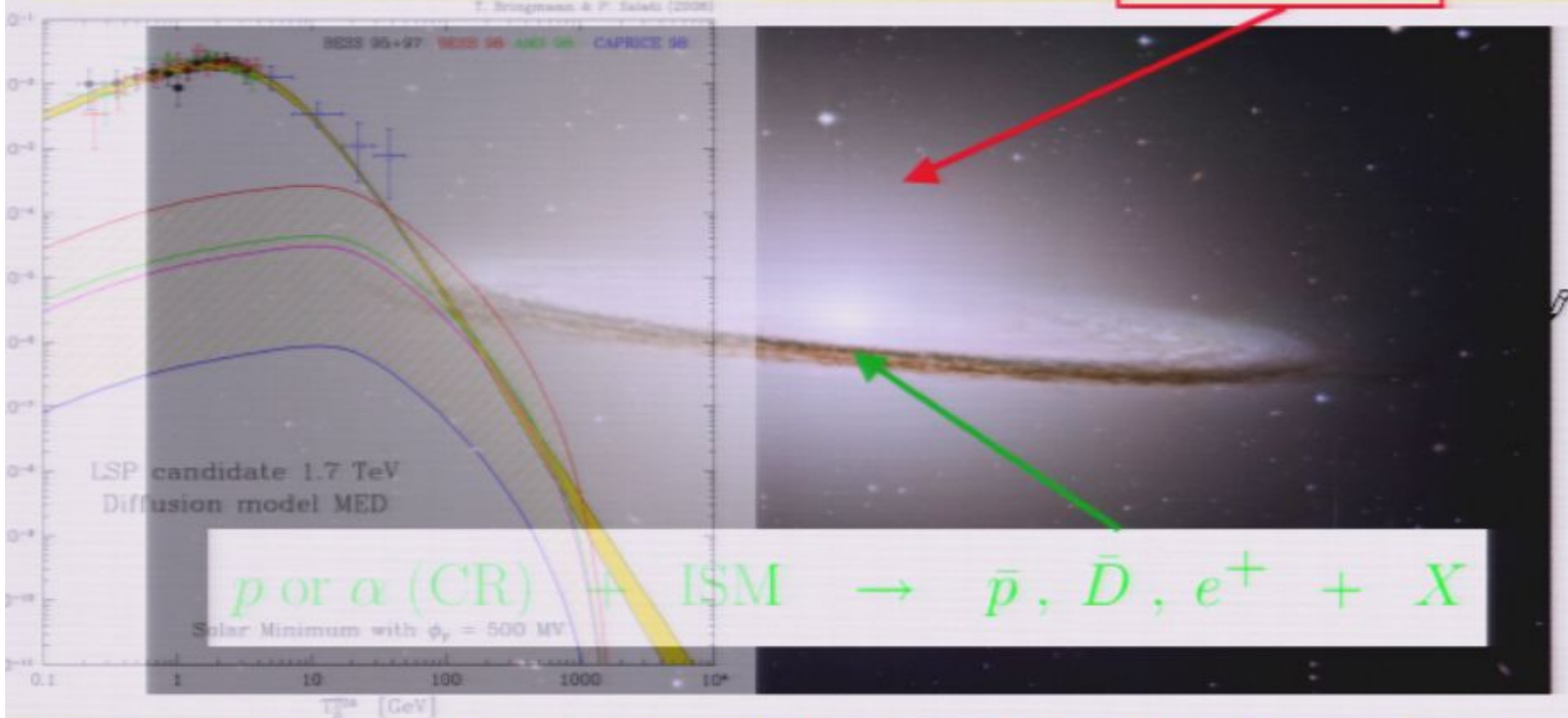
- 1) The cosmic ray anomaly 
- 2) Boosting the annihilation cross section
- 3) Astrophysical effects on DM annihilation
- 4) Perspectives



# Indirect signatures of DM species

Weakly Interacting Massive particles – WIMPs – may be the major component of the haloes of galaxies. Their mutual annihilations would produce an indirect signature of high-energy cosmic rays :

$$\chi + \chi \rightarrow q\bar{q}, W^+W^-, \dots \rightarrow \gamma, [\bar{p}, \bar{D}, e^+] \& \nu's$$



## 1) The cosmic ray anomaly

Space diffusion dominates in the master equation

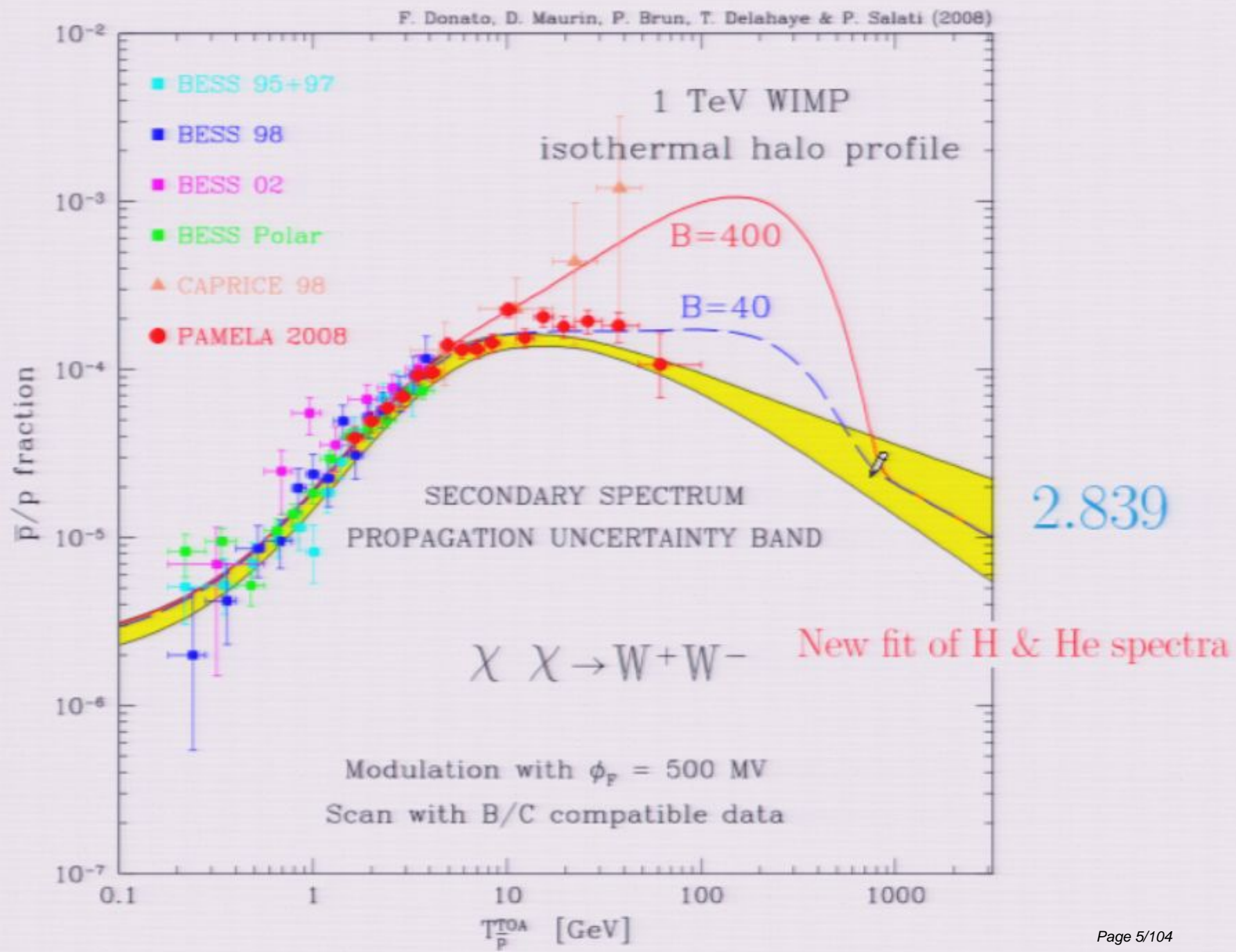
$$V_C \partial_z \Psi - K \Delta \Psi + \partial_E \{ b^{\text{loss}}(E) \Psi - K_{EE}(E) \partial_E \Psi \} = Q$$

Poisson equation  $K \Delta \Psi + Q = 0$



Long range with  $G_{\bar{P}}^{\text{3D}}(r) = \frac{Q}{4\pi Kr}$

- Evaporation at the vertical boundaries  $\pm L$
- Leakage at the radial boundaries  $R = 20 \text{ kpc}$
- Evaporation from convective wind  $\mathcal{V}_C$
- Annihilations inside the MW gaseous disk
- Energy losses and mild diffusive reacceleration



# PAMELA & the positron excess

Mostly sensitive to the local region

Energy losses dominate

IC on stellar light and CMB – synchrotron

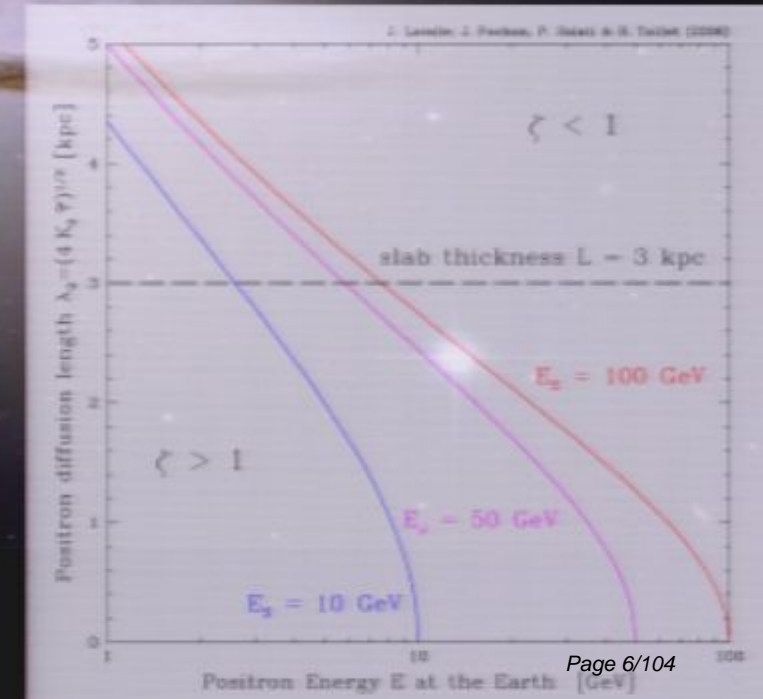
$$E_{\text{obs}} \leq E_S$$



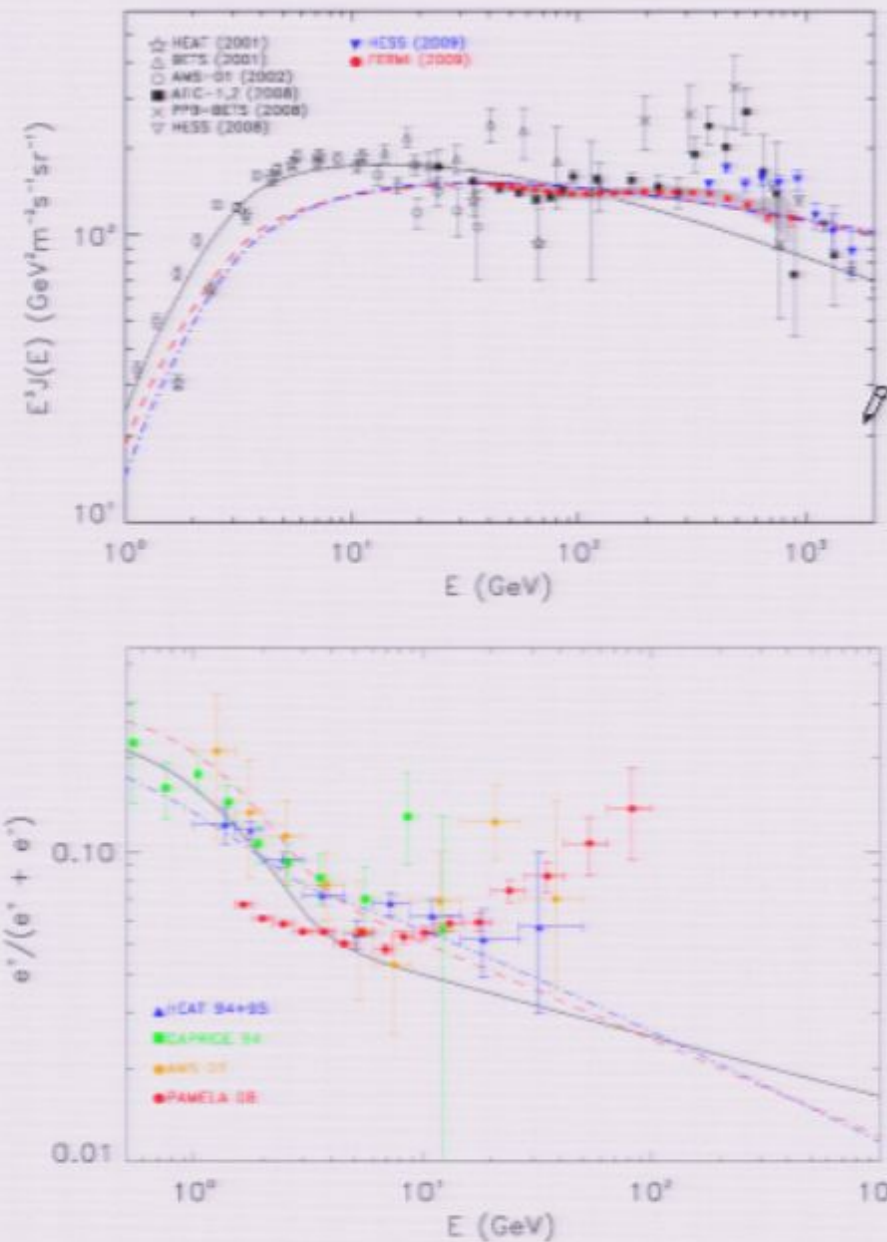
$$G_{e^+}(\vec{x}_\odot, E \leftarrow \vec{x}, E_S) = \frac{\tau_E}{E_0 \epsilon^2} \tilde{G}(\vec{x}_\odot, \tilde{t} \leftarrow \vec{x}, \tilde{t}_S)$$

$$\tilde{G}(\vec{x}_\odot, \tilde{t} \leftarrow \vec{x}, \tilde{t}_S) = \frac{\theta(r_S - r)}{V_S}$$

$$V_S = (\sqrt{2\pi} \lambda_D)^3$$



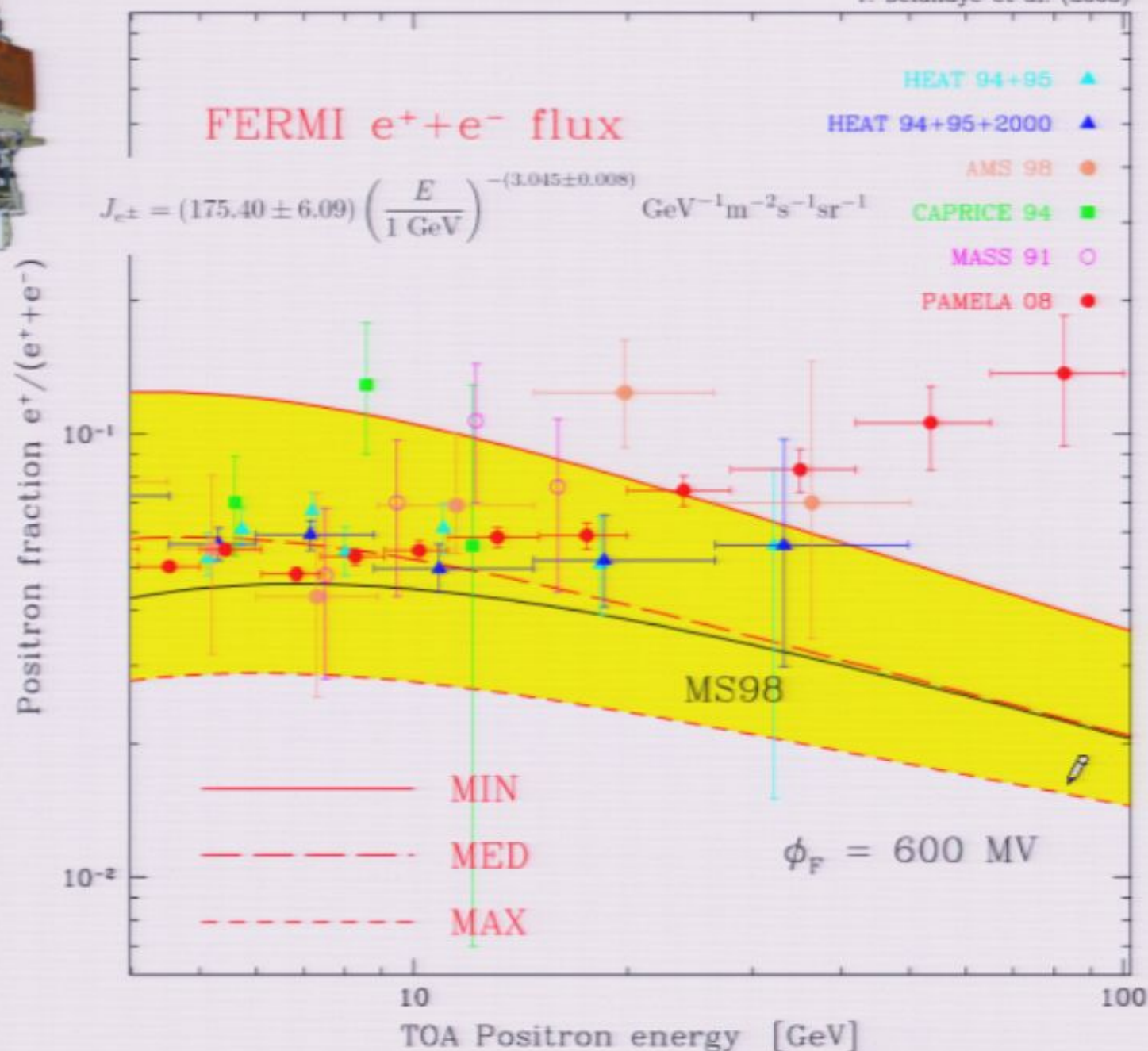
Model #	$D_0$ ( $\text{cm}^2\text{s}^{-1}$ )	$\delta$	$z_h$ (kpc)	$\gamma_0$	$N_{e^-}$ ( $\text{m}^{-2}\text{s}^{-1}\text{sr}^{-1}\text{GeV}^{-1}$ )	$\gamma_0^p$
0	$3.6 \times 10^{28}$	0.33	4	2.54	$1.3 \times 10^{-4}$	2.42
1	$3.6 \times 10^{28}$	0.33	4	2.42	$1.3 \times 10^{-4}$	2.42
2	$1.3 \times 10^{28}$	0.60	4	2.33	$1.3 \times 10^{-4}$	2.1





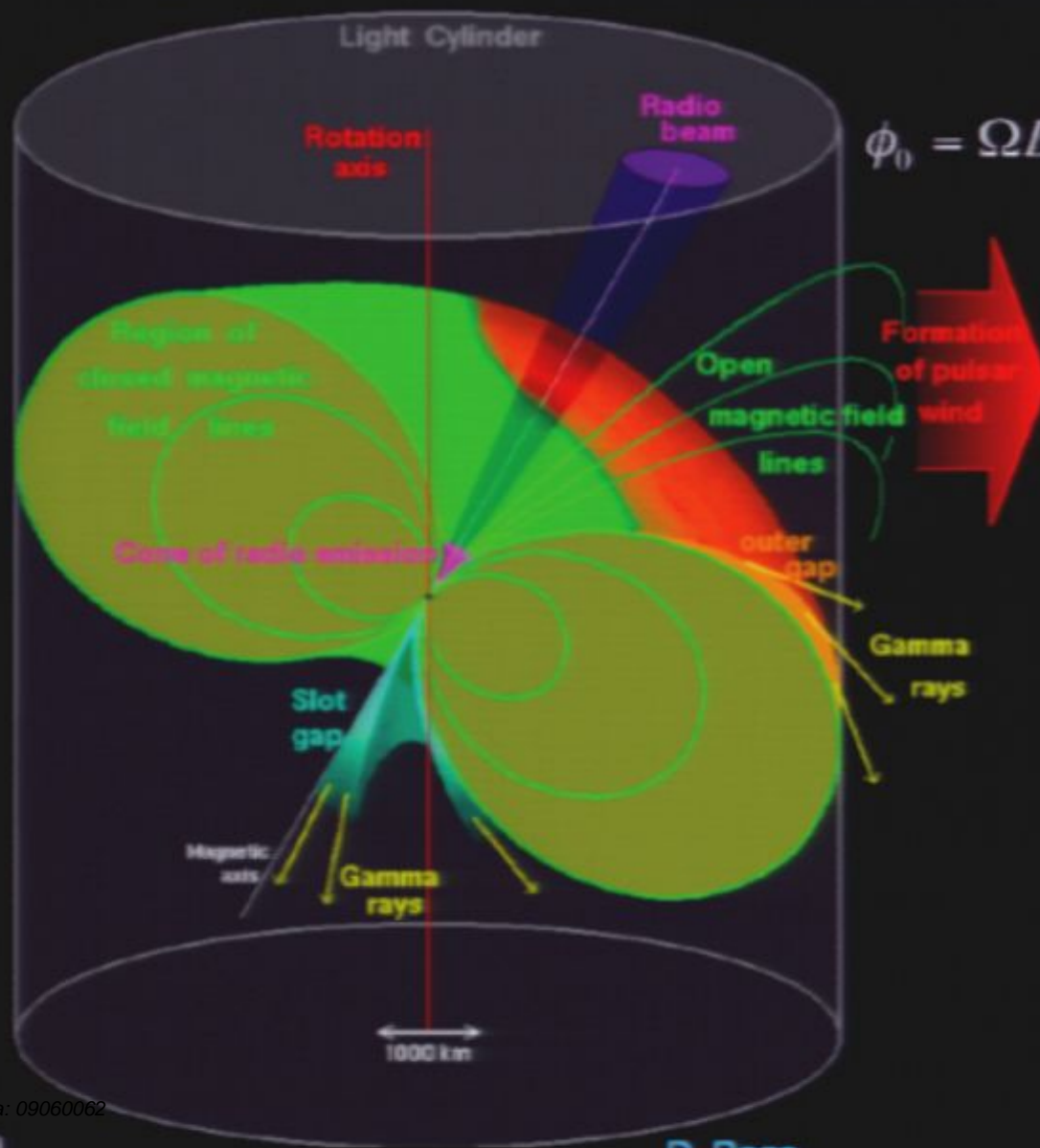
Delahaye T. et al. – arXiv:0809.5268

T. Delahaye et al. (2008)

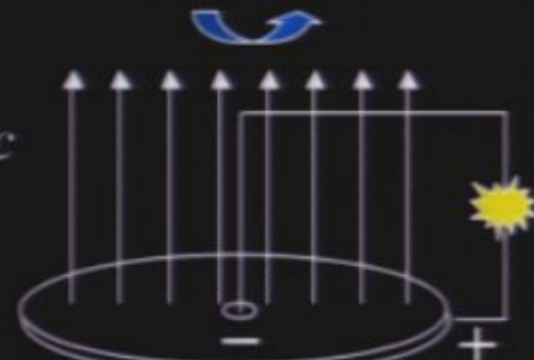


## 4) Astrophysical explanations of the PAMELA excess

Courtesy of Anatoly Spitkovsky – Princeton

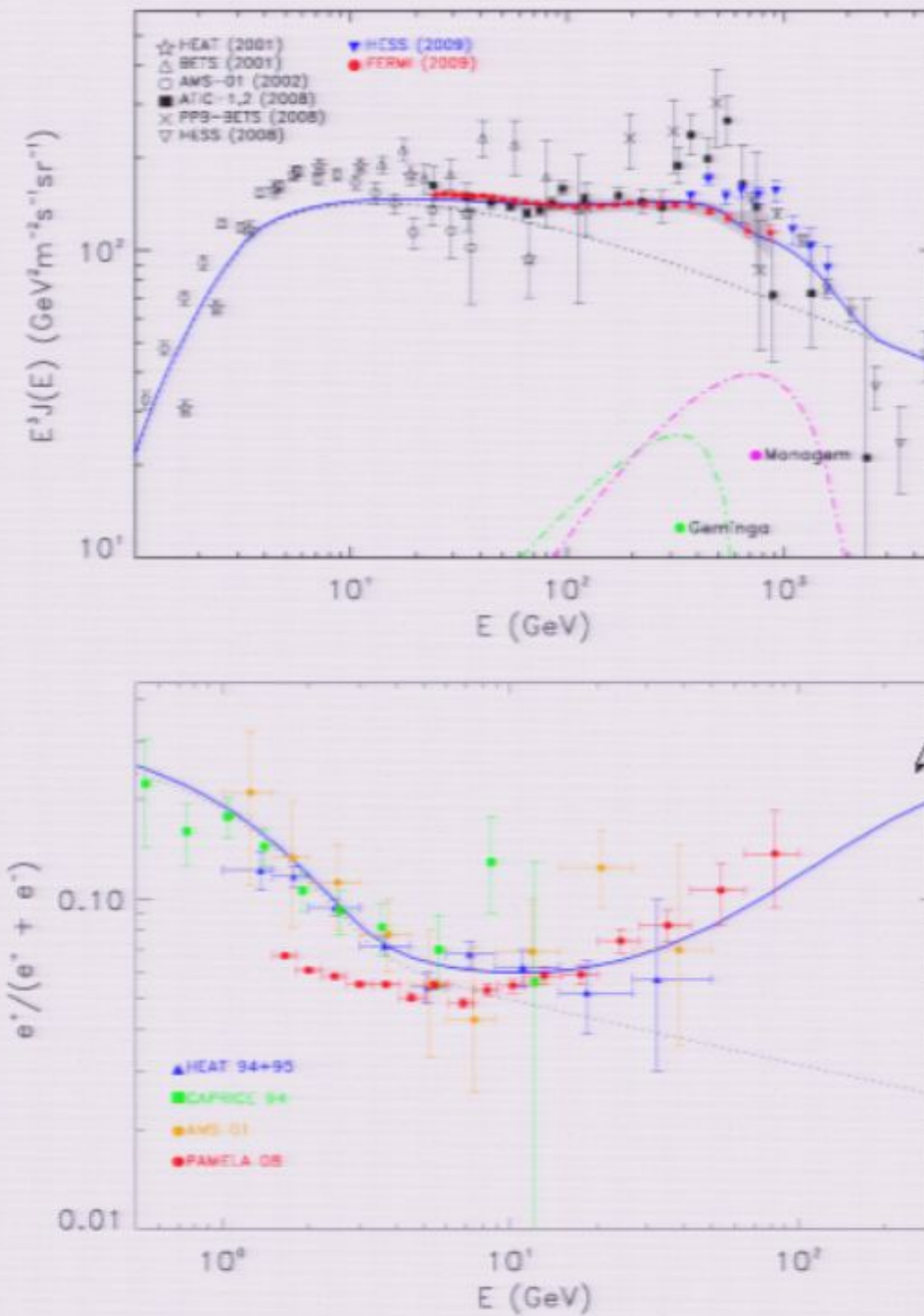


$$\phi_0 = \Omega B a^2 / c$$



**Faraday disk: unipolar induction**

- but pulsars are not in vacuum!
- Equator-pole potential difference ( $10^{15} V$  for Crab)
- Charge extraction from the surface ( $E$  field  $\gg$  gravity)
- Currents, strong magnetization
- Corotating zone; Light cylinder
- Throwing away toroidal field – energy loss (Poynting flux)
- Plasma currents modify field  
How can we model this?



## PAMELA positron excess

May be the first indirect hint that DM species annihilate in the MW.

$$\Gamma_{\text{ann}} \equiv \langle \sigma v \rangle \times \frac{\rho_\chi^2}{m_\chi^2} \text{ needs to be enhanced}$$

## 2) Boosting the annihilation cross section

- Internal bremsstrahlung from charged external legs or virtual internal particles.
- Sommerfeld effect – a non-perturbative enhancement of  $\sigma_{\text{ann}}$  at low velocity.
- Slightly or strongly modified thermal decoupling (quintessence).

Beware of the other messengers !

- Antiprotons are not produced – leptophilic WIMP ?
- Even though, strong constraints from radio and IC ?

$$\chi \chi \rightarrow \phi \phi \quad \& \quad \phi \rightarrow l^+ l^-$$

Accelerator constraints soon ?

# DM particles

The annihilation rate needs to be considerably boosted

L. Roszkowski, R. Ruiz de Austri, J. Silk & R. Trotta, arXiv:0707.0622

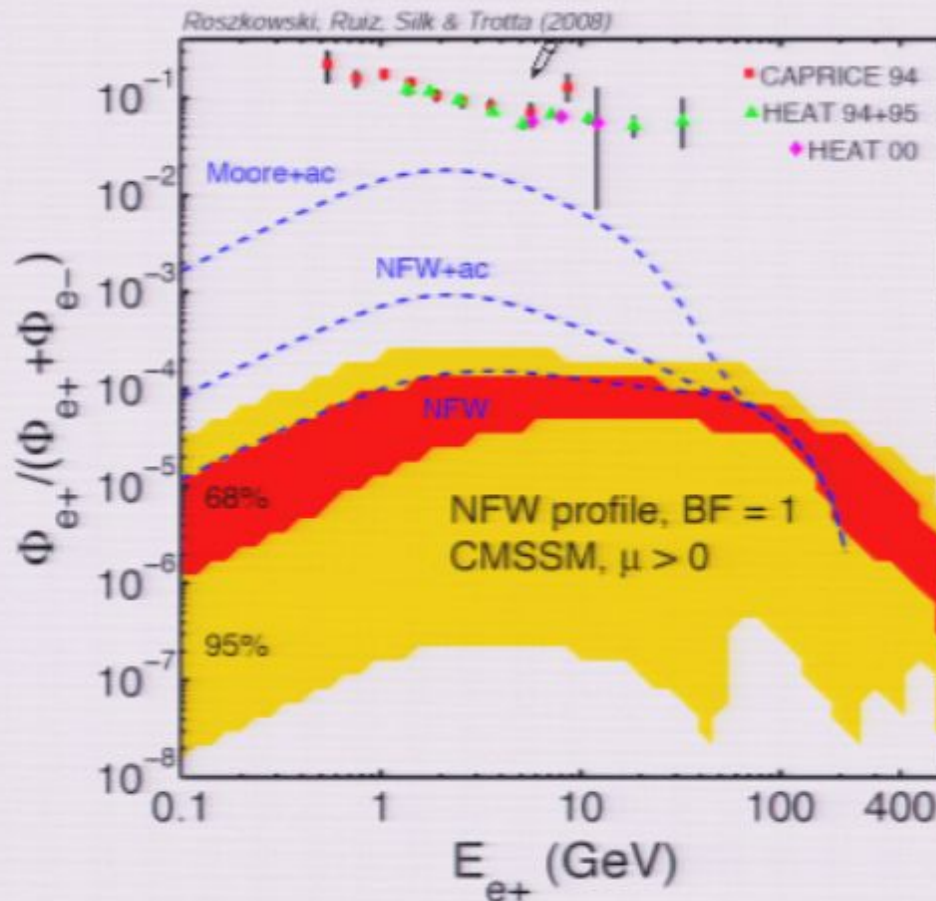


Figure 3: Predicted positron flux fraction in the CMSSM. The 68% (dark/red) and 95% (light/yellow) regions are for an NFW profile with a boost factor  $BF=1$  and a specific choice of propagation model. We also show for comparison some of the current data. To illustrate the dependency of the spectral shape at low energies on the halo model, we plot the spectrum for the same choice of CMSSM parameters (with  $m_\chi = 229$  GeV) for three different halo models as indicated. In absence of a large boost factor, the signal appears too small to be detected by PAMELA.

## PAMELA positron excess

May be the first indirect hint that DM species annihilate in the MW.

$$\Gamma_{\text{ann}} \equiv \langle \sigma v \rangle \times \frac{\rho_\chi^2}{m_\chi^2} \text{ needs to be enhanced}$$



### 2) Boosting the annihilation cross section

- Internal bremsstrahlung from charged external legs or virtual internal particles.
- Sommerfeld effect – a non-perturbative enhancement of  $\sigma_{\text{ann}}$  at low velocity.
- Slightly or strongly modified thermal decoupling (quintessence).

Beware of the other messengers !

- Antiprotons are not produced – leptophilic WIMP ?
- Even though, strong constraints from radio and IC ?

$$\chi \chi \rightarrow \phi \phi \quad \& \quad \phi \rightarrow l^+ l^-$$

Accelerator constraints soon ?

# DM particles

The annihilation rate needs to be considerably boosted

L. Roszkowski, R. Ruiz de Austri, J. Silk & R. Trotta, arXiv:0707.0622

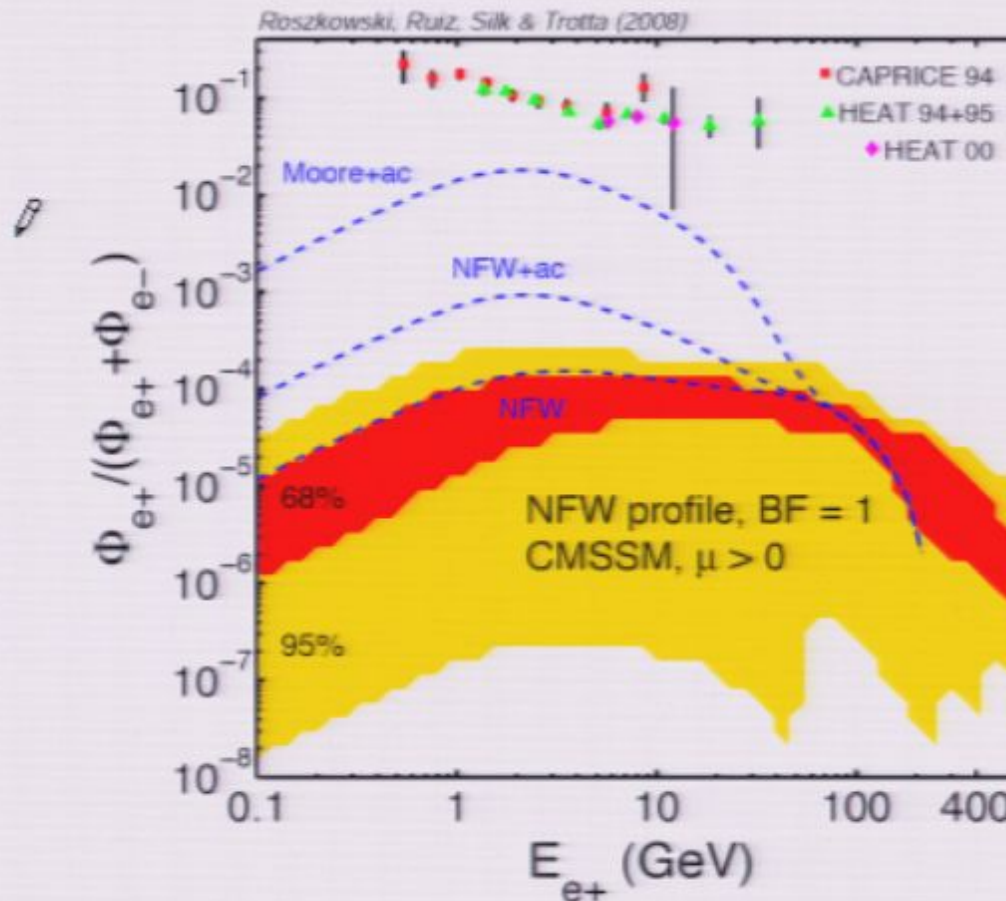


Figure 3: Predicted positron flux fraction in the CMSSM. The 68% (dark/red) and 95% (light/yellow) regions are for an NFW profile with a boost factor  $BF=1$  and a specific choice of propagation model. We also show for comparison some of the current data. To illustrate the dependency of the spectral shape at low energies on the halo model, we plot the spectrum for the same choice of CMSSM parameters (with  $m_\chi = 229$  GeV) for three different halo models as indicated. In absence of a large boost factor, the signal appears too small to be detected by PAMELA.

## PAMELA positron excess

May be the first indirect hint that DM species annihilate in the MW.

$$\Gamma_{\text{ann}} \equiv \langle \sigma v \rangle \times \frac{\rho_\chi^2}{m_\chi^2} \text{ needs to be enhanced}$$

### 2) Boosting the annihilation cross section

- Internal bremsstrahlung from charged external legs or virtual internal particles.
- Sommerfeld effect – a non-perturbative enhancement of  $\sigma_{\text{ann}}$  at low velocity.
- Slightly or strongly modified thermal decoupling (quintessence).

Beware of the other messengers !

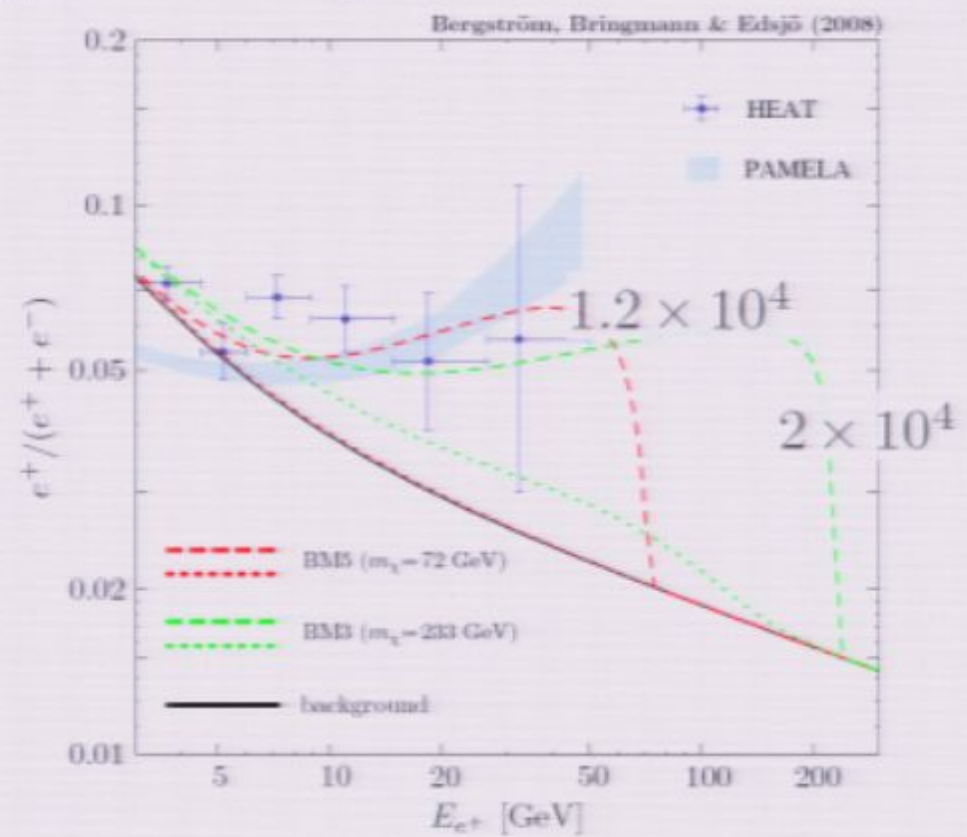
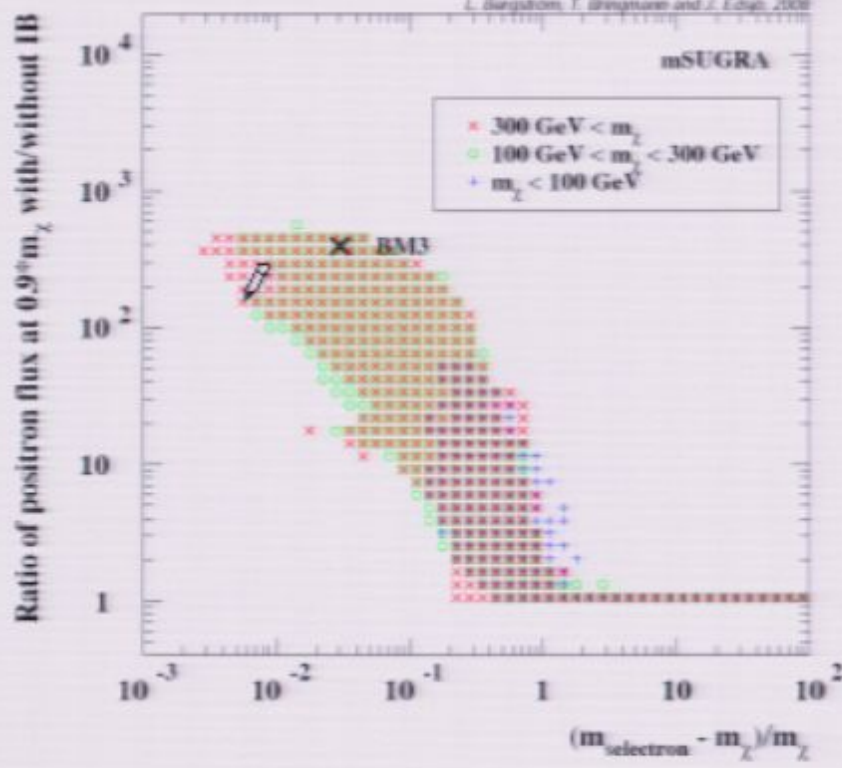
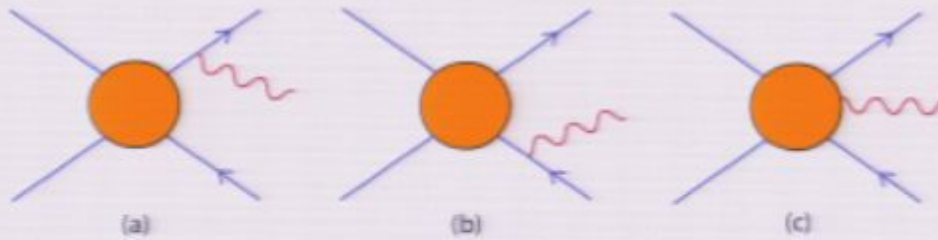
- Antiprotons are not produced – leptophilic WIMP ?
- Even though, strong constraints from radio and IC ?

$$\chi \chi \rightarrow \phi \phi \quad \& \quad \phi \rightarrow l^+ l^-$$

Accelerator constraints soon ?

# New Positron Spectral Features from Supersymmetric Dark Matter - a Way to Explain the PAMELA Data?

Lars Bergström,\* Torsten Bringmann,† and Joakim Edsjö‡



# Sommerfeld effect – a non-perturbative enhancement of $\sigma_{\text{ann}}$ at low velocity

J. Hisano, S. Matsumoto and M. M. Nojiri

M. Pospelov & A. Ritz, Phys. Lett. **B671** (2009) 391

N. Arkani-Hamed, D. P. Finkbeiner, T. R. Slatyer & N. Weiner, Phys. Rev. **D79** (2009) 015014

$$\sigma = \sigma_0 \left( 1 + \frac{v_{\text{esc}}^2}{v^2} \right)$$

$$\lambda \geq (\alpha m_\chi)^{-1}$$

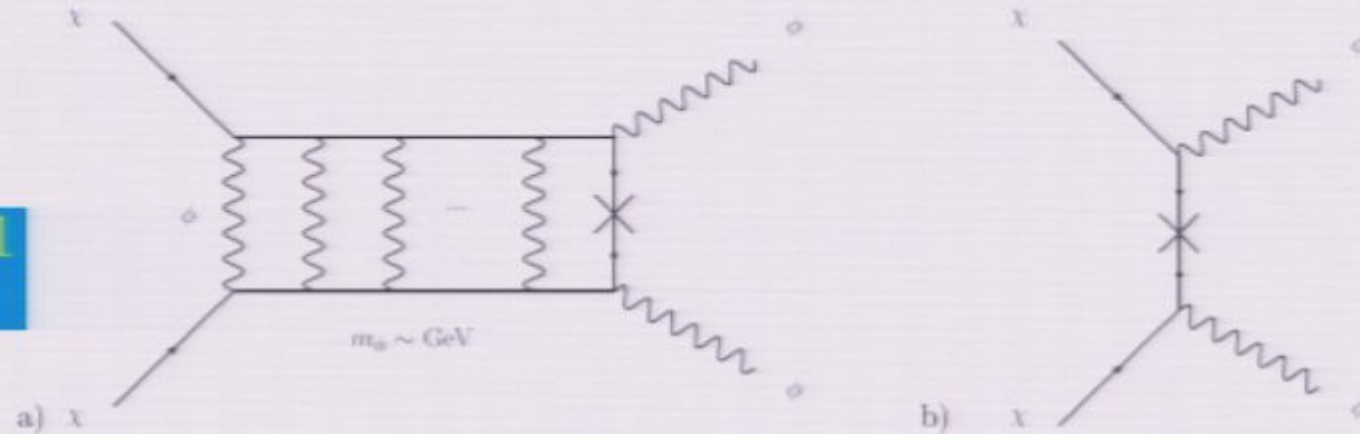
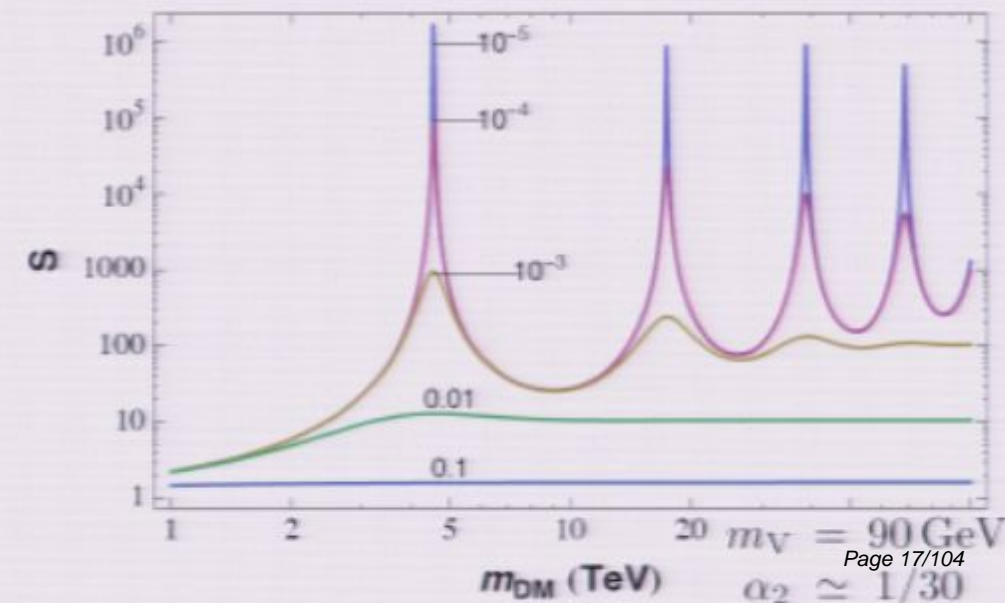
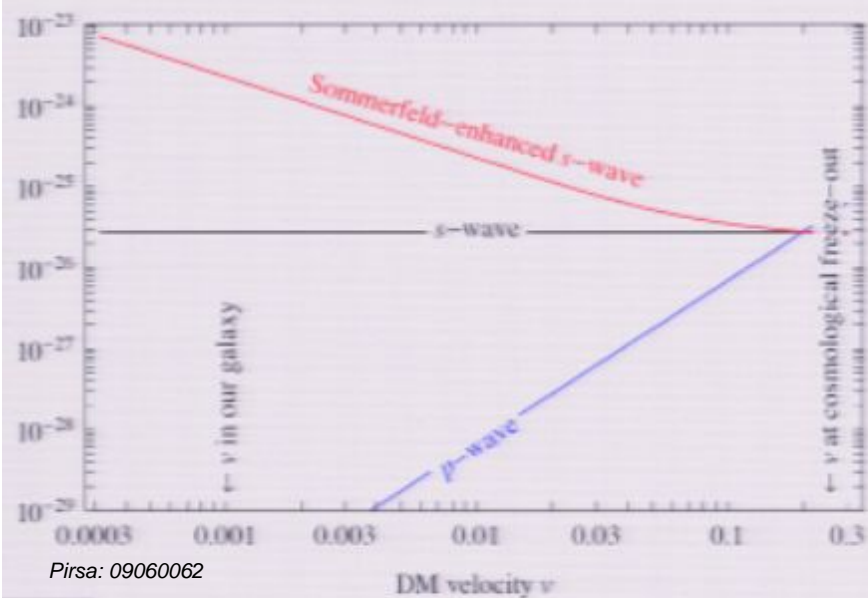


FIG. 3: The annihilation diagrams  $\chi\chi \rightarrow \phi\phi$  both with (a) and without (b) the Sommerfeld enhancements.



# DM particles

The annihilation rate needs to be considerably boosted

L. Roszkowski, R. Ruiz de Austri, J. Silk & R. Trotta, arXiv:0707.0622

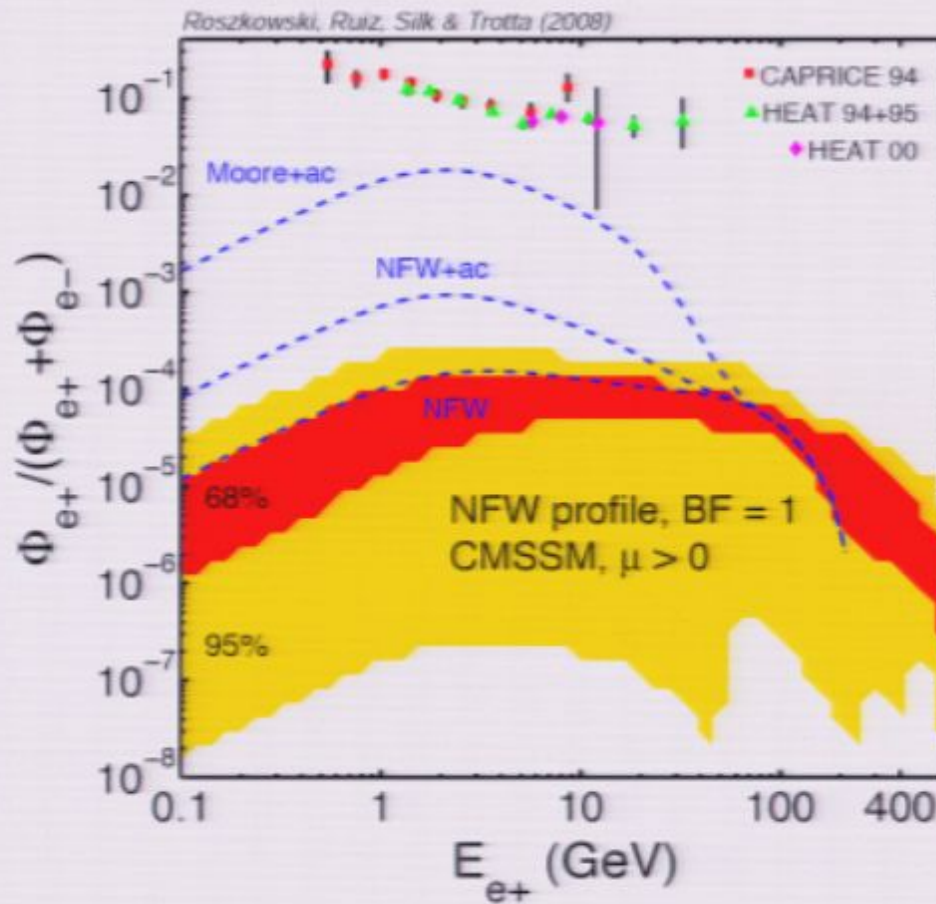


Figure 3: Predicted positron flux fraction in the CMSSM. The 68% (dark/red) and 95% (light/yellow) regions are for an NFW profile with a boost factor  $BF=1$  and a specific choice of propagation model. We also show for comparison some of the current data. To illustrate the dependency of the spectral shape at low energies on the halo model, we plot the spectrum for the same choice of CMSSM parameters (with  $m_\chi = 229$  GeV) for three different halo models as indicated. In absence of a large boost factor, the signal appears too small to be detected by PAMELA.

## PAMELA positron excess

May be the first indirect hint that DM species annihilate in the MW.

$$\Gamma_{\text{ann}} \equiv \langle \sigma v \rangle \times \frac{\rho_\chi^2}{m_\chi^2} \text{ needs to be enhanced}$$

### 2) Boosting the annihilation cross section

- Internal bremsstrahlung from charged external legs or virtual internal particles.
- Sommerfeld effect – a non-perturbative enhancement of  $\sigma_{\text{ann}}$  at low velocity.
- Slightly or strongly modified thermal decoupling (quintessence).



Beware of the other messengers !

- Antiprotons are not produced – leptophilic WIMP ?
- Even though, strong constraints from radio and IC ?

$$\chi \chi \rightarrow \phi \phi \quad \& \quad \phi \rightarrow l^+ l^-$$

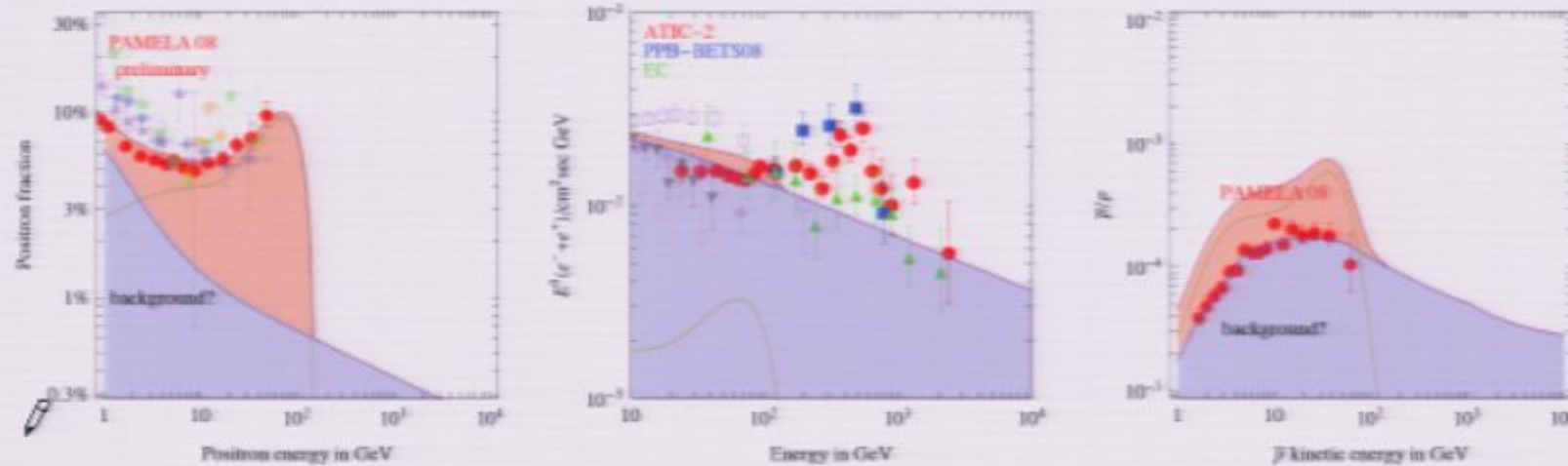
Accelerator constraints soon ?

# Other signals should not be overproduced

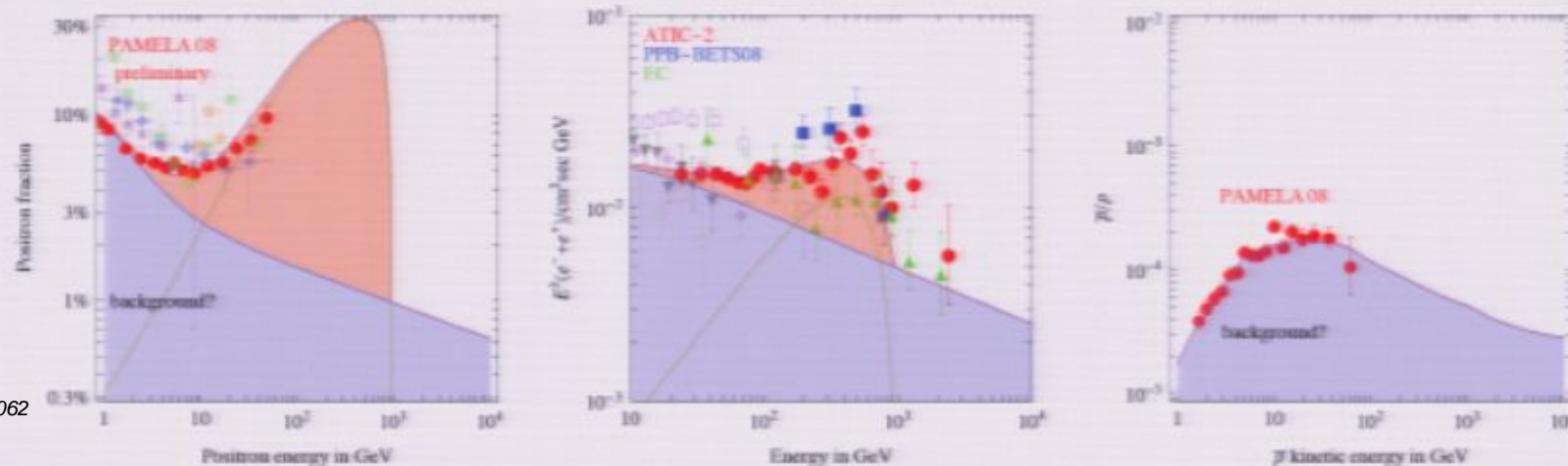
Quark channels are suppressed – purely leptophilic DM candidate

M. Cirelli<sup>a</sup>, M. Kadastik<sup>b</sup>, M. Raidal<sup>b</sup>, A. Strumia<sup>c</sup>

DM with  $M = 150$  GeV that annihilates into  $W^+ W^-$



DM with  $M = 1$  TeV that annihilates into  $\mu^+ \mu^-$



# Constraints on WIMP Dark Matter from the High Energy PAMELA $\bar{p}/p$ data

F. Donato, D. Maurin, P. Brun, T. Delahaye & P. Salati, [arXiv:0810.5292](https://arxiv.org/abs/0810.5292)

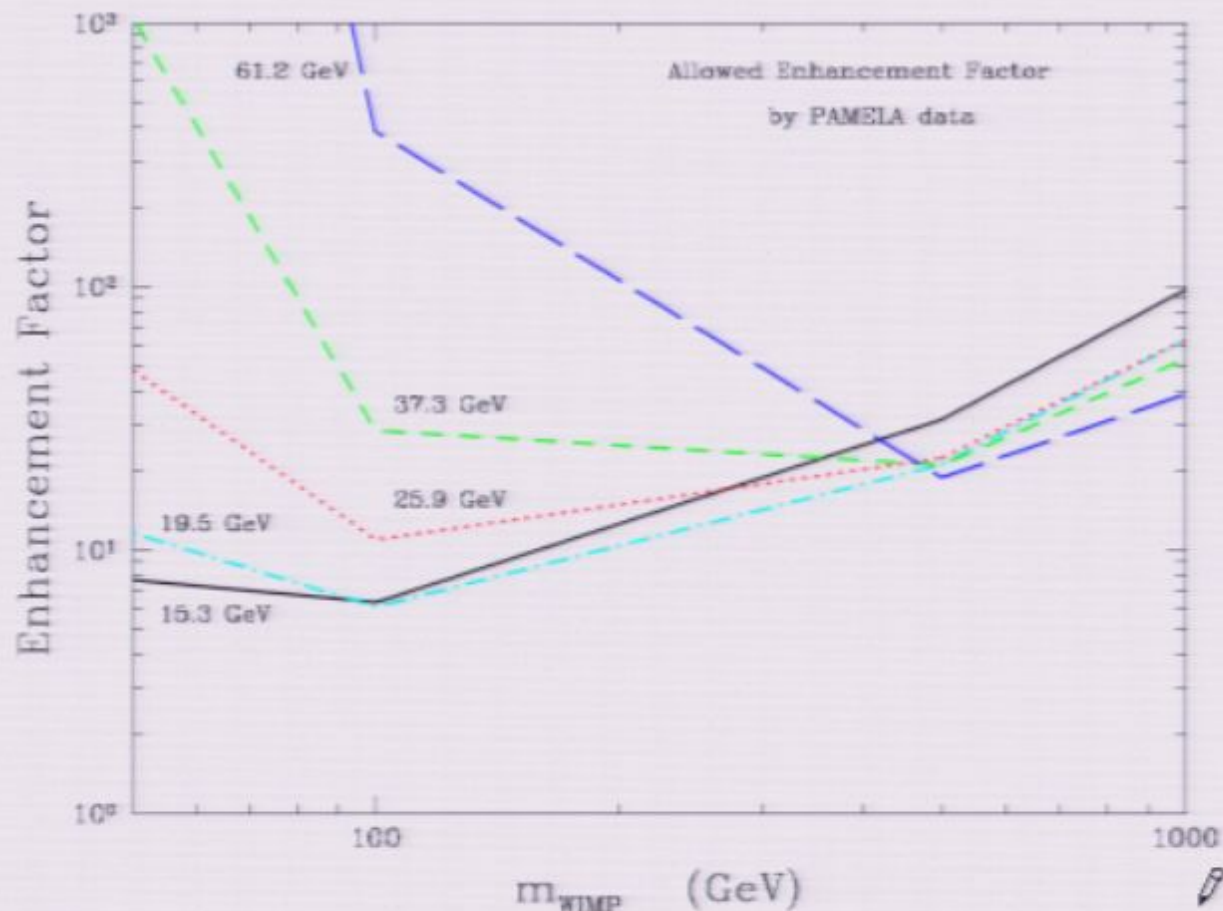


FIG. 2: Upper limits on the enhancement factor to the primary  $\bar{p}$  flux as a function of the WIMP mass, derived from a comparison with PAMELA high energy data. Each curve is labelled according to the corresponding PAMELA energy bin.

# Constraints on WIMP Dark Matter from the High Energy PAMELA $\bar{p}/p$ data

F. Donato et al. – arXiv:0810.5292 – PRL 102 (2009) 071301

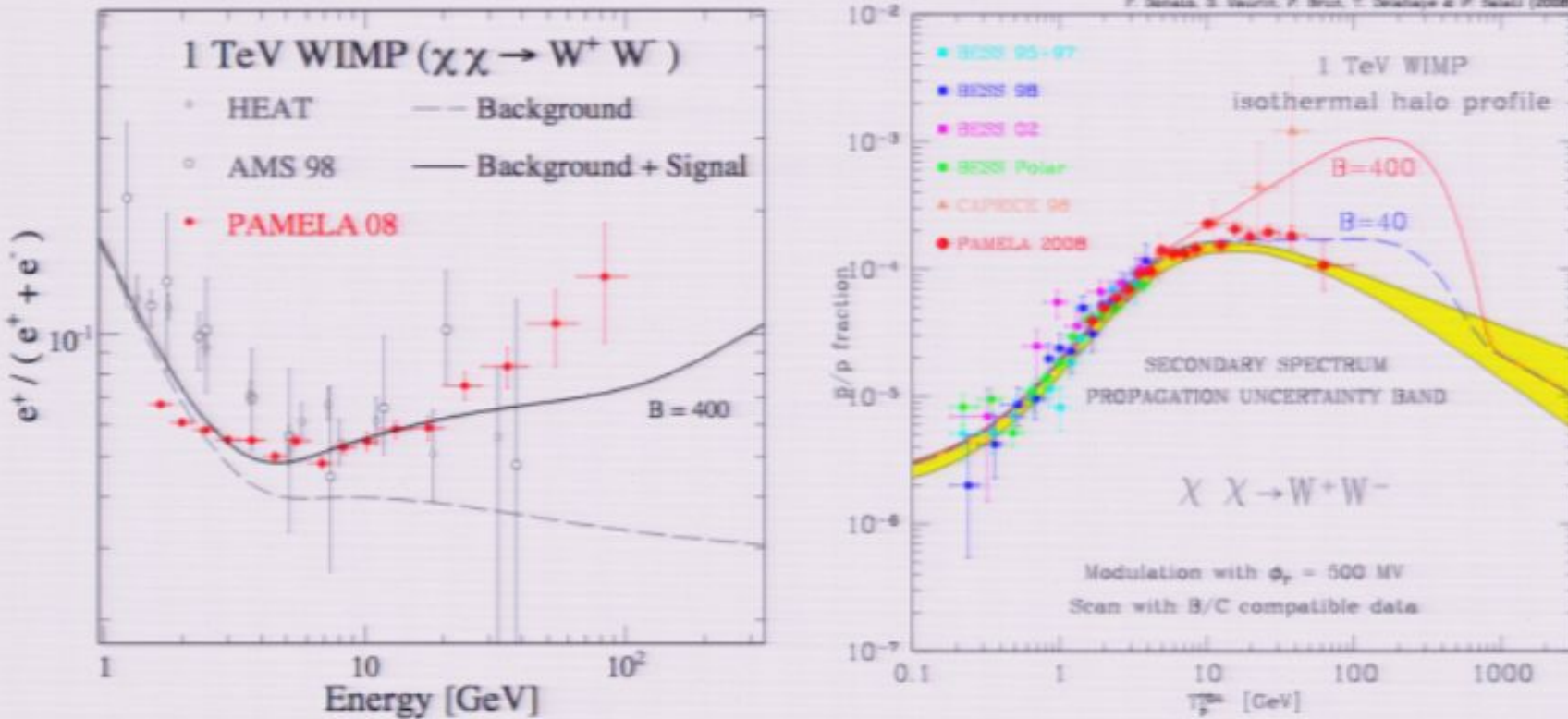


FIG. 3: The fiducial case of a 1 TeV LSP annihilating into a  $W^+W^-$  pair is featured. In the left panel, the positron signal which this DM species yields has been increased by a factor of 400, hence the solid curve and a marginal agreement with the PAMELA data. Positron fraction data are from HEAT [18], AMS-01 [5, 22] and PAMELA [2]. If the so-called Sommerfeld effect [7] is invoked to explain such a large enhancement of the annihilation cross section, the same boost applies to antiprotons and leads to an unacceptable distortion of their spectrum as indicated by the red solid line of the right panel.

# Constraints from $\gamma$ -rays and radio

Lars Bergström<sup>a</sup>, Gianfranco Bertone<sup>b</sup>, Torsten Bringmann<sup>a</sup>, Joakim Edsjö<sup>a</sup>, and Marco Taoso<sup>b,c</sup>

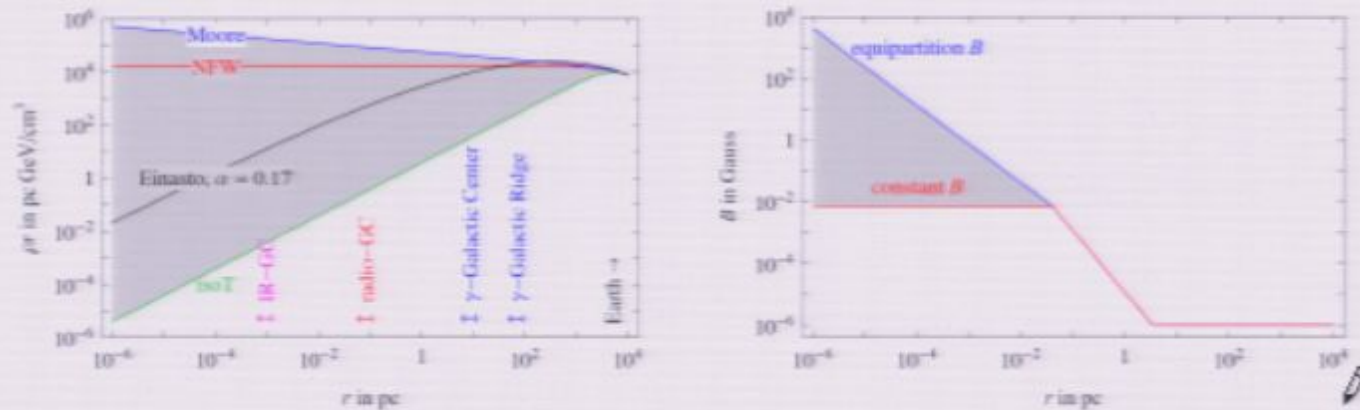
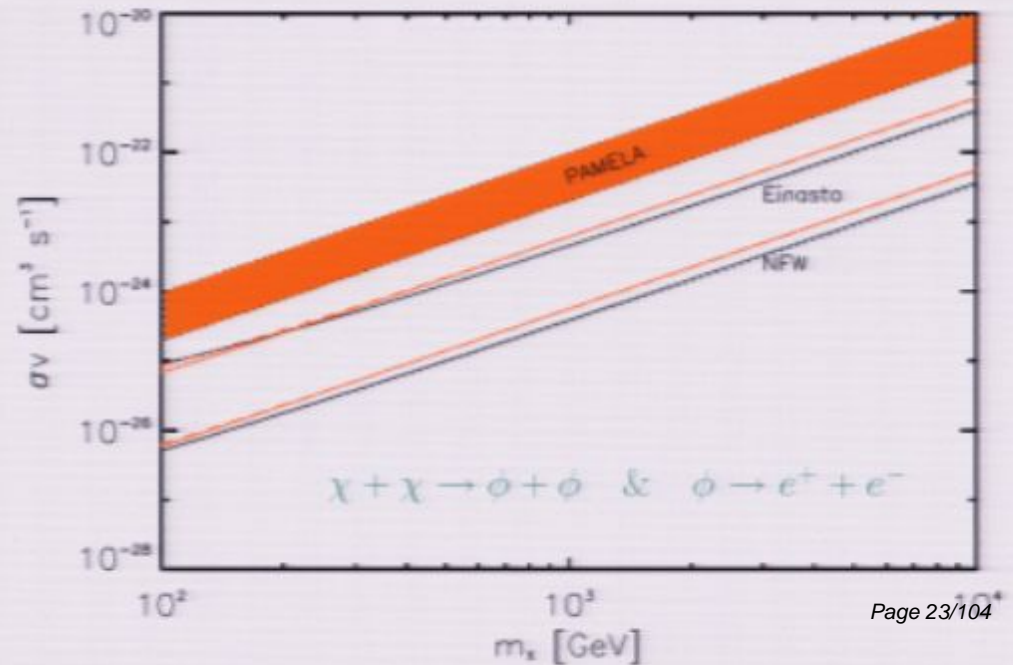
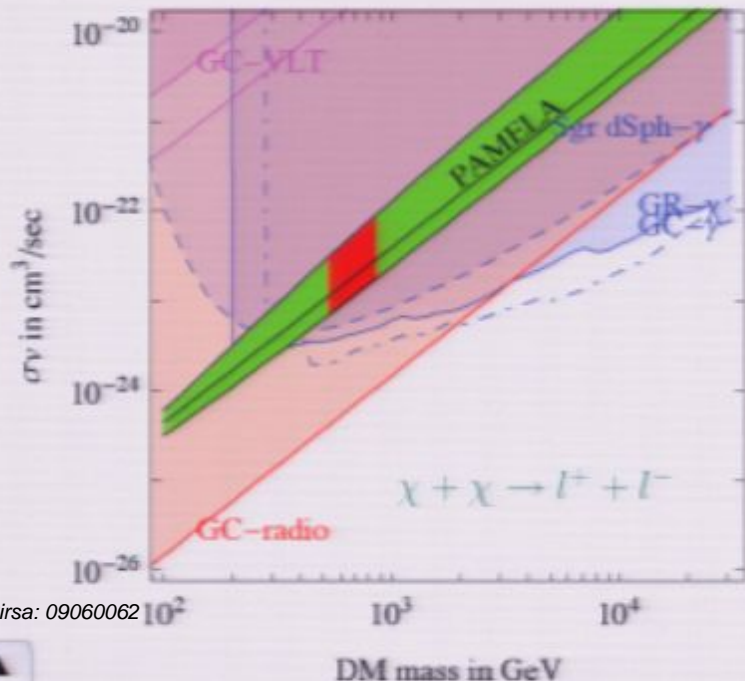
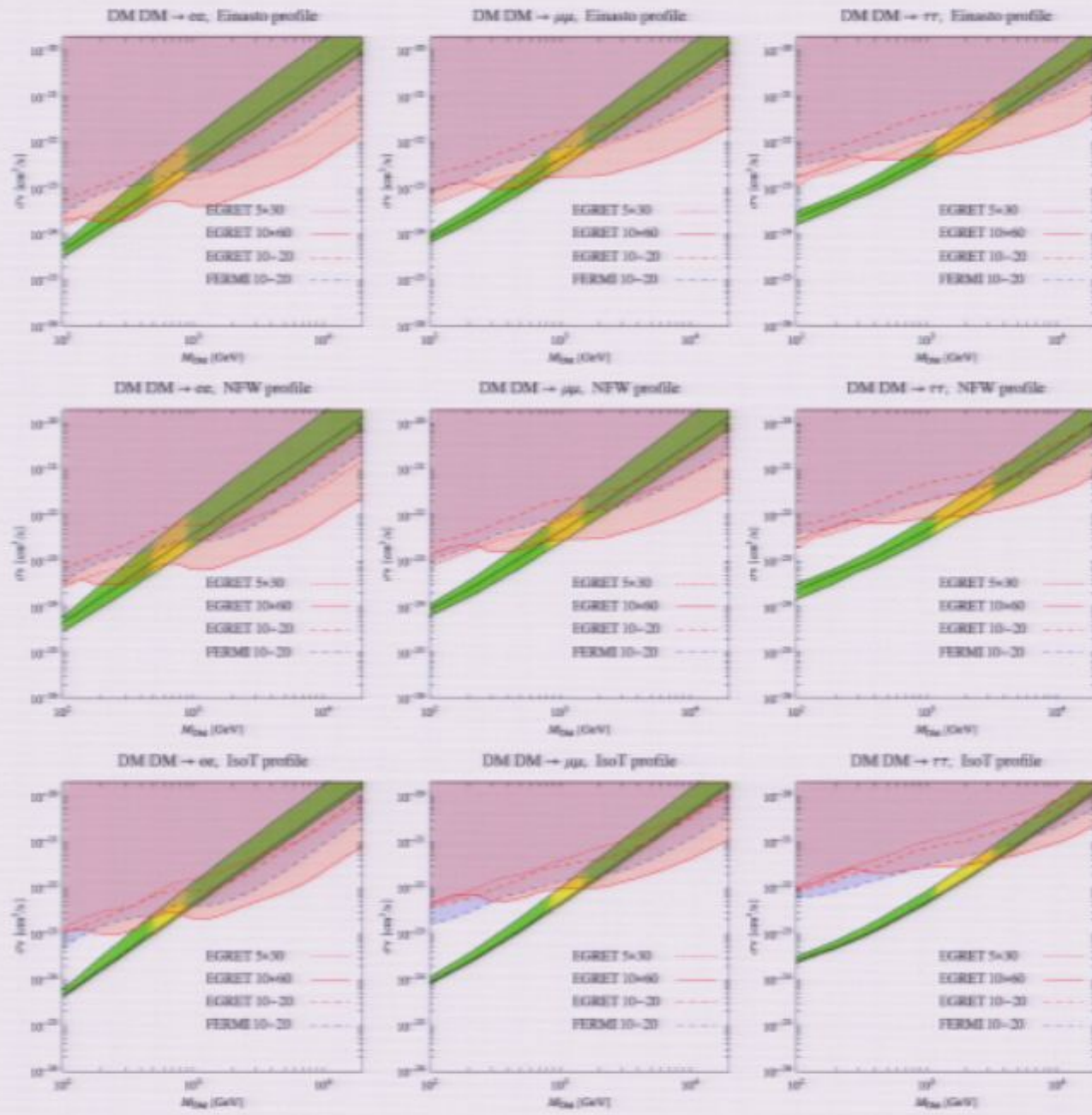


Figure 1: Shape of DM density (left) and magnetic field (right) profiles discussed in the text, as a function of the galactocentric coordinate  $r$ .

## DM $\text{DM} \rightarrow e^+ e^-$ , NFW profile



Marco Cirelli<sup>a</sup>, Paolo Panci<sup>a,b,c</sup>

# Constraints from $\gamma$ -rays and radio

Lars Bergström<sup>a</sup>, Gianfranco Bertone<sup>b</sup>, Torsten Bringmann<sup>a</sup>, Joakim Edsjö<sup>a</sup>, and Marco Taoso<sup>b,c</sup>

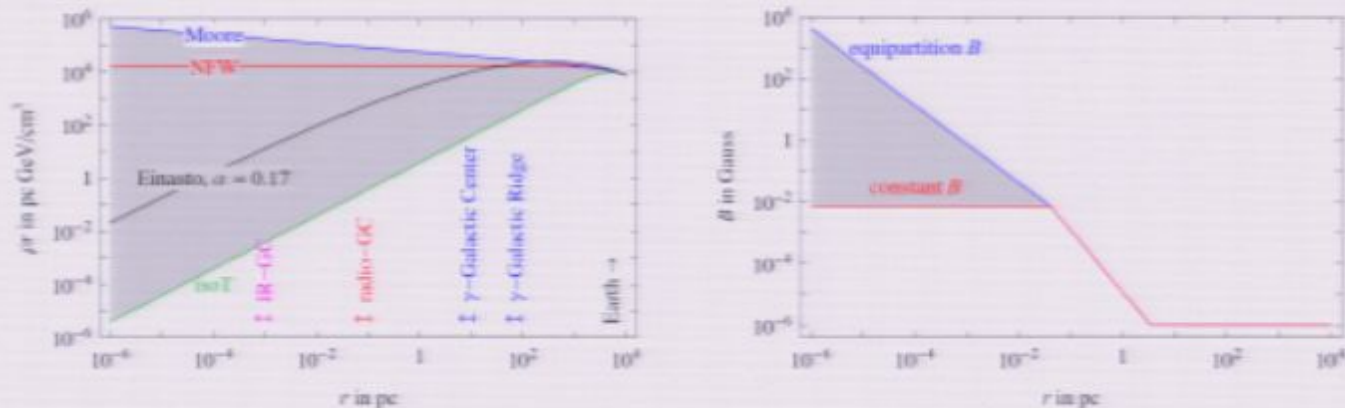
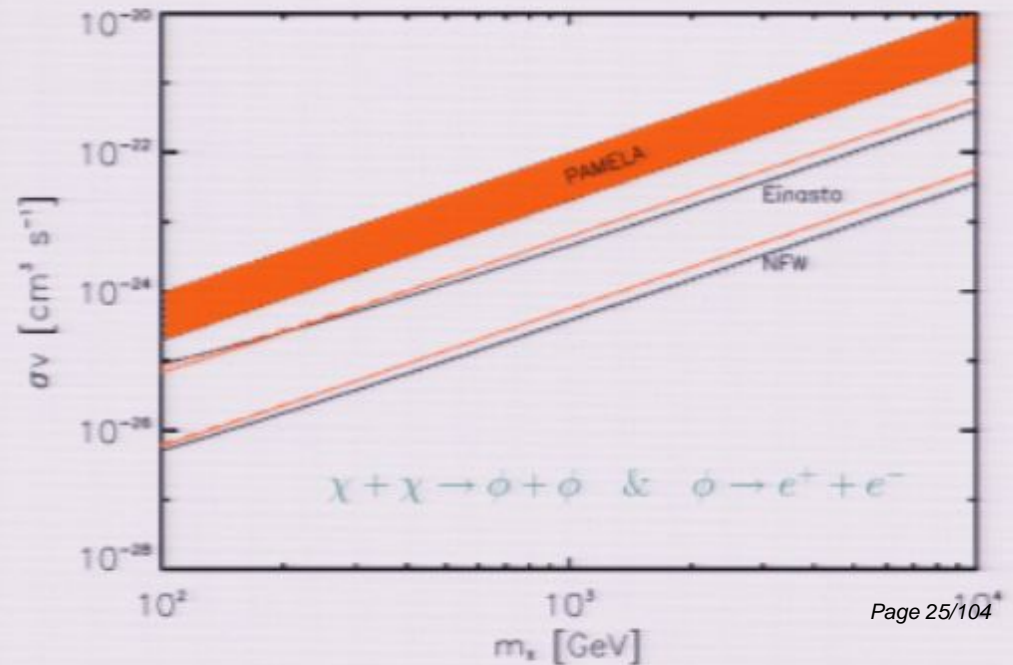
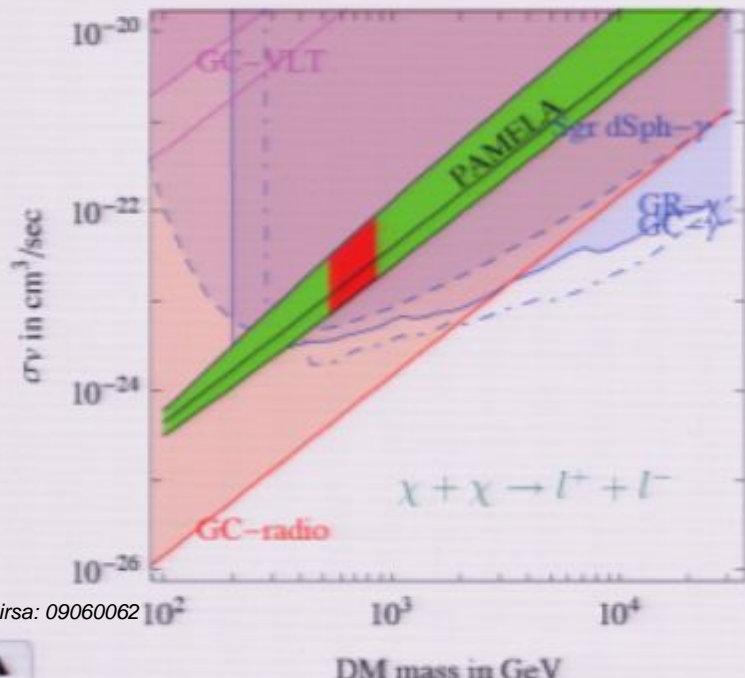
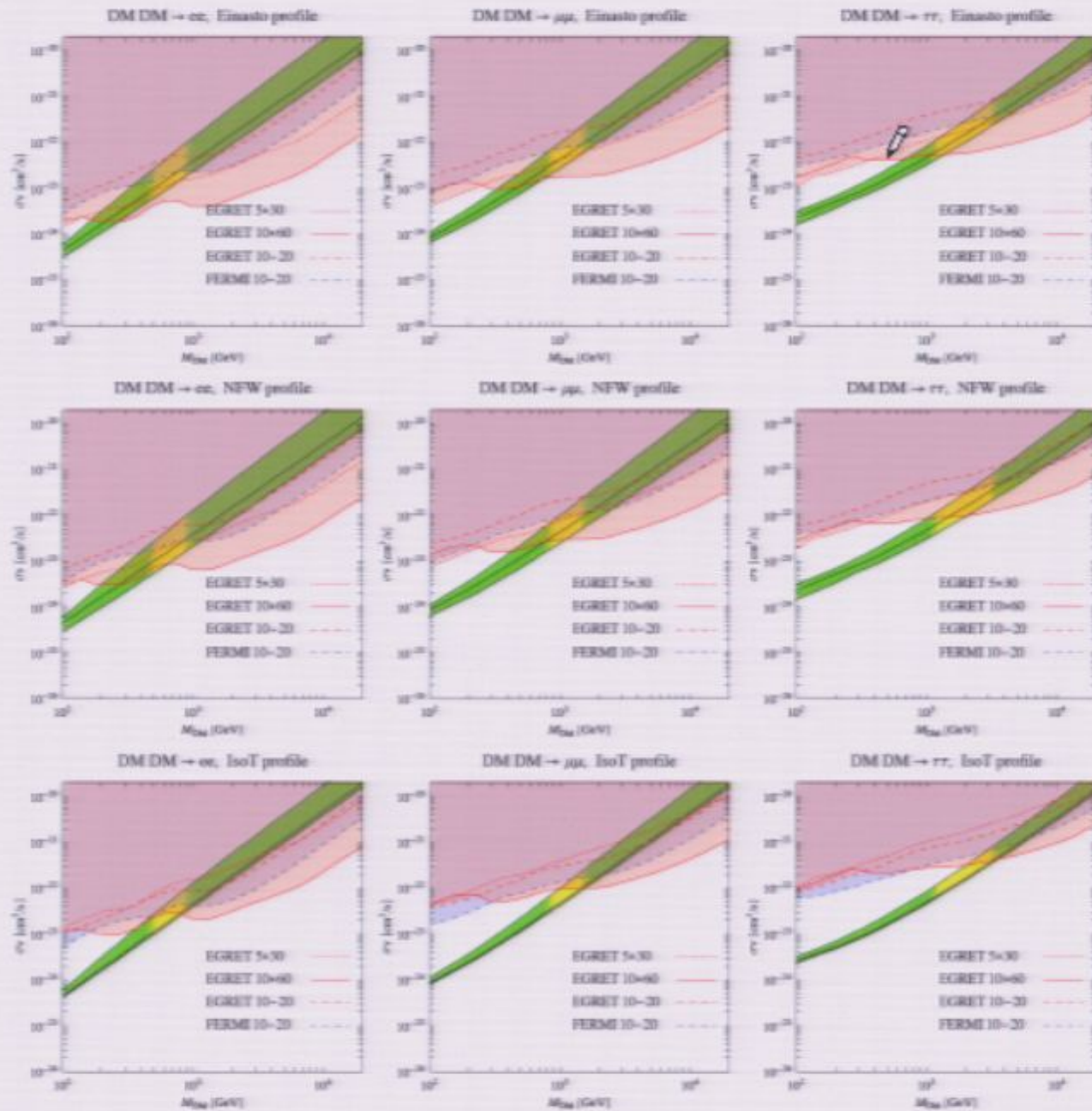


Figure 1: Shape of DM density (left) and magnetic field (right) profiles discussed in the text, as a function of the galactocentric coordinate  $r$ .

## DM $\text{DM} \rightarrow e^+ e^-$ , NFW profile



Marco Cirelli<sup>a</sup>, Paolo Panci<sup>a,b,c</sup>

# Constraints from $\gamma$ -rays and radio

Lars Bergström<sup>a</sup>, Gianfranco Bertone<sup>b</sup>, Torsten Bringmann<sup>a</sup>, Joakim Edsjö<sup>a</sup>, and Marco Taoso<sup>b,c</sup>

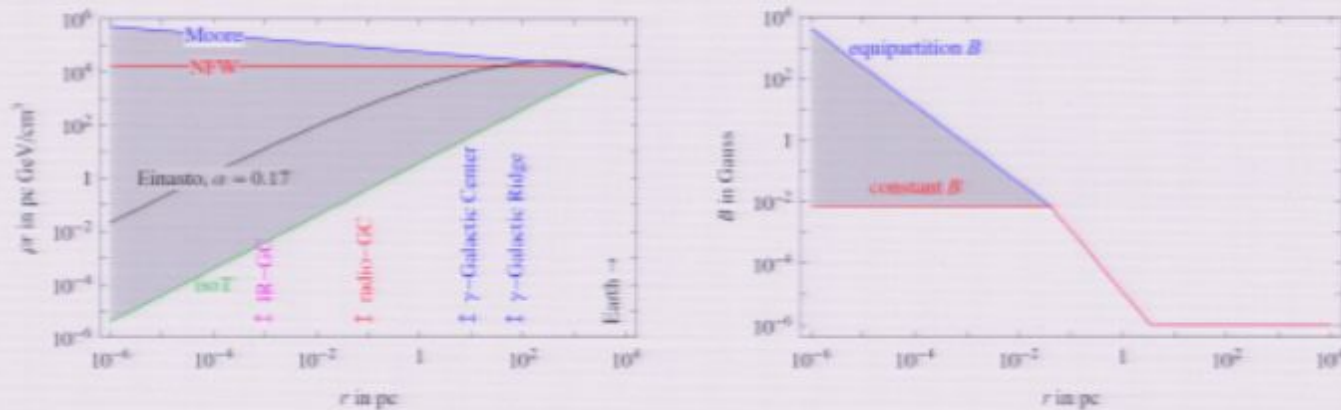
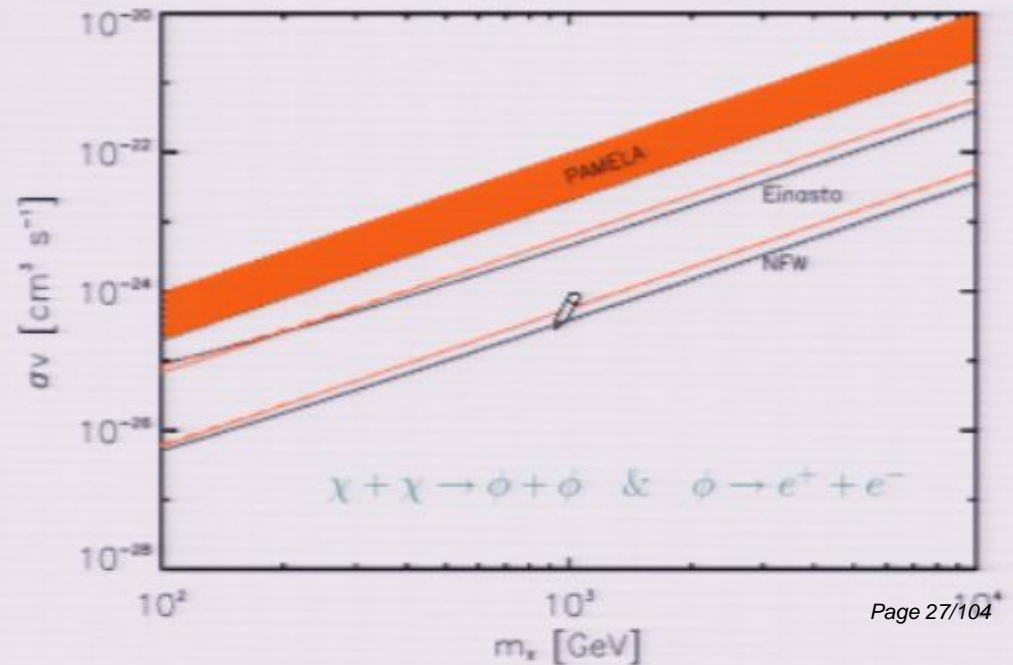
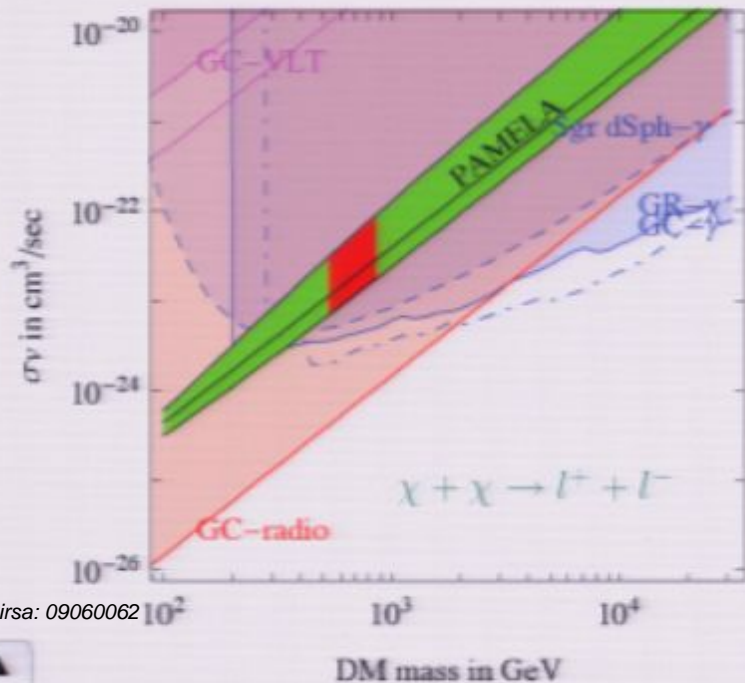


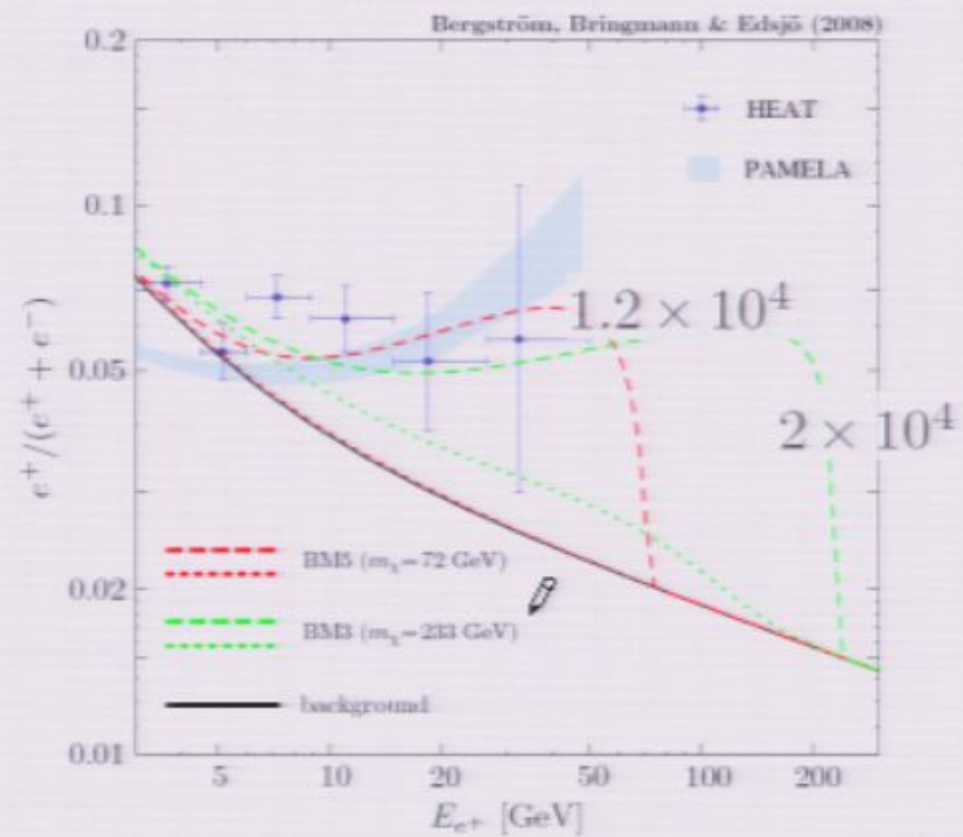
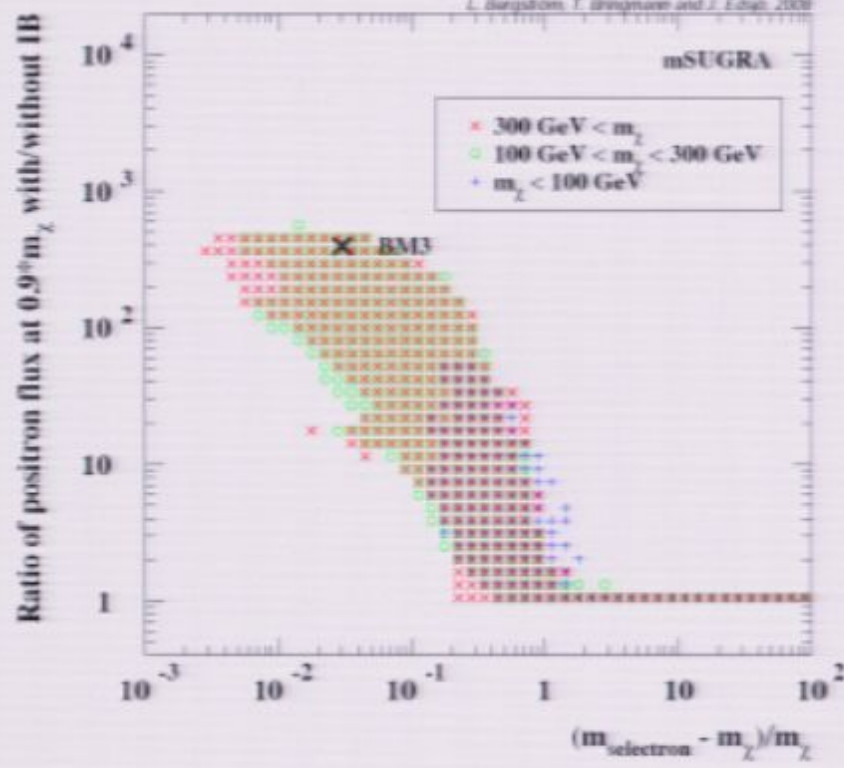
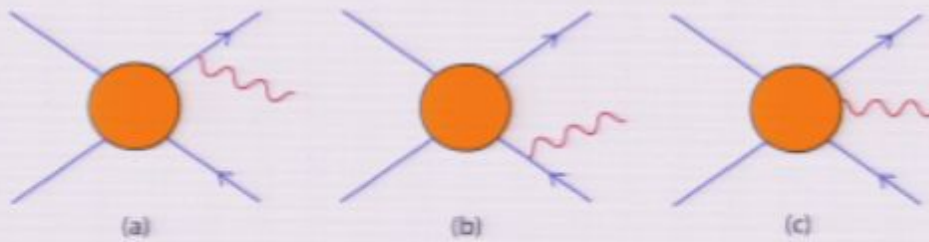
Figure 1: Shape of DM density (left) and magnetic field (right) profiles discussed in the text, as a function of the galactocentric coordinate  $r$ .

## DM $\text{DM} \rightarrow e^+ e^-$ , NFW profile



# New Positron Spectral Features from Supersymmetric Dark Matter - a Way to Explain the PAMELA Data?

Lars Bergström,\* Torsten Bringmann,† and Joakim Edsjö‡



## PAMELA positron excess

May be the first indirect hint that DM species annihilate in the MW.

$$\Gamma_{\text{ann}} \equiv \langle \sigma v \rangle \times \frac{\rho_\chi^2}{m_\chi^2} \text{ needs to be enhanced}$$

### 2) Boosting the annihilation cross section

- Internal bremsstrahlung from charged external legs or virtual internal particles.
- Sommerfeld effect – a non-perturbative enhancement of  $\sigma_{\text{ann}}$  at low velocity.
- Slightly or strongly modified thermal decoupling (quintessence).

Beware of the other messengers !

- Antiprotons are not produced – leptophilic WIMP ?
- Even though, strong constraints from radio and IC ?

$$\chi \chi \rightarrow \phi \phi \quad \& \quad \phi \rightarrow l^+ l^-$$

Accelerator constraints soon ?

# Constraints on WIMP Dark Matter from the High Energy PAMELA $\bar{p}/p$ data

F. Donato et al. – arXiv:0810.5292 – PRL **102** (2009) 071301

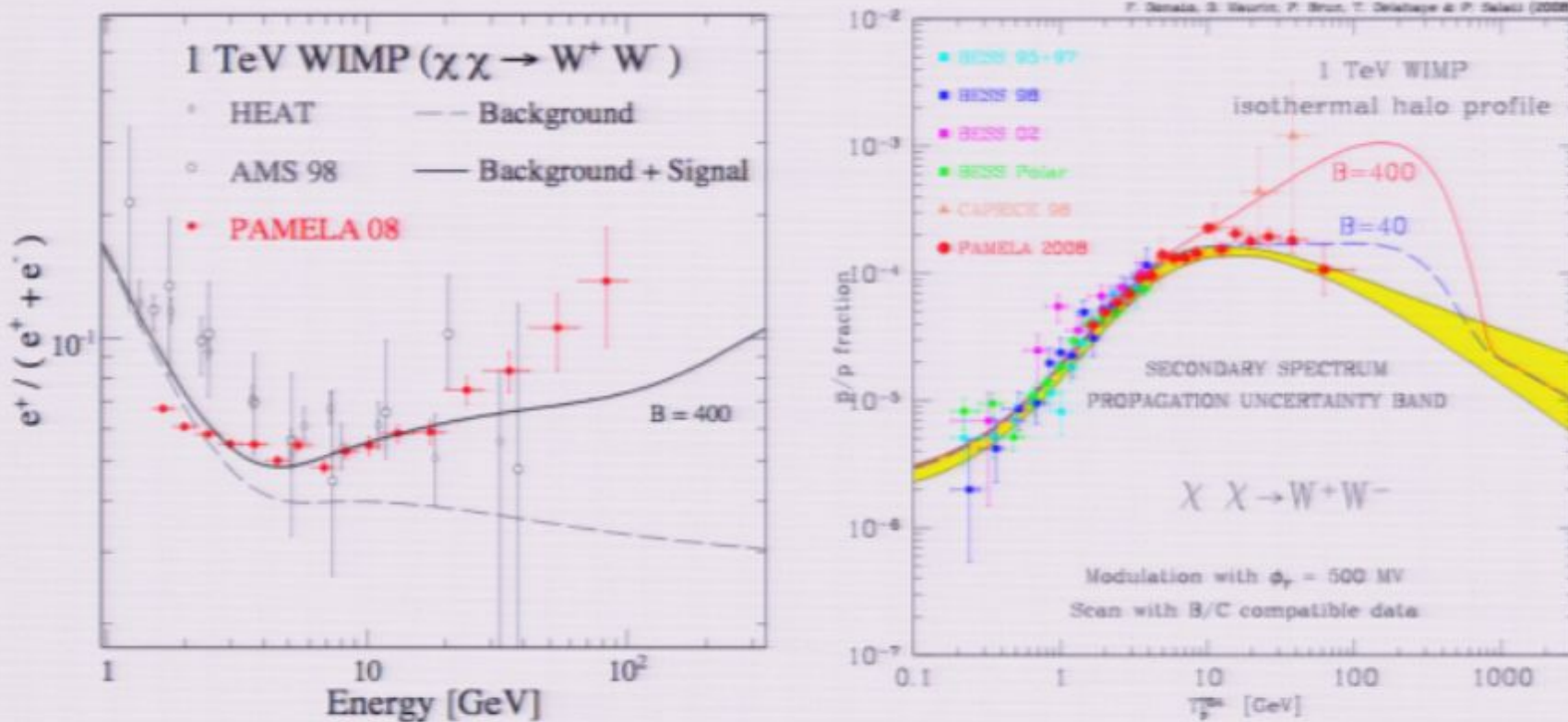


FIG. 3: The fiducial case of a 1 TeV LSP annihilating into a  $W^+W^-$  pair is featured. In the left panel, the positron signal which this DM species yields has been increased by a factor of 400, hence the solid curve and a marginal agreement with the PAMELA data. Positron fraction data are from HEAT [18], AMS-01 [5, 22] and PAMELA [2]. If the so-called Sommerfeld effect [7] is invoked to explain such a large enhancement of the annihilation cross section, the same boost applies to antiprotons and leads to an unacceptable distortion of their spectrum as indicated by the red solid line of the right panel.

## PAMELA positron excess

May be the first indirect hint that DM species annihilate in the MW.

$$\Gamma_{\text{ann}} \equiv \langle \sigma v \rangle \times \frac{\rho_\chi^2}{m_\chi^2} \text{ needs to be enhanced}$$

### 3) Astrophysical effects on DM annihilation

DM substructures have  $\langle \rho^2 \rangle \geq \langle \rho \rangle^2$ .

- A statistical analysis is necessary to compute the signal enhancement.

$$B_{\text{Milky Way}} \leq 20 \text{ in } \Lambda\text{CDM}$$

- A single nearby clump – how probable is it ?
- A single nearby clump – what about the other messengers ?
- Are minispikes about IMBHs a myth ?

# Boost factors : a hazardous kind of magic

JÜRG DIEMAND<sup>1,2</sup>, MICHAEL KUHLEN<sup>1,3</sup>, & PIERO MADAU<sup>1,4</sup>

FIG. 2.—Projected dark matter density-squared map of our simulated Milky Way-size halo (“Via Lactea”) at the present epoch. The image covers an area of  $800 \times 600$  kpc, and the projection goes through a 600 kpc-deep cuboid containing a total of 110 million particles. The logarithmic color scale covers 20 decades in density-square.

# Boost factors : a hazardous kind of magic



CURRENT JACKPOT

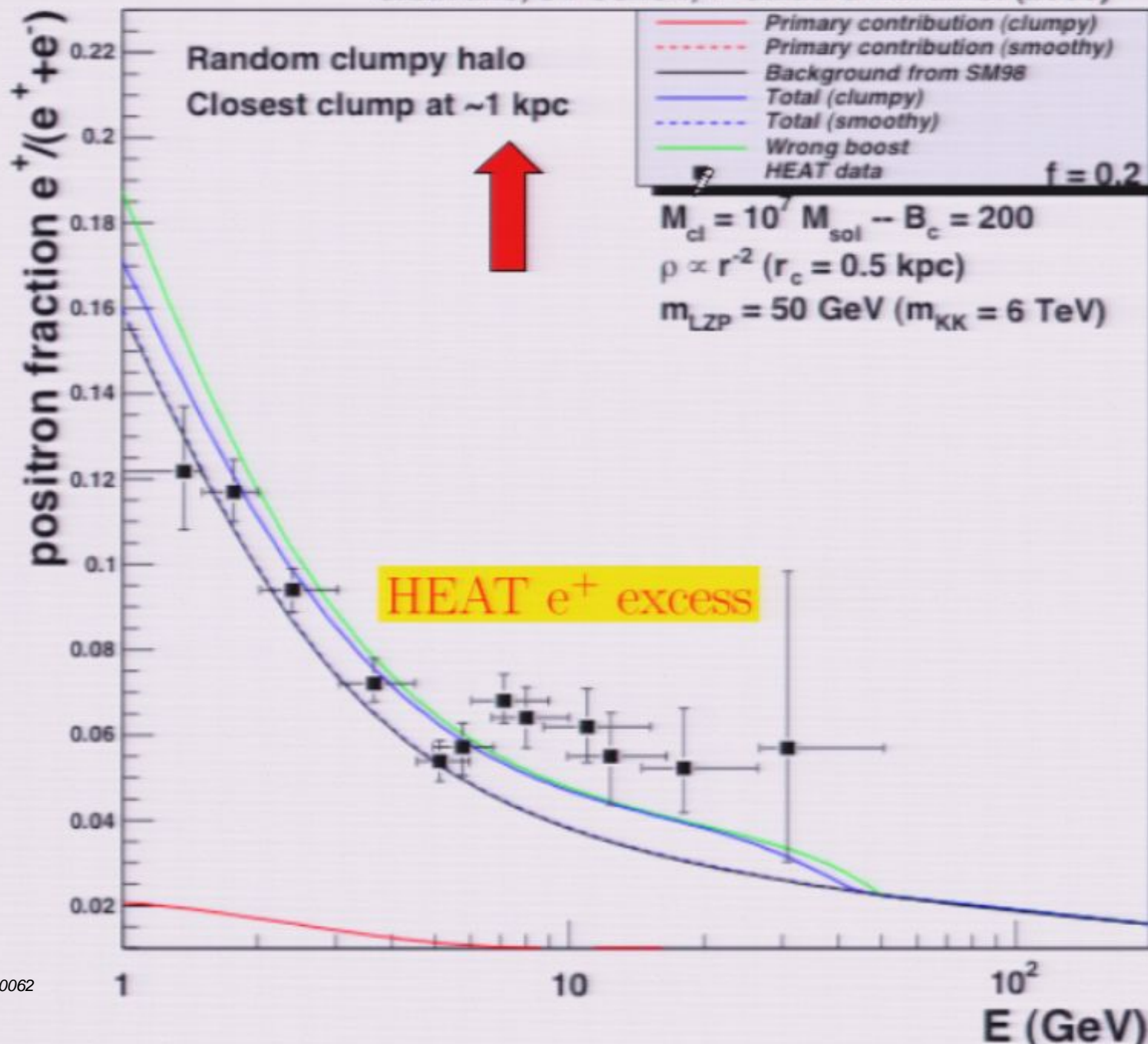
\$  $10^{66}$  neutralinos

Estimated for 3/31/2006

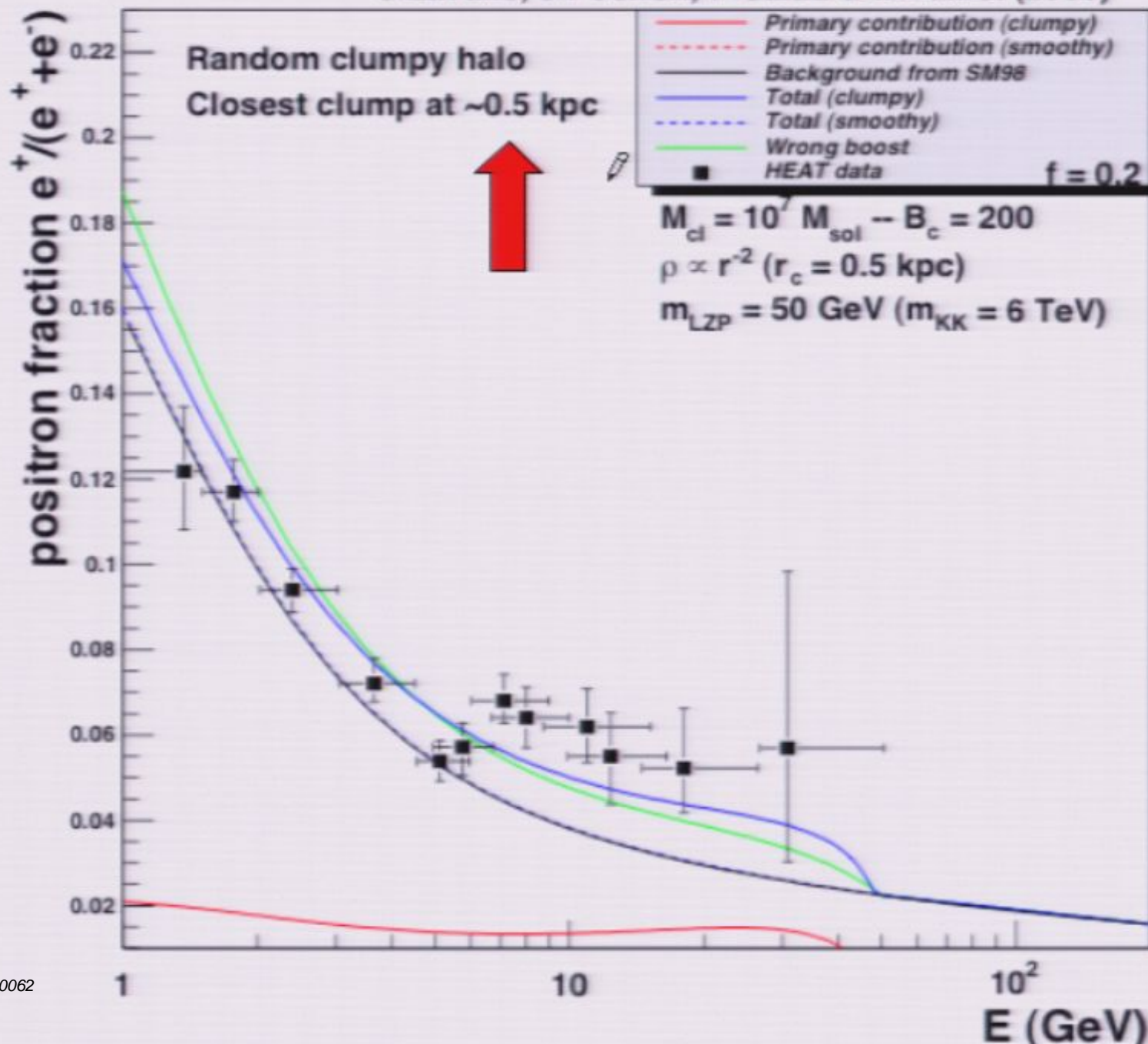
JÜRG DIEMAND<sup>1,2</sup>, MICHAEL KUHLEN<sup>1,3</sup>, & PIERO MADAU<sup>1,4</sup>

FIG. 2.—Projected dark matter density-squared map of our simulated Milky Way-size halo (“Via Lactea”) at the present epoch. The image covers an area of  $800 \times 600$  kpc, and the projection goes through a 600 kpc-deep cuboid containing a total of 110 million particles. The logarithmic color scale covers 20 decades in density-square.

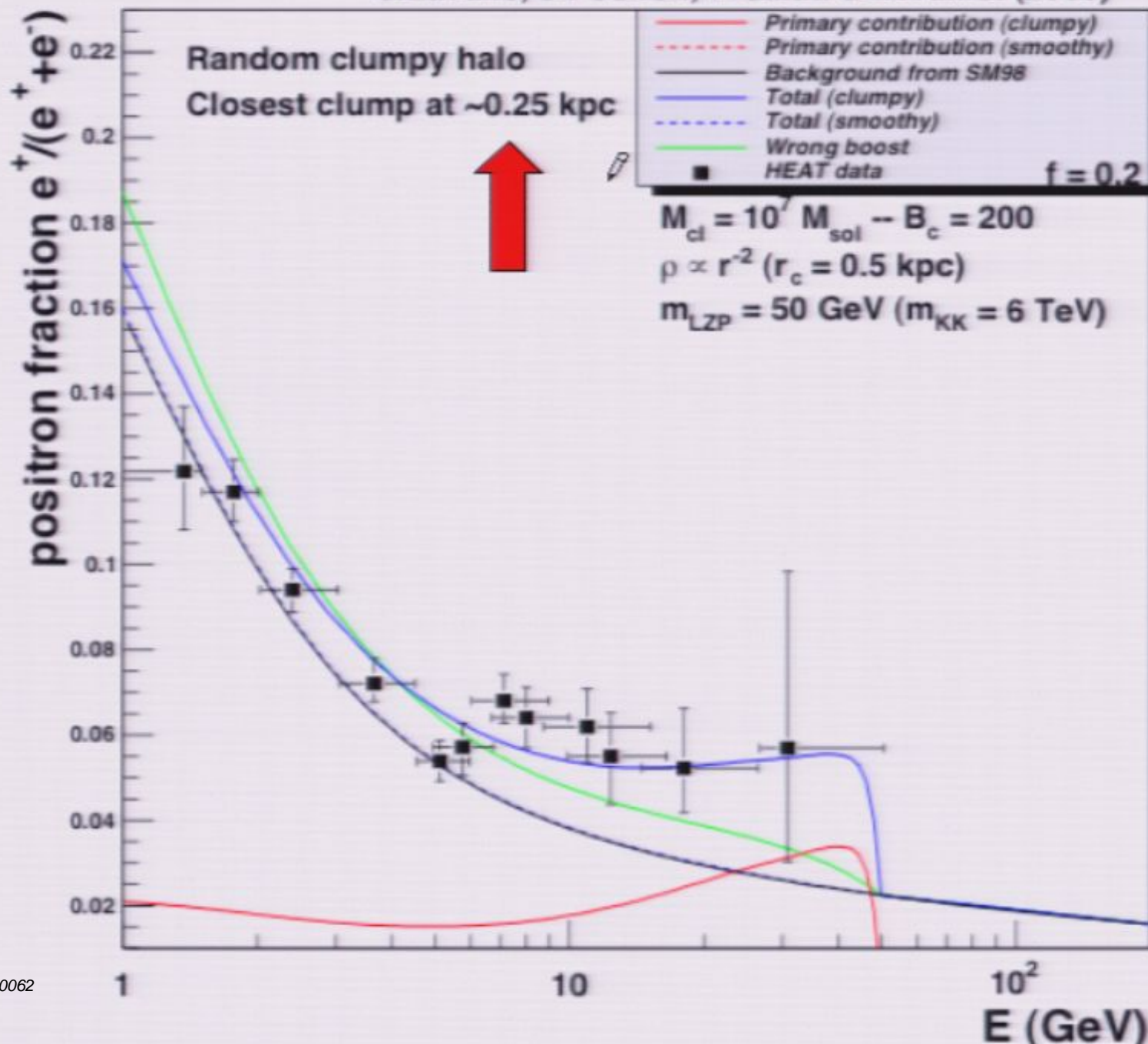
J.Lavalle, J.Pochon, P.Salati & R.Taillet (2006)



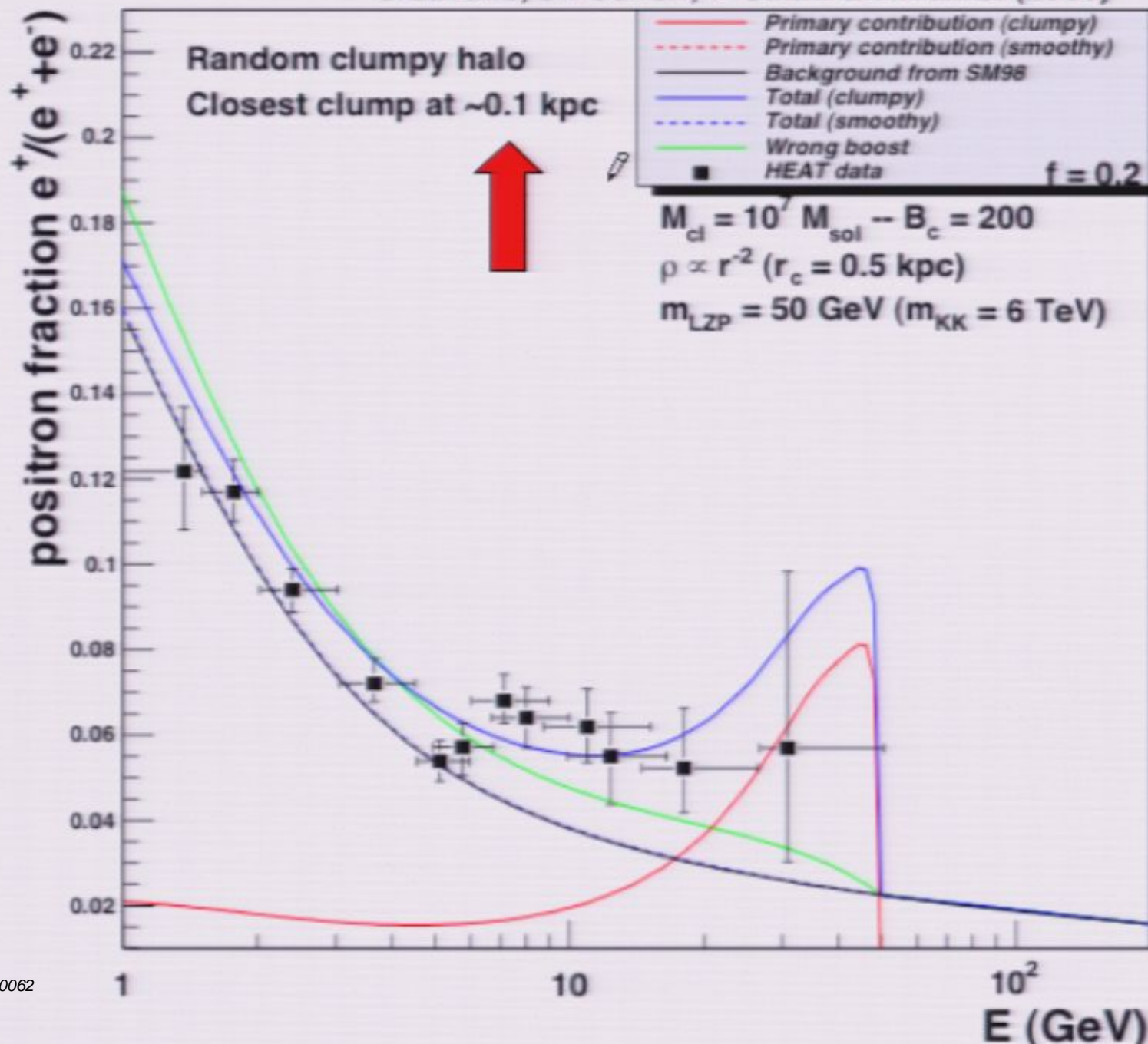
J.Lavalle, J.Pochon, P.Salati & R.Taillet (2006)



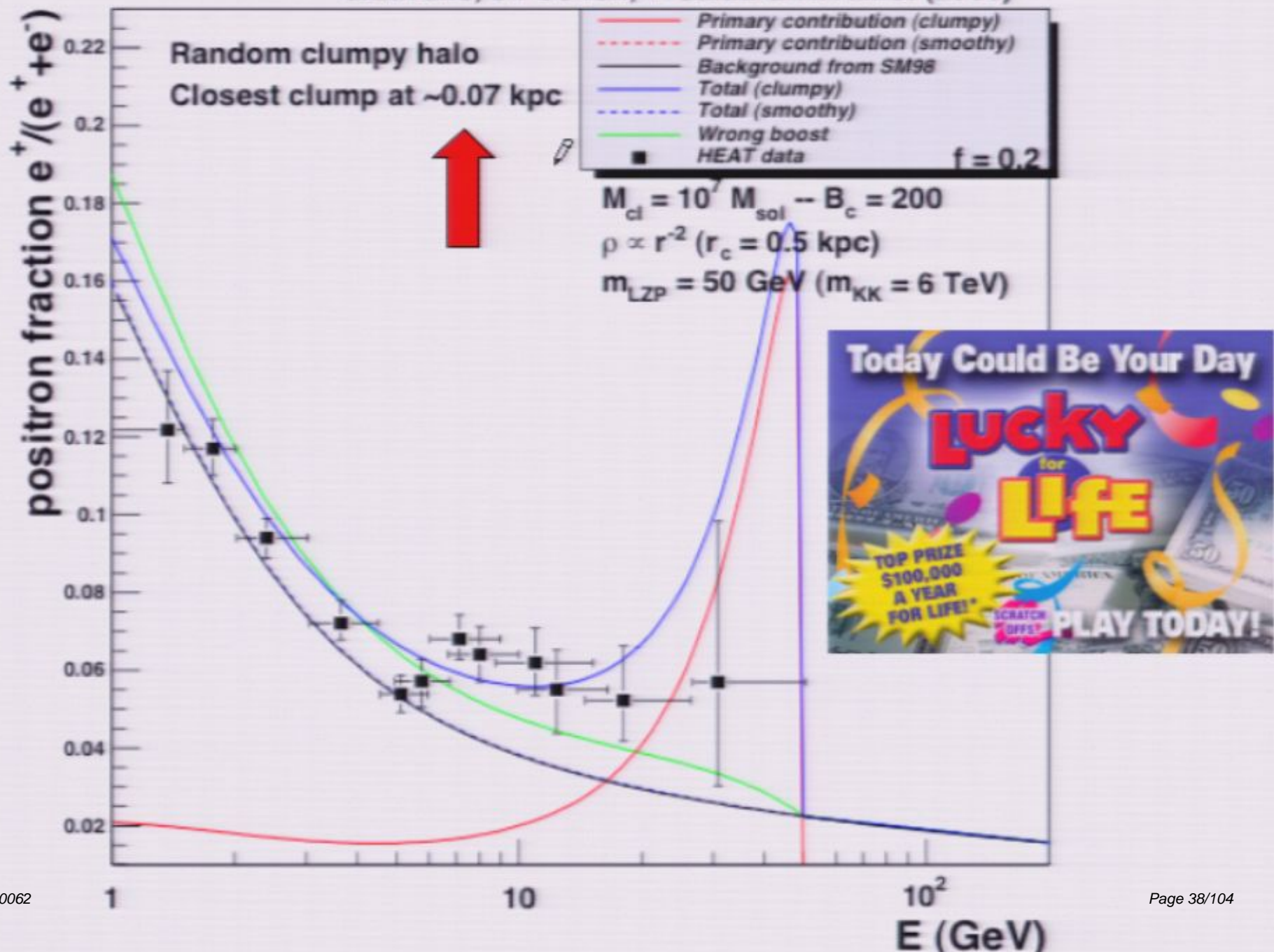
J.Lavalle, J.Pochon, P.Salati & R.Taillet (2006)



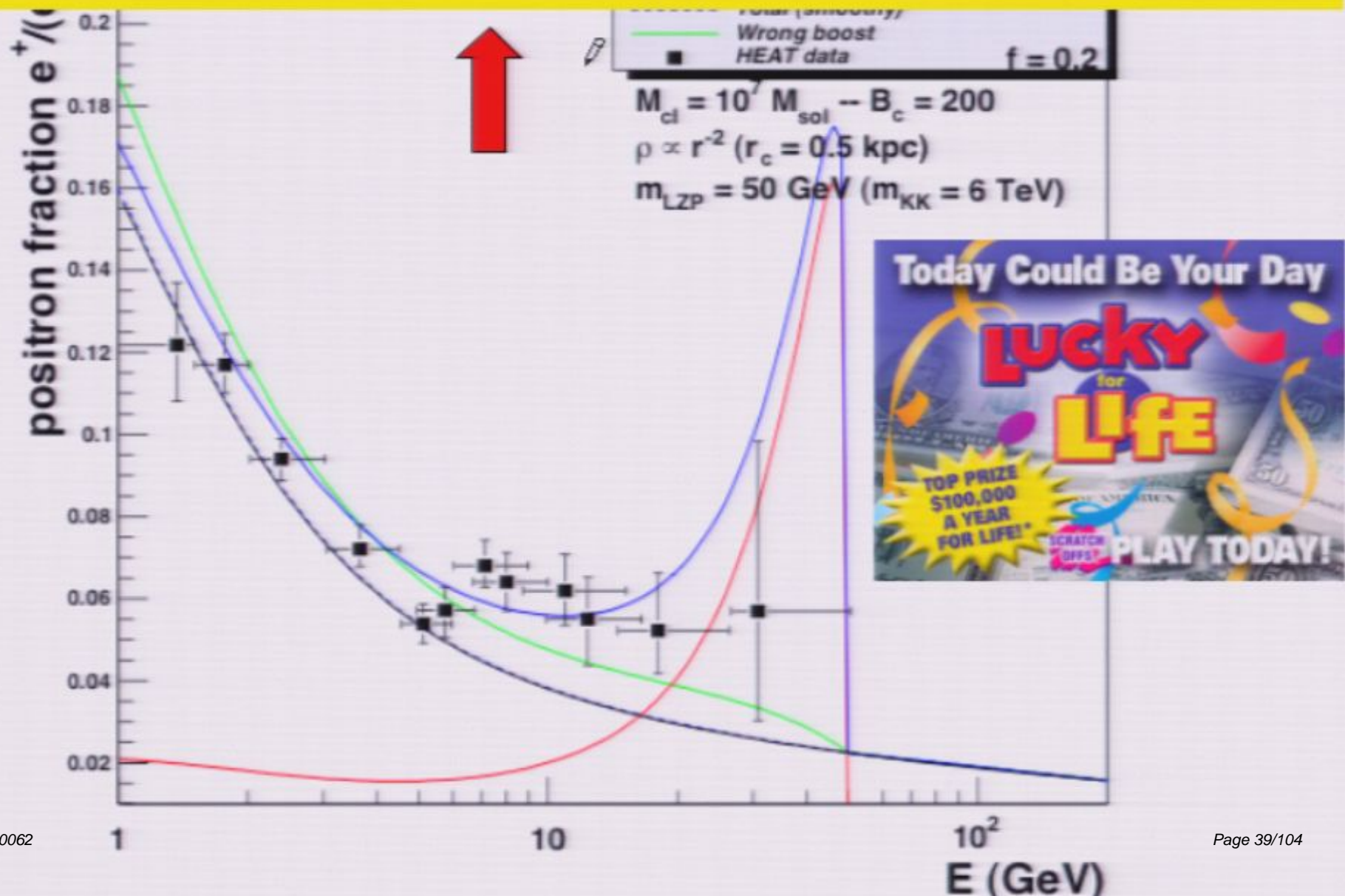
J.Lavalle, J.Pochon, P.Salati & R.Taillet (2006)



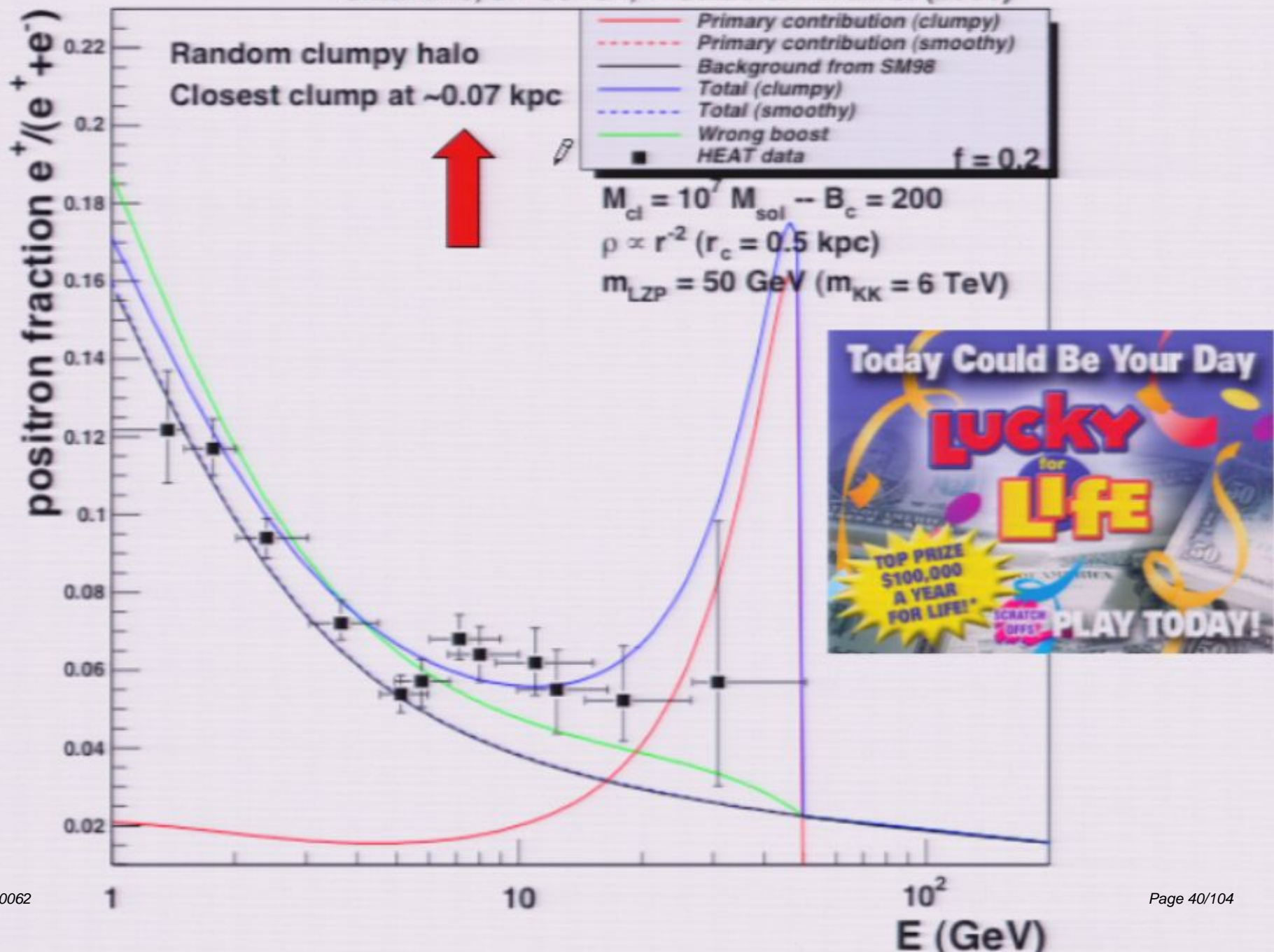
J.Lavalle, J.Pochon, P.Salati & R.Taillet (2006)



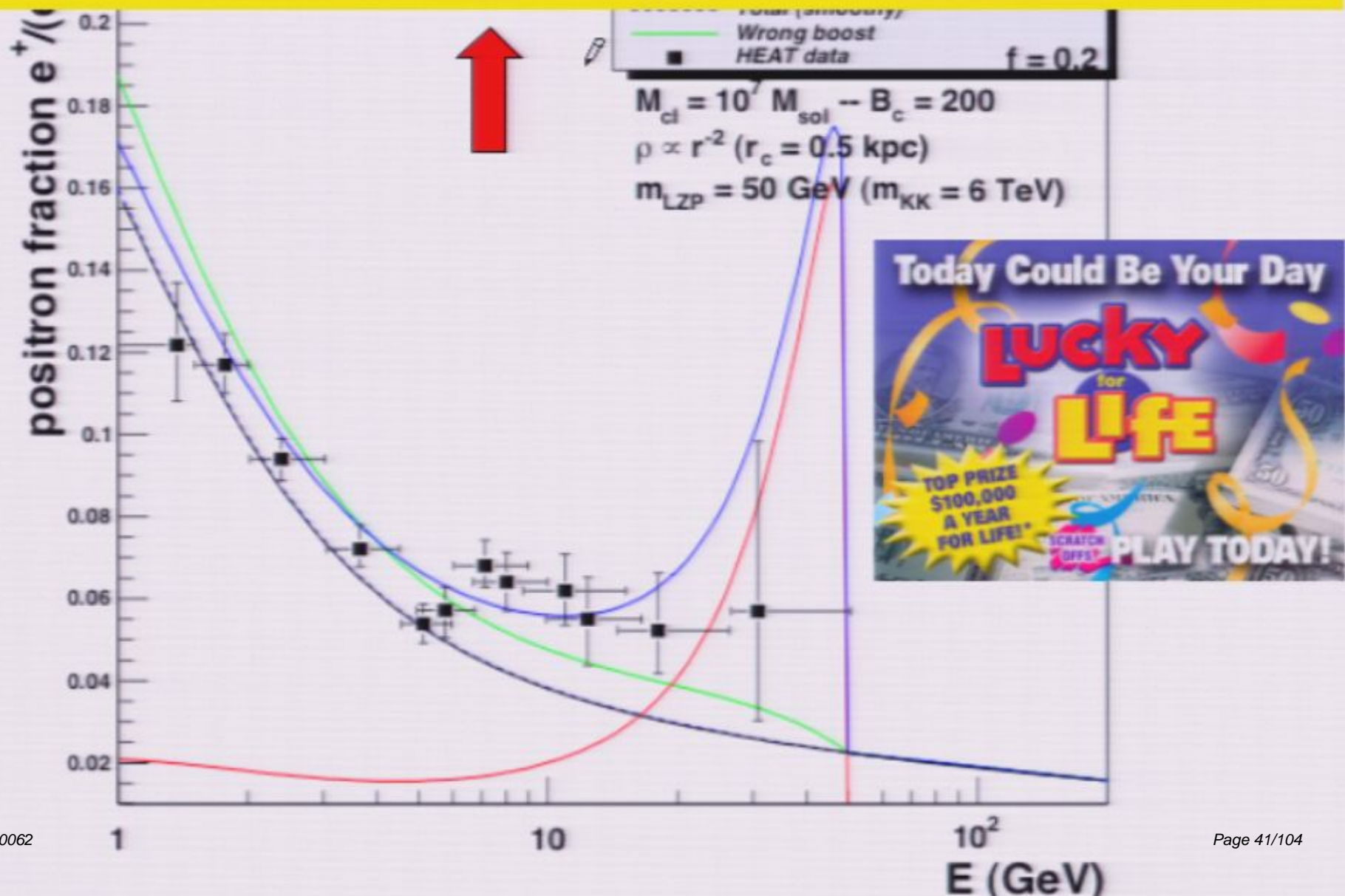
# How probable is that ?



J.Lavalle, J.Pochon, P.Salati & R.Taillet (2006)



# How probable is that ?



# Recipe for a statistical analysis

- Without clumps – with the smooth DM distribution  $\rho_s$

$$\phi_s = \left\{ \mathcal{S} \equiv \frac{\beta \delta}{4\pi} \langle \sigma_{\text{ann}} v \rangle \frac{\rho_\odot^2}{m_\chi^2} \frac{dN}{dE} \right\} \times \left\{ \mathcal{I} \equiv \int_{\text{DZ}} G(\mathbf{x}) \frac{\rho_s^2(\mathbf{x})}{\rho_\odot^2} d^3\mathbf{x} \right\}$$

- With clumps – with the DM distribution  $\rho = \rho'_s + \delta\rho$

$$\phi = \{\phi'_s \simeq \phi_s\} + \left\{ \phi_r = \sum_i \varphi_i \right\}$$

$$\varphi_i = \mathcal{S} \times G(\mathbf{x}_i) \times \left\{ \xi_i = \frac{B_i M_i}{\rho_\odot} = \int_{\text{ith clump}} \frac{\delta\rho^2(\mathbf{x})}{\rho_\odot^2} d^3\mathbf{x} \right\}$$



$$\text{Boost factor } B \equiv \frac{\phi}{\phi_s}$$

# Recipe for a statistical analysis

- Without clumps – with the smooth DM distribution  $\rho_s$

$$\phi_s = \left\{ \mathcal{S} \equiv \frac{\beta \delta}{4\pi} \langle \sigma_{\text{ann}} v \rangle \frac{\rho_\odot^2}{m_\chi^2} \frac{dN}{dE} \right\} \times \left\{ \mathcal{I} \equiv \int_{\text{DZ}} G(\mathbf{x}) \frac{\rho_s^2(\mathbf{x})}{\rho_\odot^2} d^3\mathbf{x} \right\}$$

- With clumps – with the DM distribution  $\rho = \rho'_s + \delta\rho$

$$\phi = \{\phi'_s \simeq \phi_s\} + \left\{ \phi_r = \sum_i \varphi_i \right\}$$
$$\varphi_i = \mathcal{S} \times G(\mathbf{x}_i) \times \left\{ \xi_i = \frac{B_i M_i}{\rho_\odot} = \int_{\text{ith clump}} \frac{\delta\rho^2(\mathbf{x})}{\rho_\odot^2} d^3\mathbf{x} \right\}$$

random behaviour !



$$\text{Boost factor } B \equiv \frac{\phi}{\phi_s}$$

# Recipe for a statistical analysis

- (i) The actual distribution of DM substructures is one particular realization  $\in$  statistical ensemble of all the possible **random** distributions.

$$\langle \phi_r \rangle \quad \text{and} \quad \sigma_r^2 = \langle \phi_r^2 \rangle - \langle \phi_r \rangle^2$$

$$B_{\text{eff}} = \langle B = \phi/\phi_s \rangle \quad \text{and} \quad \sigma_B = \sigma_r/\phi_s$$

- (ii) Clumps are distributed independently of each other. Therefore, we just need to determine how a single clump is distributed inside the galactic halo in order to derive the statistical properties of an entire constellation of  $N_H$  such substructures.

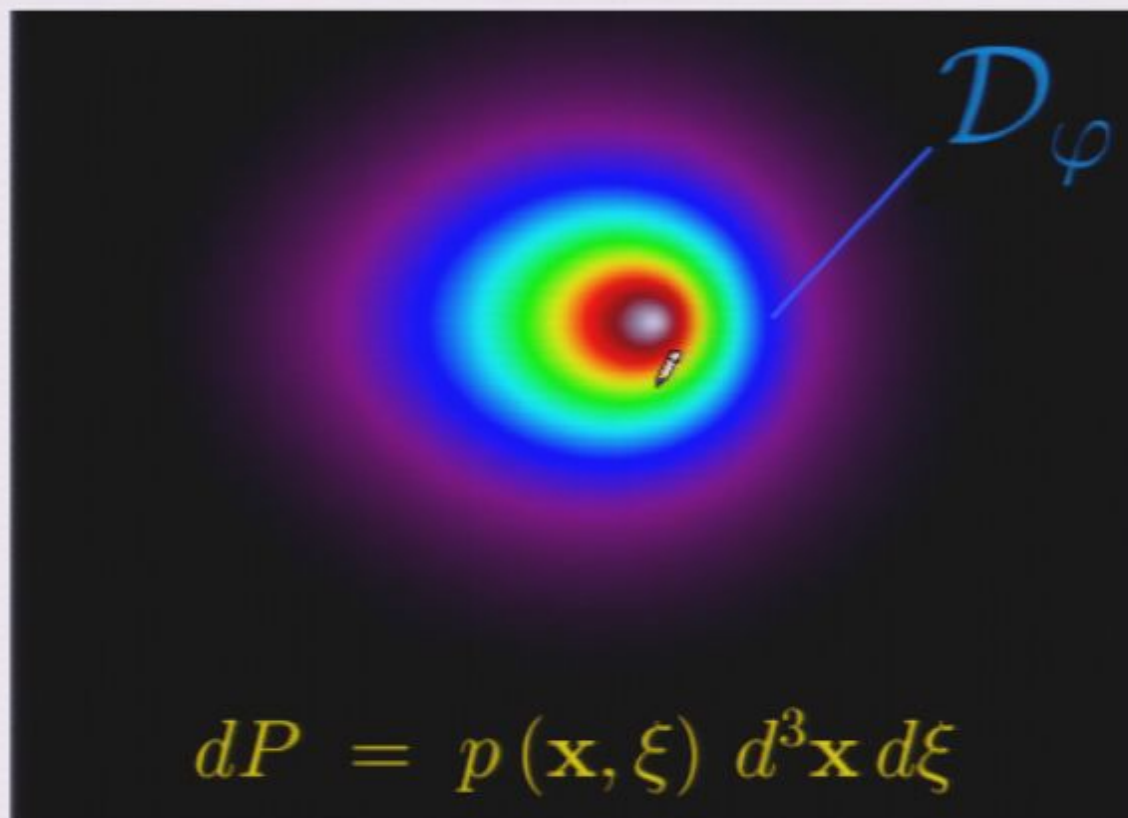
$$\langle \phi_r \rangle = N_H \langle \varphi \rangle \quad \text{and} \quad \sigma_r^2 = N_H \sigma^2 = N_H \{ \langle \varphi^2 \rangle - \langle \varphi \rangle^2 \}$$



(iii) The set of the random distributions of one single clump inside the domain  $\mathcal{D}_H$  forms the statistical ensemble  $\mathcal{T}$  which we need to consider. An event from that ensemble consists in a clump characterized by the annihilation volume  $\xi$  up to  $d\xi$  and located at position  $\mathbf{x}$  within the elementary volume  $d^3\mathbf{x}$ .

$$\mathcal{P}(\varphi) d\varphi = dP = \int_{\mathcal{D}_\varphi} p(\mathbf{x}, \xi) d^3\mathbf{x} d\xi$$

$$\langle \mathcal{F} \rangle = \int \mathcal{F}(\varphi) \mathcal{P}(\varphi) d\varphi = \int_{\mathcal{D}_H} \mathcal{F}\{\varphi(\mathbf{x}, \xi)\} p(\mathbf{x}, \xi) d^3\mathbf{x} d\xi$$



(iv) This naturally leads to the effective boost factor

$$B_{\text{eff}} = \left\{ \frac{\phi'_s}{\phi_s} \simeq 1 \right\} + \frac{\langle \phi_r \rangle}{\phi_s} = 1 + N_H \frac{\langle \xi G \rangle}{\mathcal{I}}$$

and to the boost variance

$\delta$

$$\frac{\sigma_B}{B_{\text{eff}}} = \frac{\sigma_r / \phi_s}{1 + \langle \phi_r \rangle / \phi_s} \simeq \frac{\sigma_r}{\langle \phi_r \rangle}$$

where

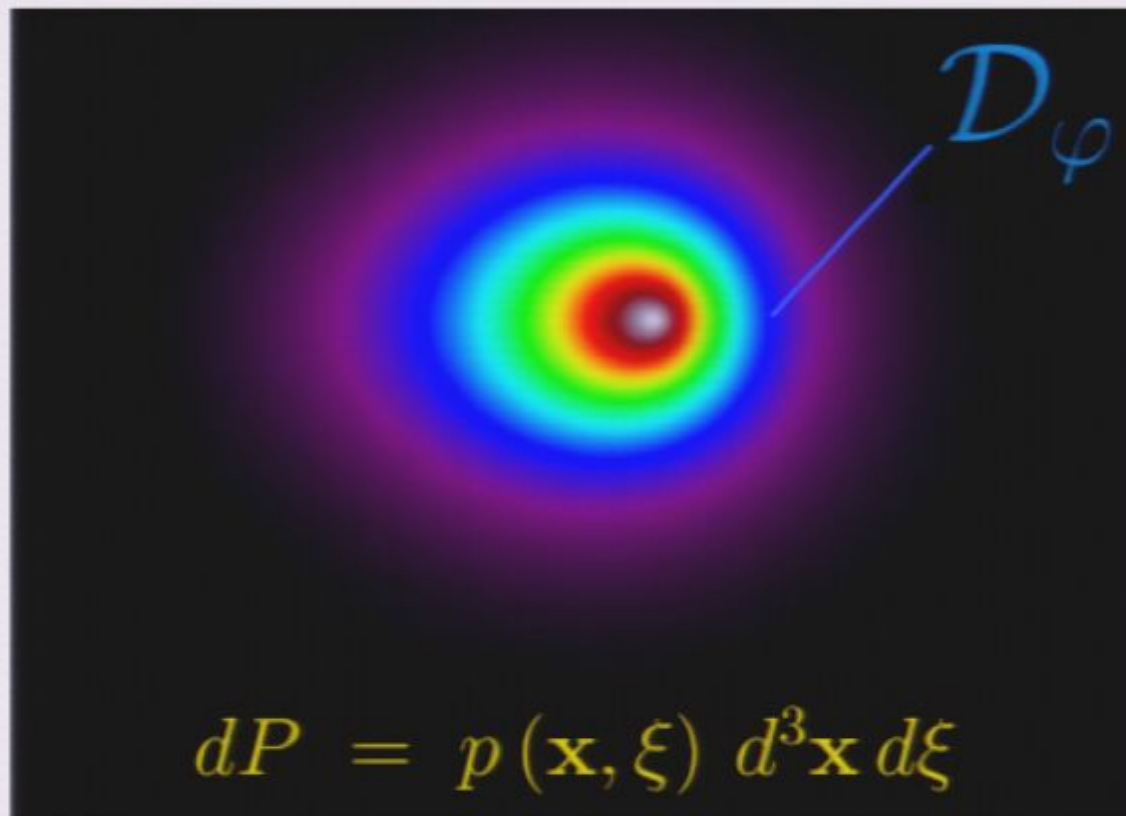
$$\frac{\sigma_r^2}{\langle \phi_r \rangle^2} = \frac{1}{N_H} \left\{ \frac{\langle \xi^2 G^2 \rangle}{\langle \xi G \rangle^2} - 1 \right\}$$

(iii) The set of the random distributions of one single clump inside the domain  $\mathcal{D}_H$  forms the statistical ensemble  $\mathcal{T}$  which we need to consider. An event from that ensemble consists in a clump characterized by the annihilation volume  $\xi$  up to  $d\xi$  and located at position  $\mathbf{x}$  within the elementary volume  $d^3\mathbf{x}$ .



$$\mathcal{P}(\varphi) d\varphi = dP = \int_{\mathcal{D}_{\varphi}} p(\mathbf{x}, \xi) d^3\mathbf{x} d\xi$$

$$\langle \mathcal{F} \rangle = \int \mathcal{F}(\varphi) \mathcal{P}(\varphi) d\varphi = \int_{\mathcal{D}_H} \mathcal{F}\{\varphi(\mathbf{x}, \xi)\} p(\mathbf{x}, \xi) d^3\mathbf{x} d\xi$$



(iv) This naturally leads to the effective boost factor

$$B_{\text{eff}} = \left\{ \frac{\phi'_s}{\phi_s} \simeq 1 \right\} + \frac{\langle \phi_r \rangle}{\phi_s} = 1 + N_H \frac{\langle \xi G \rangle}{\mathcal{I}}$$

and to the boost variance

$$\frac{\sigma_B}{B_{\text{eff}}} = \frac{\sigma_r / \phi_s}{1 + \langle \phi_r \rangle / \phi_s} \simeq \frac{\sigma_r}{\langle \phi_r \rangle}$$

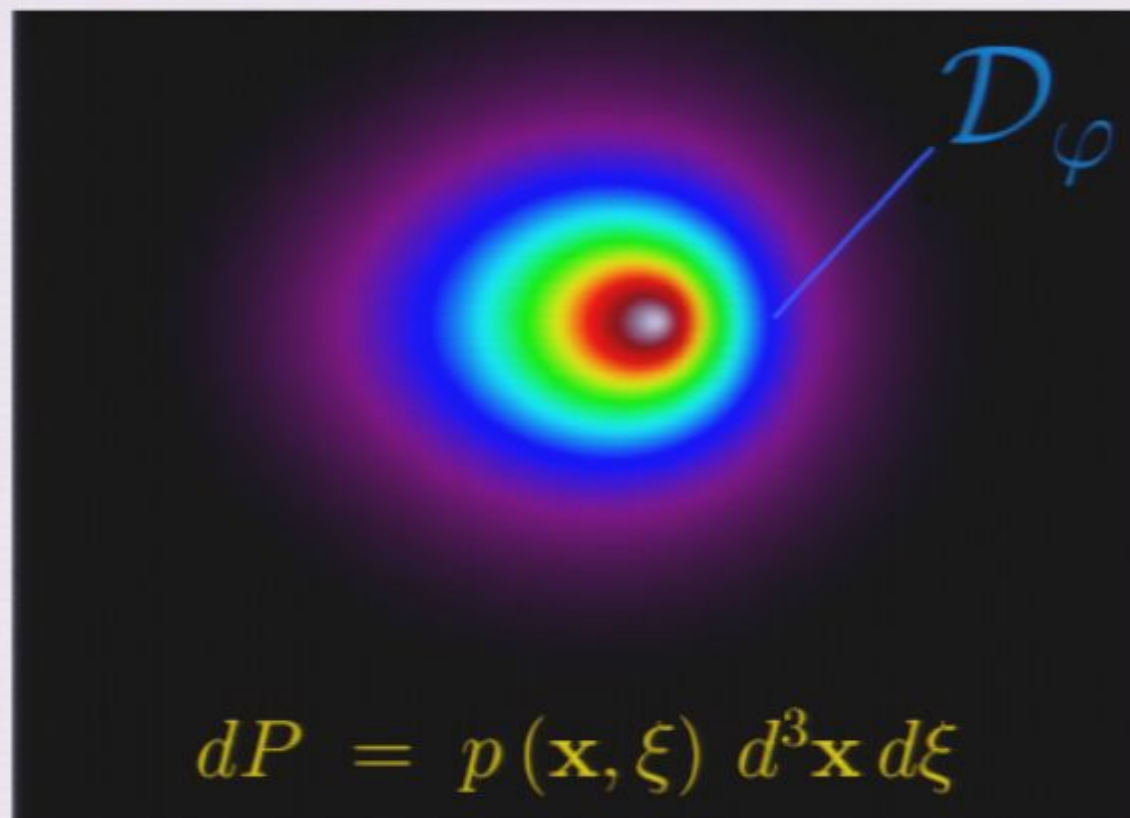
where

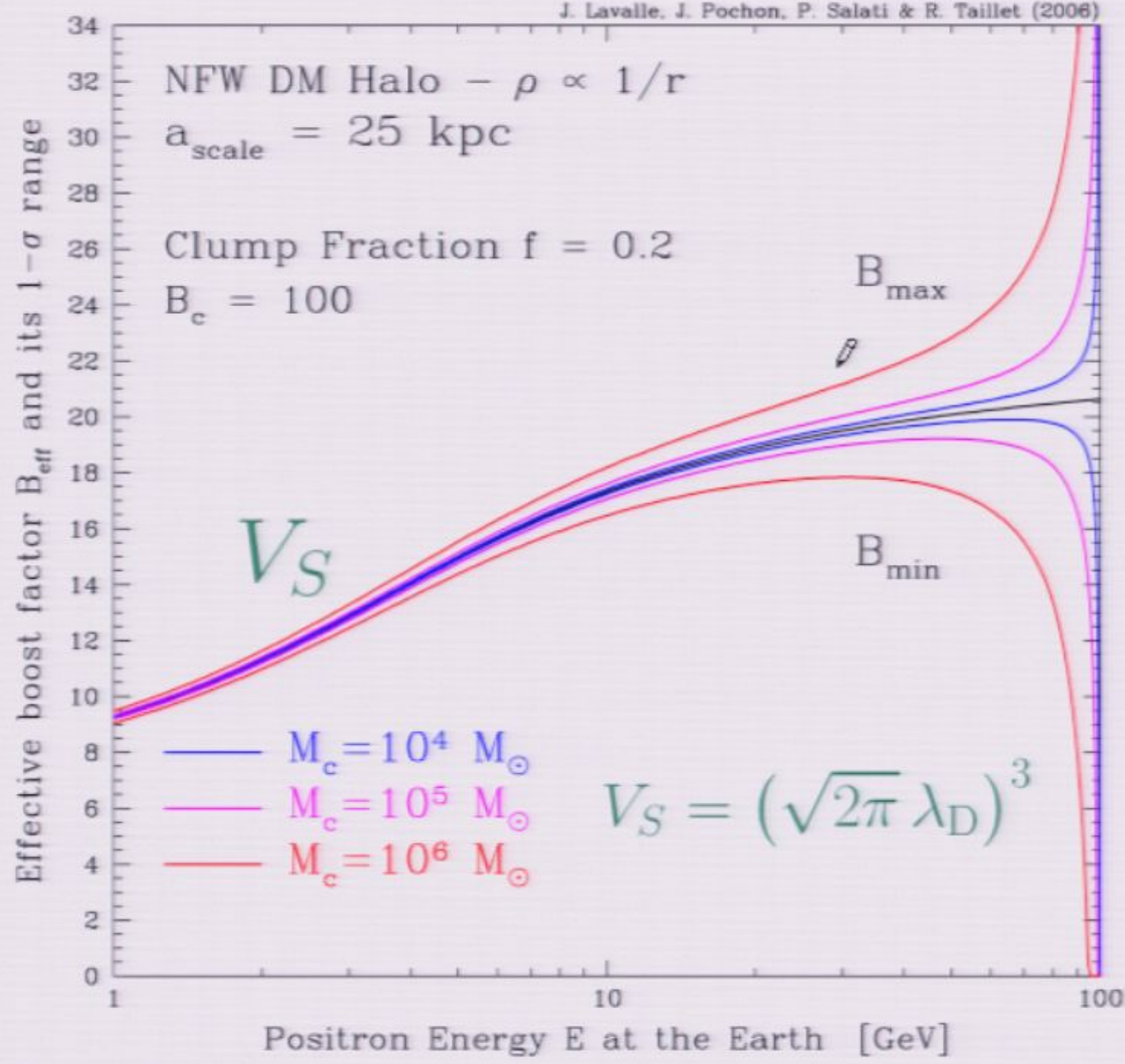
$$\frac{\sigma_r^2}{\langle \phi_r \rangle^2} = \frac{1}{N_H} \left\{ \frac{\langle \xi^2 G^2 \rangle}{\langle \xi G \rangle^2} - 1 \right\}$$

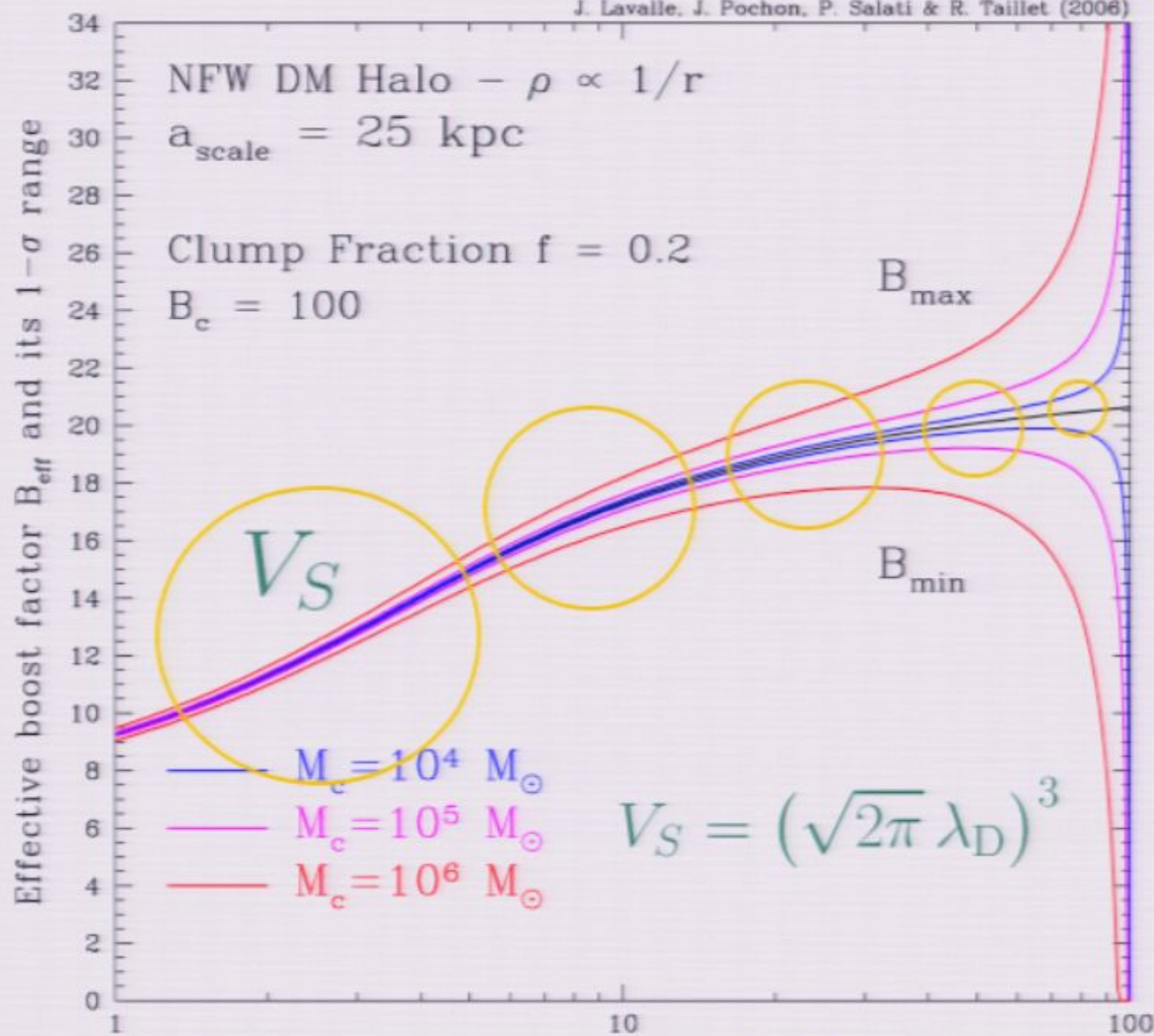
(iii) The set of the random distributions of one single clump inside the domain  $\mathcal{D}_H$  forms the statistical ensemble  $\mathcal{T}$  which we need to consider. An event from that ensemble consists in a clump characterized by the annihilation volume  $\xi$  up to  $d\xi$  and located at position  $\mathbf{x}$  within the elementary volume  $d^3\mathbf{x}$ .

$$\mathcal{P}(\varphi) d\varphi = dP = \int_{\mathcal{D}_{\varphi}} p(\mathbf{x}, \xi) d^3\mathbf{x} d\xi$$

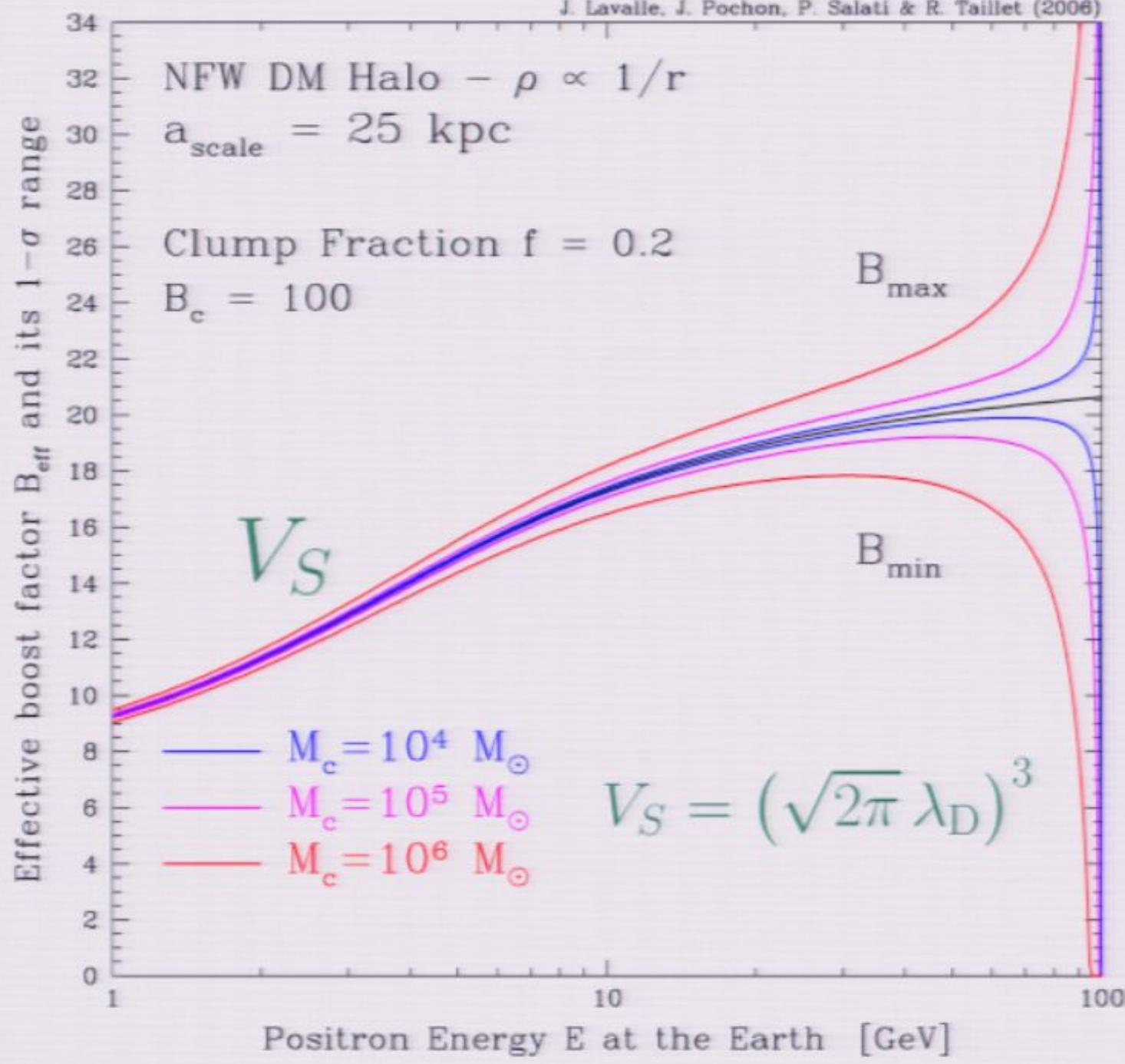
$$\langle \mathcal{F} \rangle = \int \mathcal{F}(\varphi) \mathcal{P}(\varphi) d\varphi = \int_{\mathcal{D}_H} \mathcal{F}\{\varphi(\mathbf{x}, \xi)\} p(\mathbf{x}, \xi) d^3\mathbf{x} d\xi$$

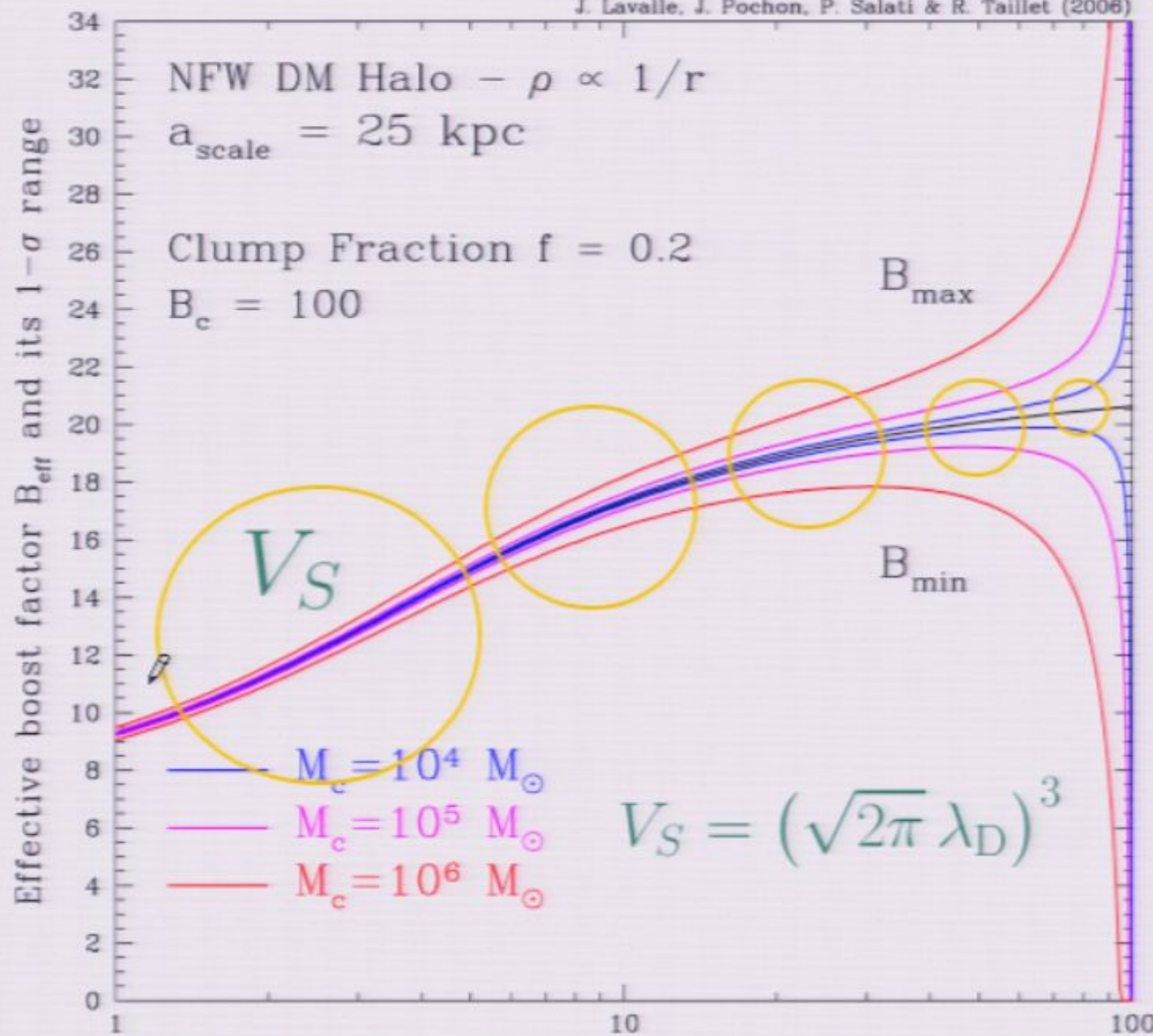






$V_S$  increases as  $E$  decreases





$V_S$  increases as  $E$  decreases

# Recipe for a statistical analysis

- Without clumps – with the smooth DM distribution  $\rho_s$

$$\phi_s = \left\{ \mathcal{S} \equiv \frac{\beta \delta}{4\pi} \langle \sigma_{\text{ann}} v \rangle \frac{\rho_\odot^2}{m_\chi^2} \frac{dN}{dE} \right\} \times \left\{ \mathcal{I} \equiv \int_{\text{DZ}} G(\mathbf{x}) \frac{\rho_s^2(\mathbf{x})}{\rho_\odot^2} d^3\mathbf{x} \right\}$$

- With clumps – with the DM distribution  $\rho = \rho'_s + \delta\rho$

$$\phi = \{\phi'_s \simeq \phi_s\} + \left\{ \phi_r = \sum_i \varphi_i \right\}$$
$$\varphi_i = \mathcal{S} \times G(\mathbf{x}_i) \times \left\{ \xi_i = \frac{B_i M_i}{\rho_\odot} = \int_{\text{ith clump}} \frac{\delta\rho^2(\mathbf{x})}{\rho_\odot^2} d^3\mathbf{x} \right\}$$

random behaviour !



$$\text{Boost factor } B \equiv \frac{\phi}{\phi_s}$$

# Recipe for a statistical analysis

- Without clumps – with the smooth DM distribution  $\rho_s$

$$\phi_s = \left\{ \mathcal{S} \equiv \frac{\beta \delta}{4\pi} \langle \sigma_{\text{ann}} v \rangle \frac{\rho_\odot^2}{m_\chi^2} \frac{dN}{dE} \right\} \times \left\{ \mathcal{I} \equiv \int_{\text{DZ}} G(\mathbf{x}) \frac{\rho_s^2(\mathbf{x})}{\rho_\odot^2} d^3\mathbf{x} \right\}$$

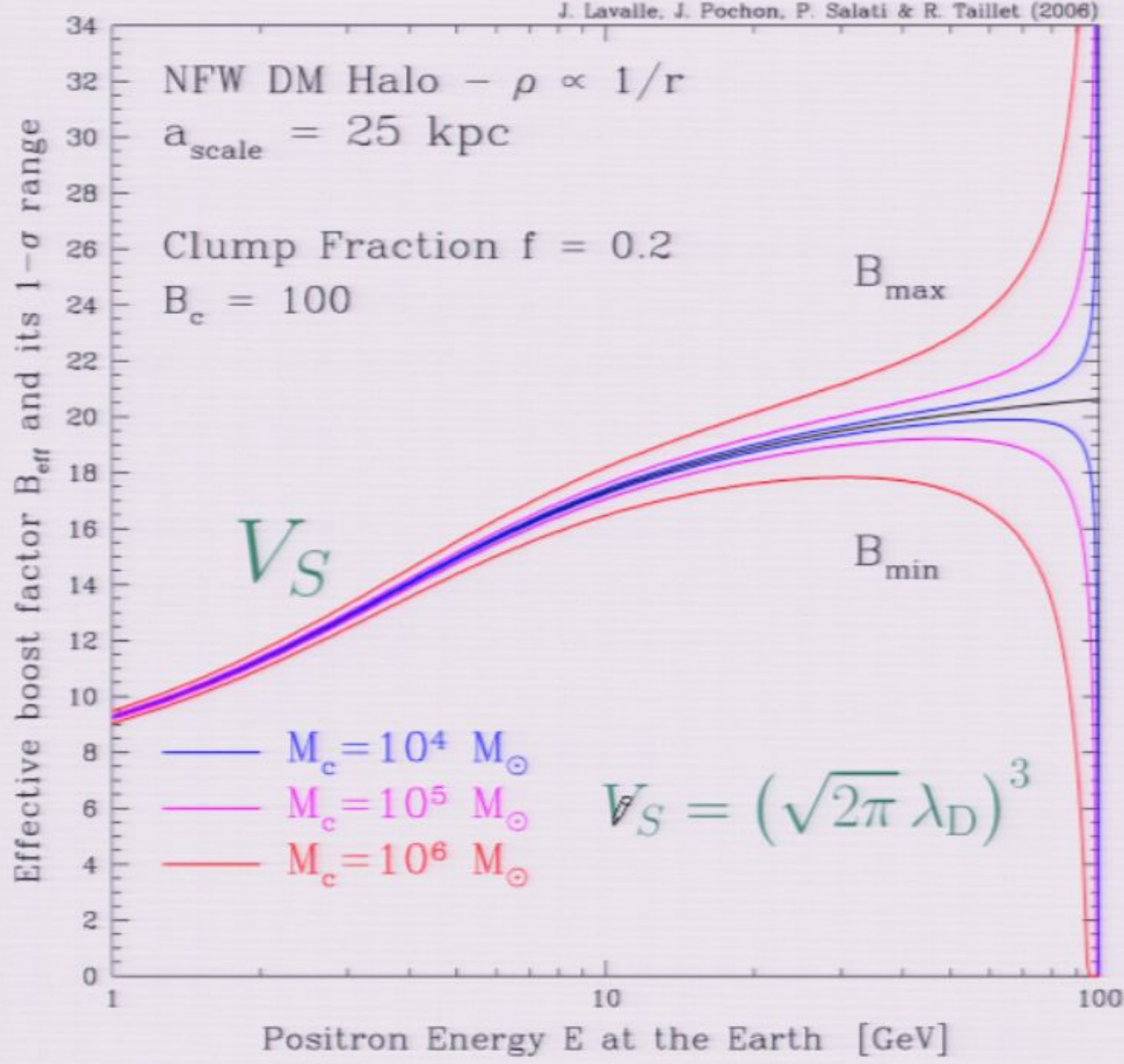
- With clumps – with the DM distribution  $\rho = \rho'_s + \delta\rho$

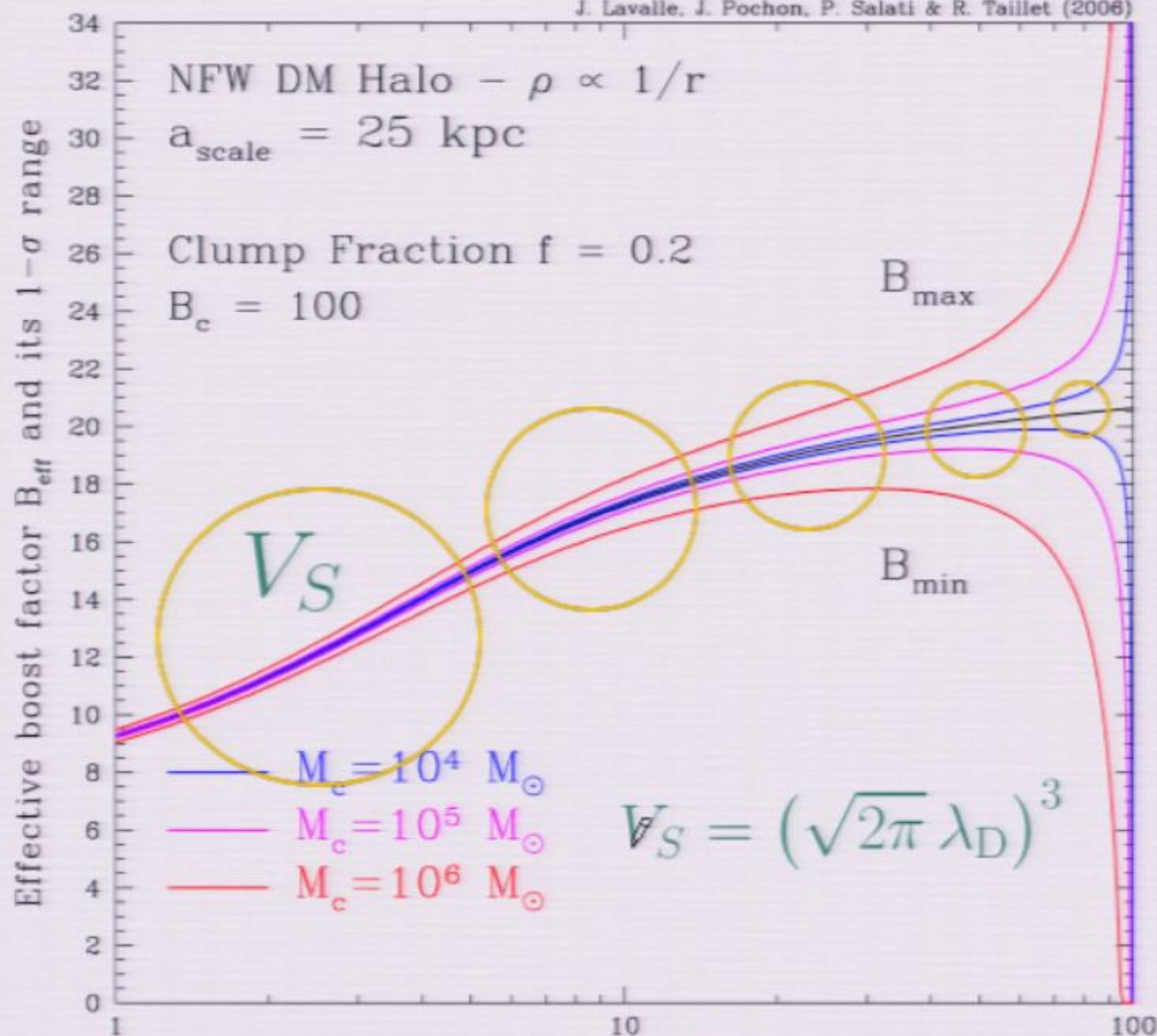
$$\phi = \{\phi'_s \simeq \phi_s\} + \left\{ \phi_r = \sum_i \varphi_i \right\}$$

$$\varphi_i = \mathcal{S} \times G(\mathbf{x}_i) \times \left\{ \xi_i = \frac{B_i M_i}{\rho_\odot} = \int_{\text{ith clump}} \frac{\delta\rho^2(\mathbf{x})}{\rho_\odot^2} d^3\mathbf{x} \right\}$$



$$\text{Boost factor } B \equiv \frac{\phi}{\phi_s}$$





$V_S$  increases as  $E$  decreases

# Full Calculation of Clumpiness Boost factors for Antimatter Cosmic Rays in the light of $\Lambda$ CDM N-body simulation results

## Abandoning hope in clumpiness enhancement?

J. Lavalle<sup>1</sup>, Q. Yuan<sup>2</sup>, D. Maurin<sup>3</sup>, and X.-J. Bi<sup>2</sup>

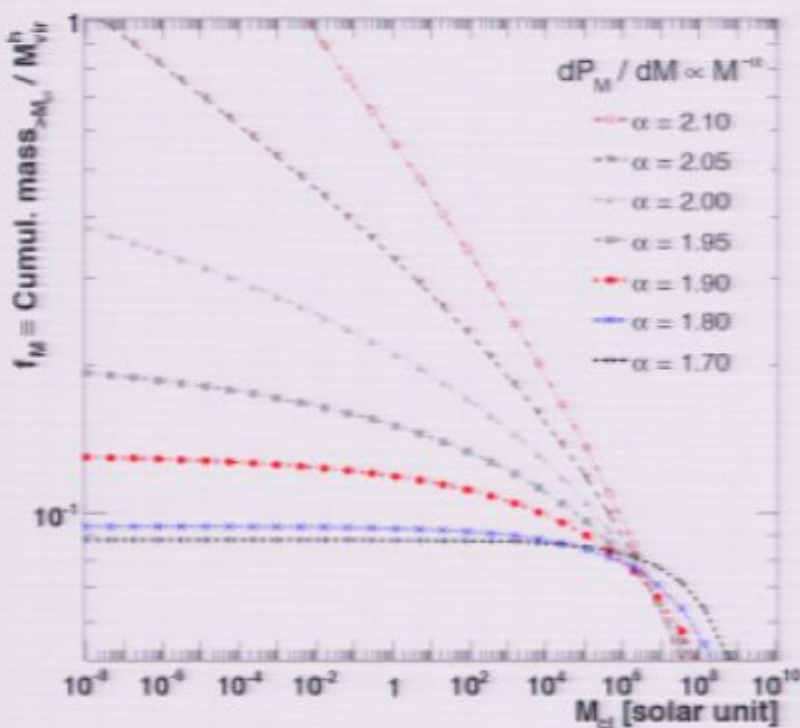


**Fig. 1.** The mass fraction  $f_M$  of DM in clumps is set once  $M_{\text{min}}$  and  $\alpha_m$  are chosen. This fraction can be directly read off the graph for various  $\alpha_m$  (from 2.1 down to 1.7—top to bottom curves) and various  $M_{\text{min}}$  (from  $10^8 M_\odot$  down to  $10^{-8} M_\odot$ , x-axis).

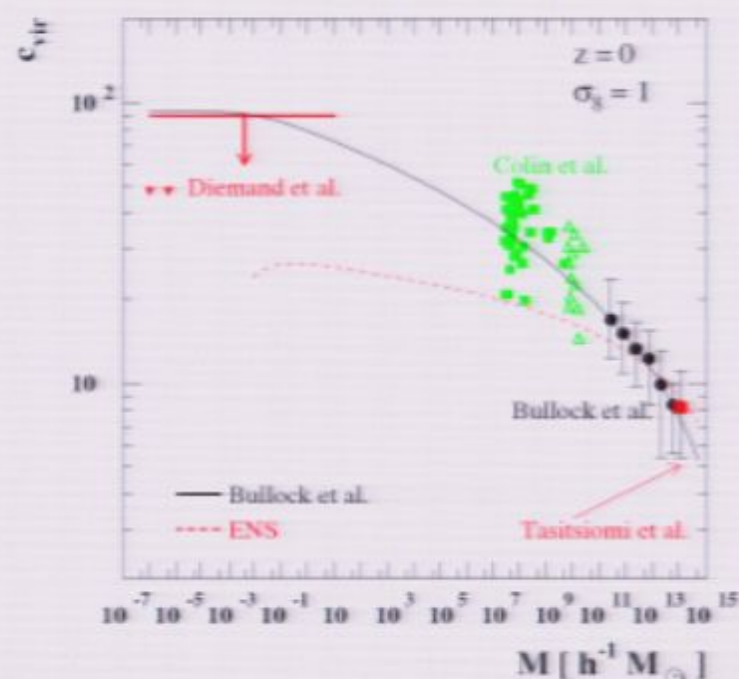


**Fig. 1.** The dependence of  $c_{\text{vir}}$  on the halo mass  $M$ , at  $z = 0$ , as in the Bullock et al. toy model (solid line) and in the ENS toy model (dashed line); predictions are compared to a few sets of simulation results in different mass ranges. A flat, vacuum-dominated cosmology with  $\Omega_M = 0.3$ ,  $\Omega_\Lambda = 0.7$ ,  $h = 0.7$  and  $\sigma_8 = 1$  is assumed here.

Clump description	Values
$dP_V(r)/dV$	Cored <sup>†</sup> or NFW
Inner profile	NFW <sup>†</sup> or Moore
$\alpha_m$	[1.8 – 1.9 <sup>‡</sup> – 2.0]
$M_{\min}$	$[10^{-6} \text{ } ^{\dagger} - 1 - 10^6] M_{\odot}$
$c_{\text{vir}} - M_{\text{vir}}$	B01 <sup>‡</sup> or ENS01

<sup>†</sup> Reference configuration.

**Table 2.** Description of the various configurations used in the paper for the sub-halo parameters.

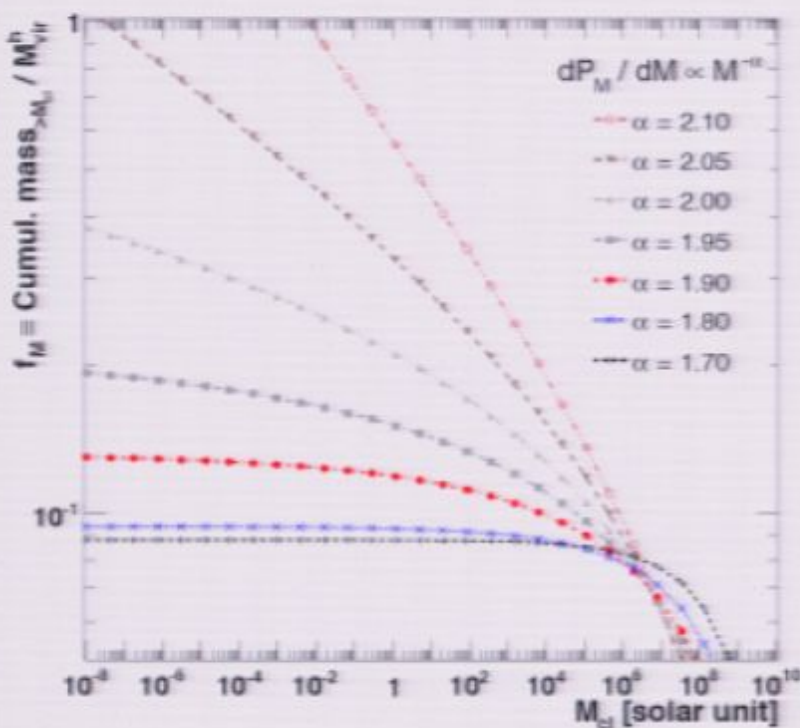


**Fig. 1.** The mass fraction  $f_M$  of DM in clumps is set once  $M_{\min}$  and  $\alpha_m$  are chosen. This fraction can be directly read off the graph for various  $\alpha_m$  (from 2.1 down to 1.7—top to bottom curves) and various  $M_{\min}$  (from  $10^8 M_{\odot}$  down to  $10^{-8} M_{\odot}$ , x-axis).

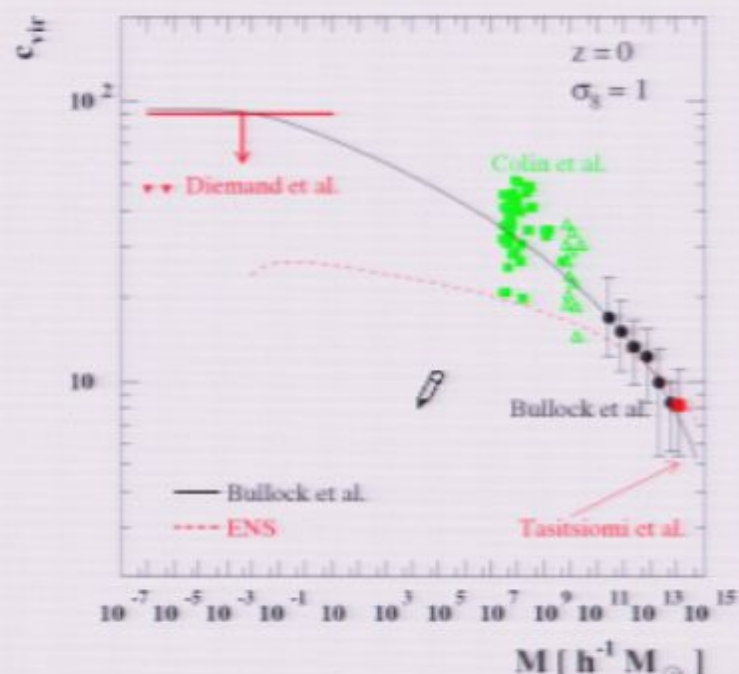


**Fig. 1.** The dependence of  $c_{\text{vir}}$  on the halo mass  $M$ , at  $z = 0$ , as in the Bullock et al. toy model (solid line) and in the ENS toy model (dashed line); predictions are compared to a few sets of simulation results in different mass ranges. A flat, vacuum-dominated cosmology with  $\Omega_M = 0.3$ ,  $\Omega_\Lambda = 0.7$ ,  $h = 0.7$  and  $\sigma_8 = 1$  is assumed here.

# $B_{\text{Milky Way}} \leq 20$ in $\Lambda\text{CDM}$

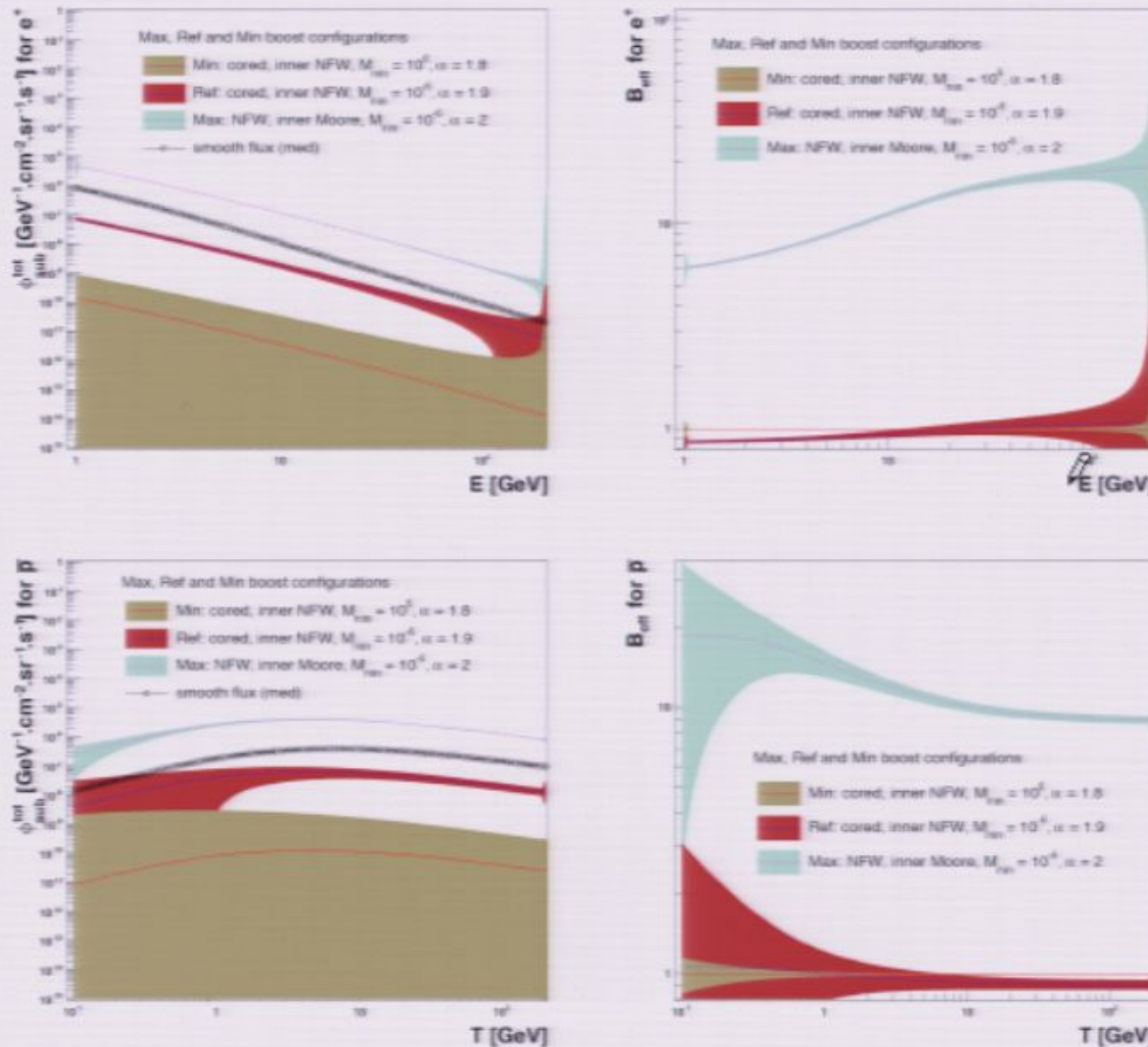


Fig. 6. Extreme cases for the DM configurations: sub-halo antimatter fluxes associated with the maximal, reference and minimal DM configurations (medium set of propagation parameters). Left/right: fluxes/boosts and corresponding 1- $\sigma$  contours. Top/bottom: no-neutrinos/anti-neutrinos. See details in the text.

# The cosmic ray lepton puzzle in the light of cosmological N-body simulations

P. Brun, T. Delahaye, J. Diemand, S. Profumo & P. Salati, arXiv:0904.0812

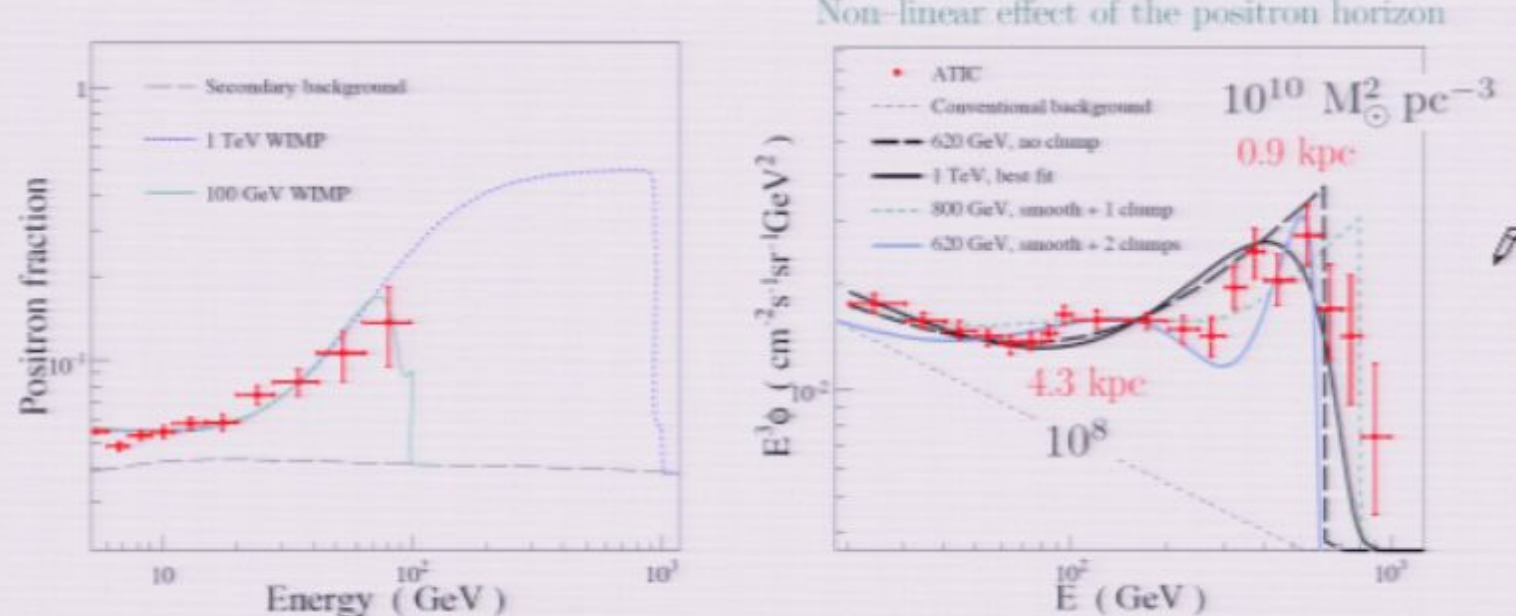


FIG. 1: Best fits to the PAMELA data in the case of a positronic line (see the  $e^+/e^-$  row of Tab. I) (left panel) and fits to the ATIC data (right panel).

	PAMELA		ATIC
$m_\chi$ (GeV)	100	1 000	1 000
$e^+/e^-$	(1.22; $1.07 \cdot 10^7$ )	(0.78; $3.56 \cdot 10^9$ )	(1.64; $4.81 \cdot 10^9$ )
$e^\pm + \mu^\pm + \tau^\pm$	(0.44; $2.51 \cdot 10^7$ )	(0.27; $9.84 \cdot 10^9$ )	(1.45; $9.44 \cdot 10^9$ )

TABLE I: Best fit values of the ( $D; L$ ) couple in units of ( $\text{kpc}; M_\odot^2 \text{pc}^{-3}$ ) for various DM particle masses and annihilation channels.

# The cosmic ray lepton puzzle in the light of cosmological N-body simulations

P. Brun, T. Delahaye, J. Diemand, S. Profumo & P. Salati, arXiv:0904.0812

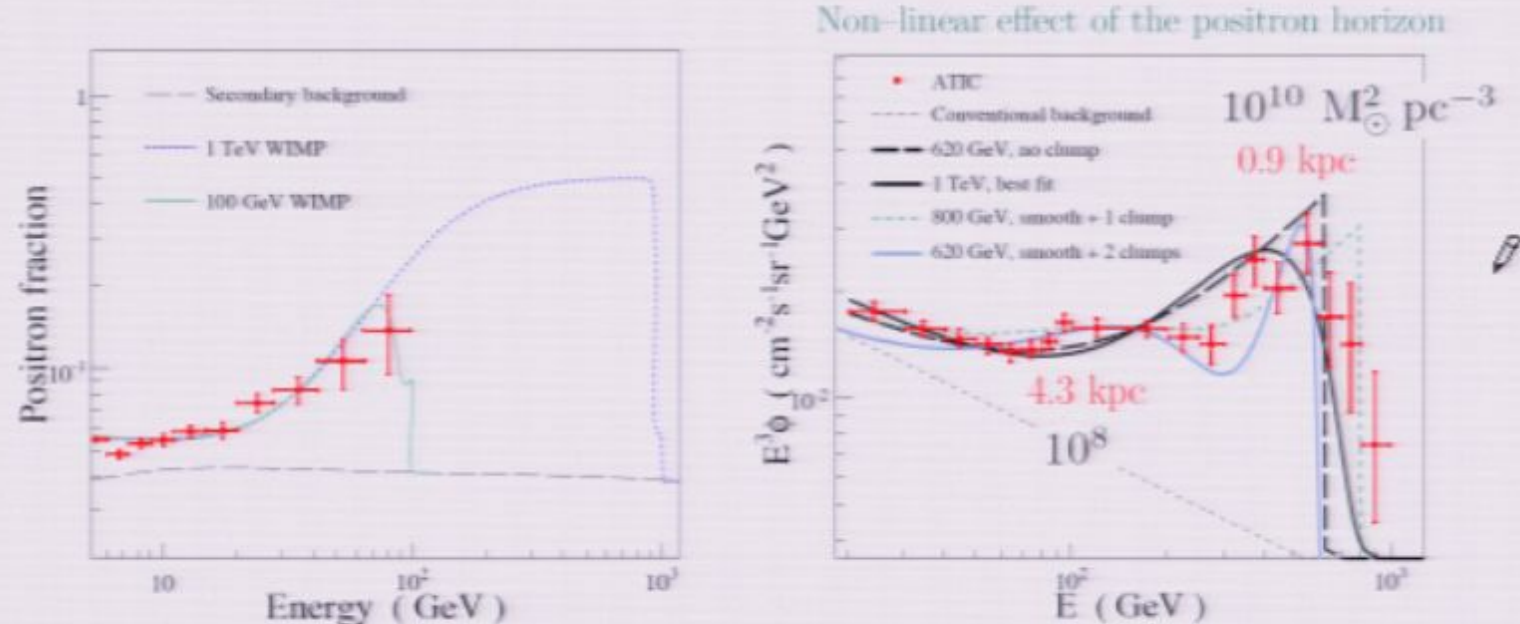


FIG. 1: Best fits to the PAMELA data in the case of a positronic line (see the  $e^+/e^-$  row of Tab. I) (left panel) and fits to the ATIC data (right panel).

	PAMELA		ATIC
$m_\chi$ (GeV)	100	1 000	1 000
$e^+/e^-$	(1.22; $1.07 \cdot 10^7$ )	(0.78; $3.56 \cdot 10^9$ )	(1.64; $4.81 \cdot 10^9$ )
$e^\pm + \mu^\pm + \tau^\pm$	(0.44; $2.51 \cdot 10^7$ )	(0.27; $9.84 \cdot 10^9$ )	(1.45; $9.44 \cdot 10^9$ )

TABLE I: Best fit values of the ( $D; L$ ) couple in units of (kpc;  $M_\odot^2 pc^{-3}$ ) for various DM particle masses and annihilation channels.

# $B_{\text{Milky Way}} \leq 20$ in $\Lambda\text{CDM}$

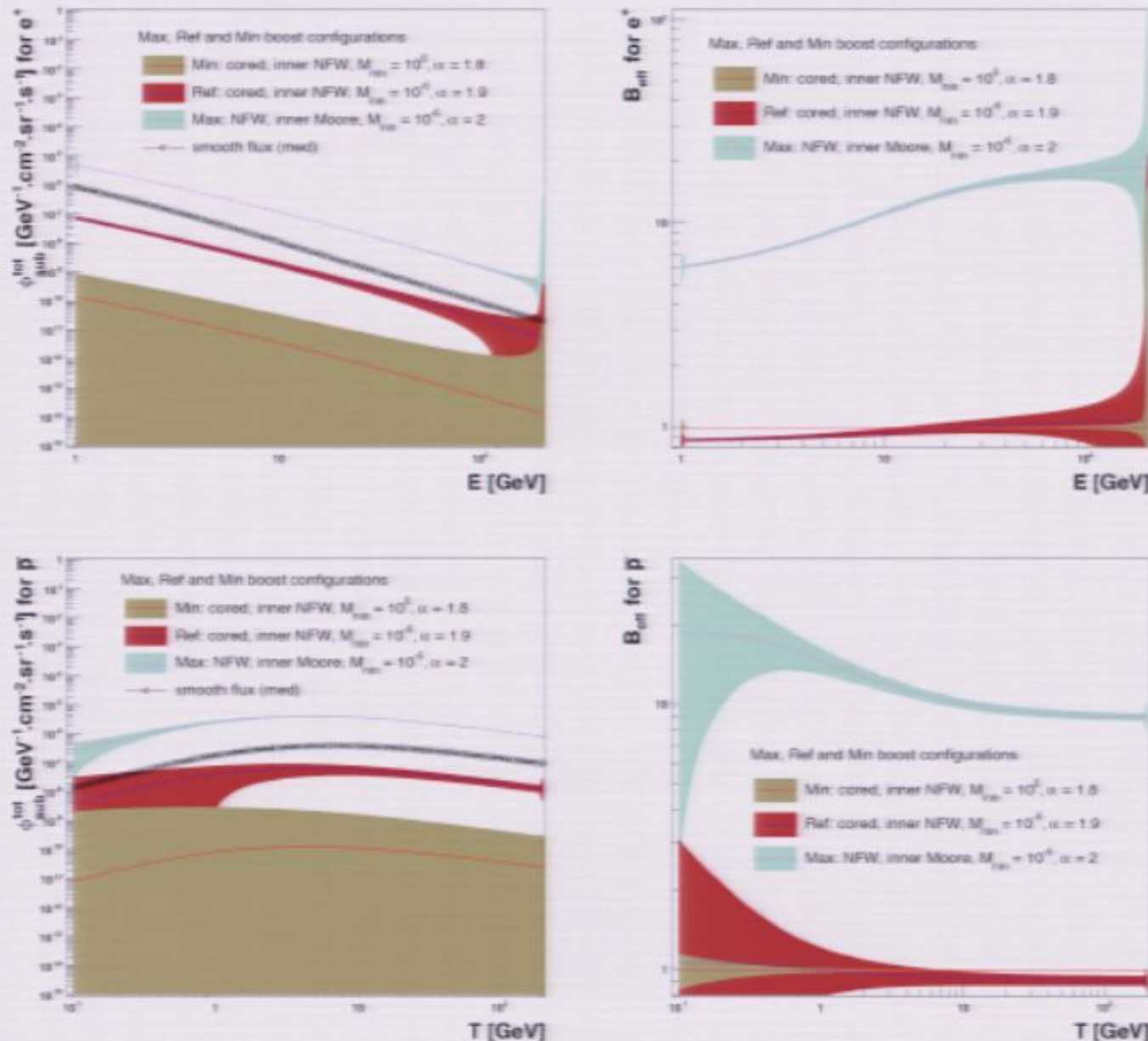


Fig. 6. Extreme cases for the DM configurations: sub-halo antimatter fluxes associated with the maximal, reference and minimal DM configurations (medium set of propagation parameters). Left/right: fluxes/boosts and corresponding  $1-\sigma$  contours. Top/bottom: positrons/anti-protons. See details in the text.

# The cosmic ray lepton puzzle in the light of cosmological N-body simulations

P. Brun, T. Delahaye, J. Diemand, S. Profumo & P. Salati, arXiv:0904.0812

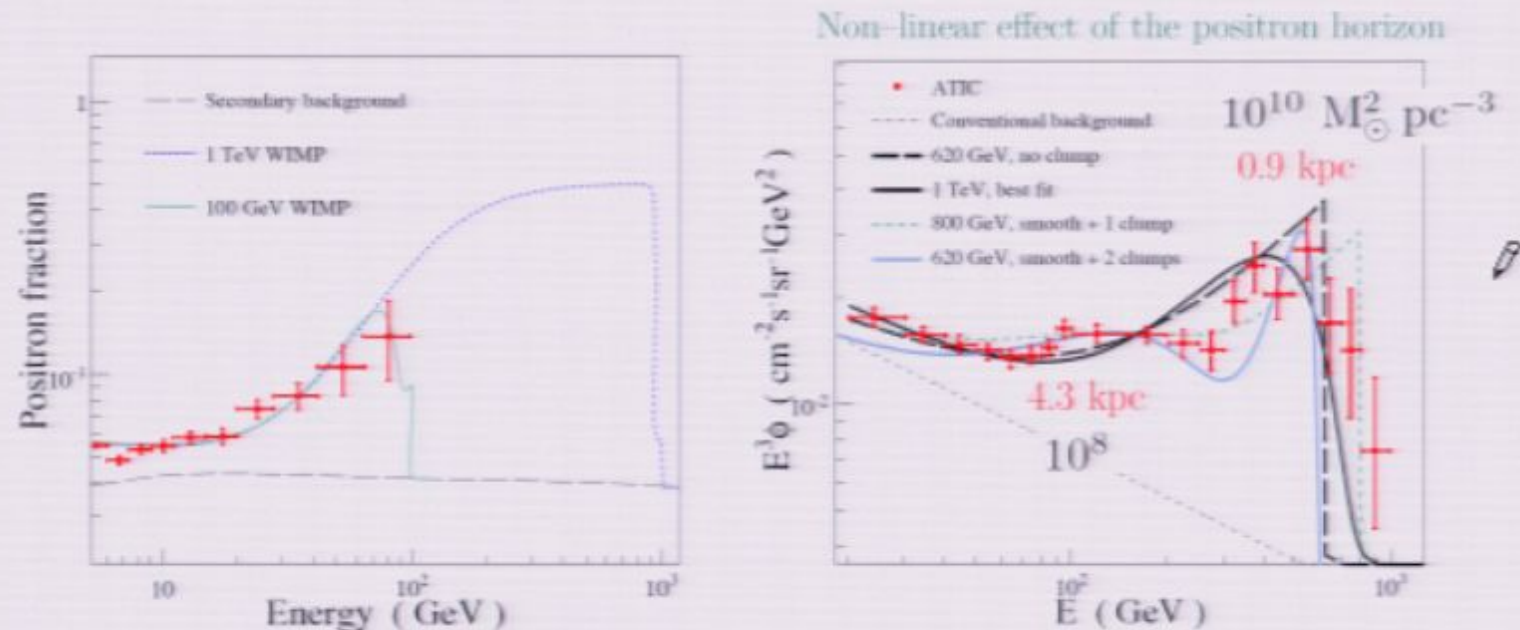


FIG. 1: Best fits to the PAMELA data in the case of a positronic line (see the  $e^+/e^-$  row of Tab. I) (left panel) and fits to the ATIC data (right panel).

	PAMELA		ATIC
$m_\chi$ (GeV)	100	1 000	1 000
$e^+/e^-$	(1.22; $1.07 \cdot 10^7$ )	(0.78; $3.56 \cdot 10^9$ )	(1.64; $4.81 \cdot 10^9$ )
$e^\pm + \mu^\pm + \tau^\pm$	(0.44; $2.51 \cdot 10^7$ )	(0.27; $9.84 \cdot 10^9$ )	(1.45; $9.44 \cdot 10^9$ )

TABLE I: Best fit values of the ( $D; L$ ) couple in units of (kpc;  $M_\odot^2 pc^{-3}$ ) for various DM particle masses and annihilation channels.

# $B_{\text{Milky Way}} \leq 20$ in $\Lambda\text{CDM}$

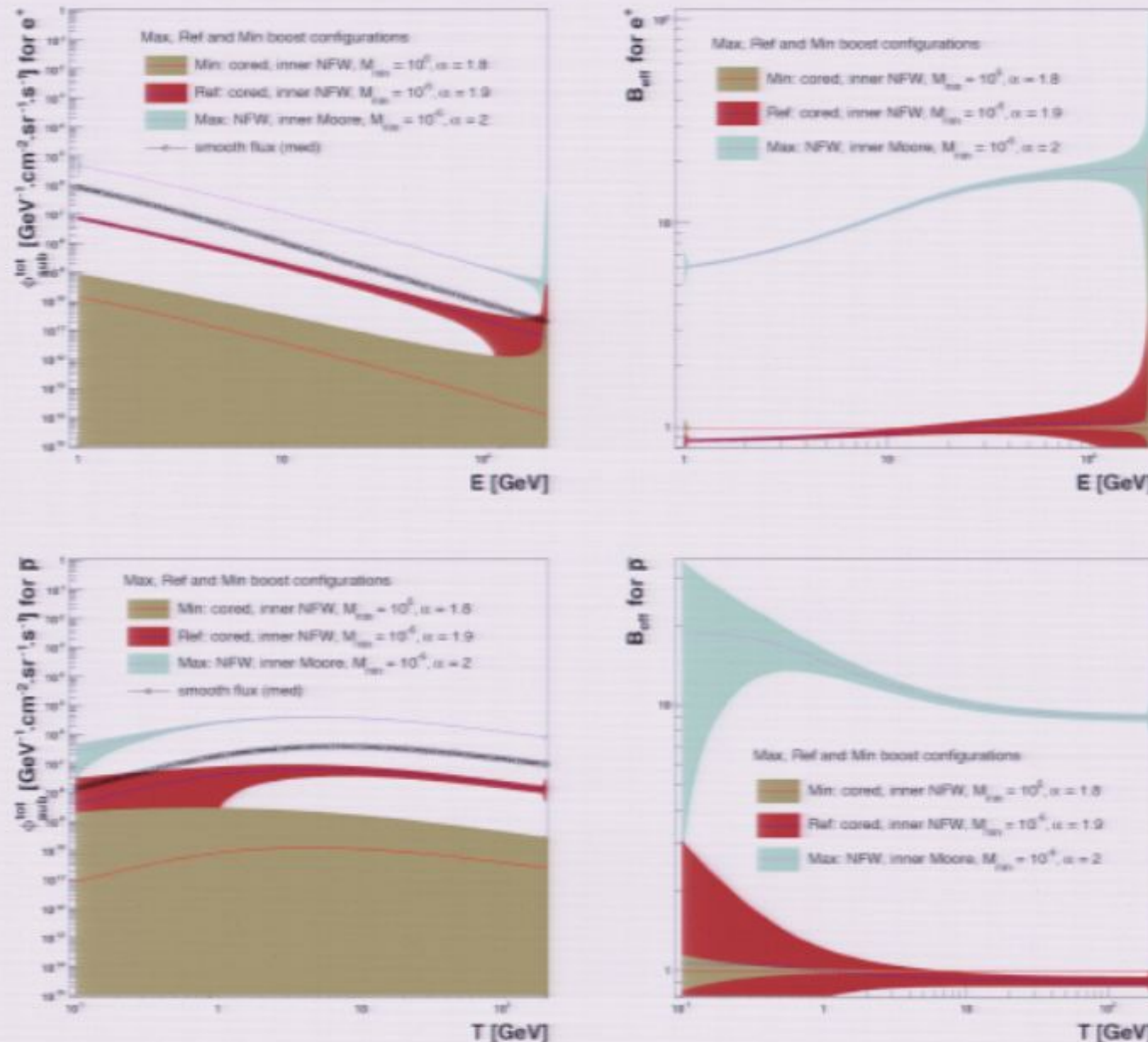


Fig. 6. Extreme cases for the DM configurations: sub-halo antimatter fluxes associated with the maximal, reference and minimal DM configurations (medium set of propagation parameters). Left/right: fluxes/boosts and corresponding 1- $\sigma$  contours. Top/bottom: positrons/anti-neutrinos. See details in the text.

# The cosmic ray lepton puzzle in the light of cosmological N-body simulations

P. Brun, T. Delahaye, J. Diemand, S. Profumo & P. Salati, arXiv:0904.0812

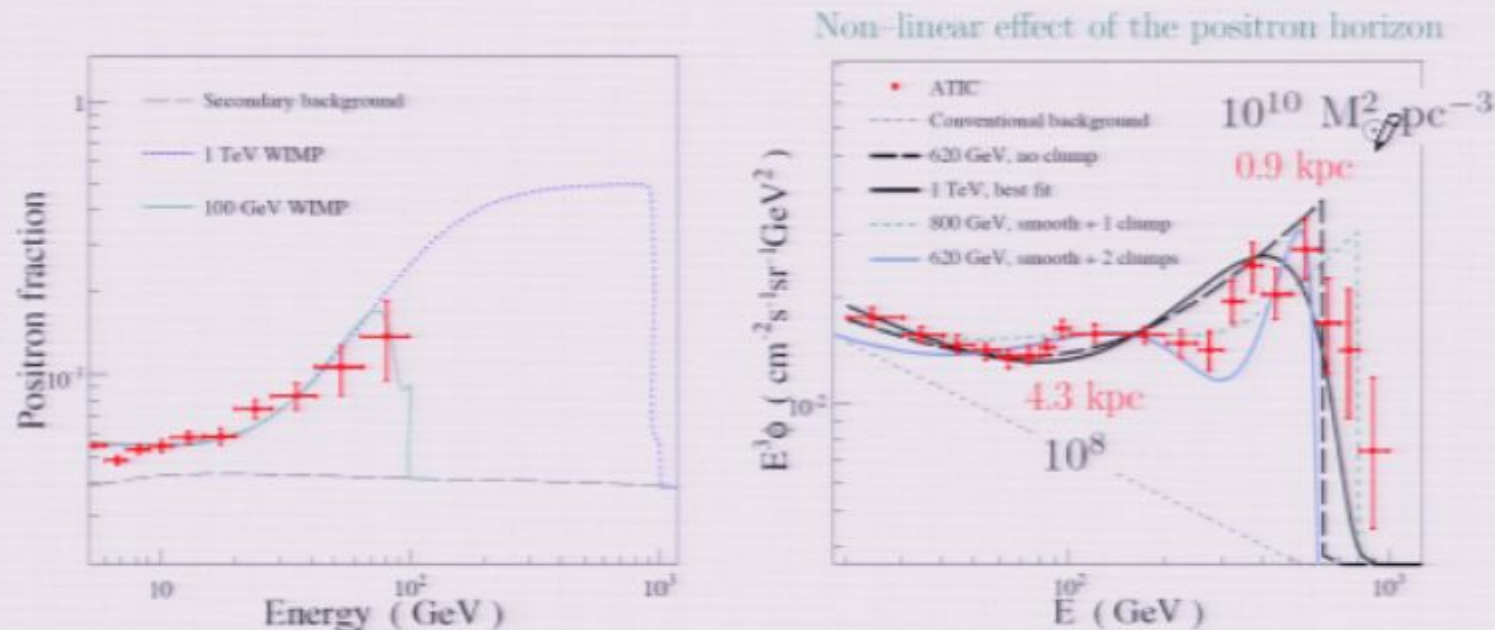


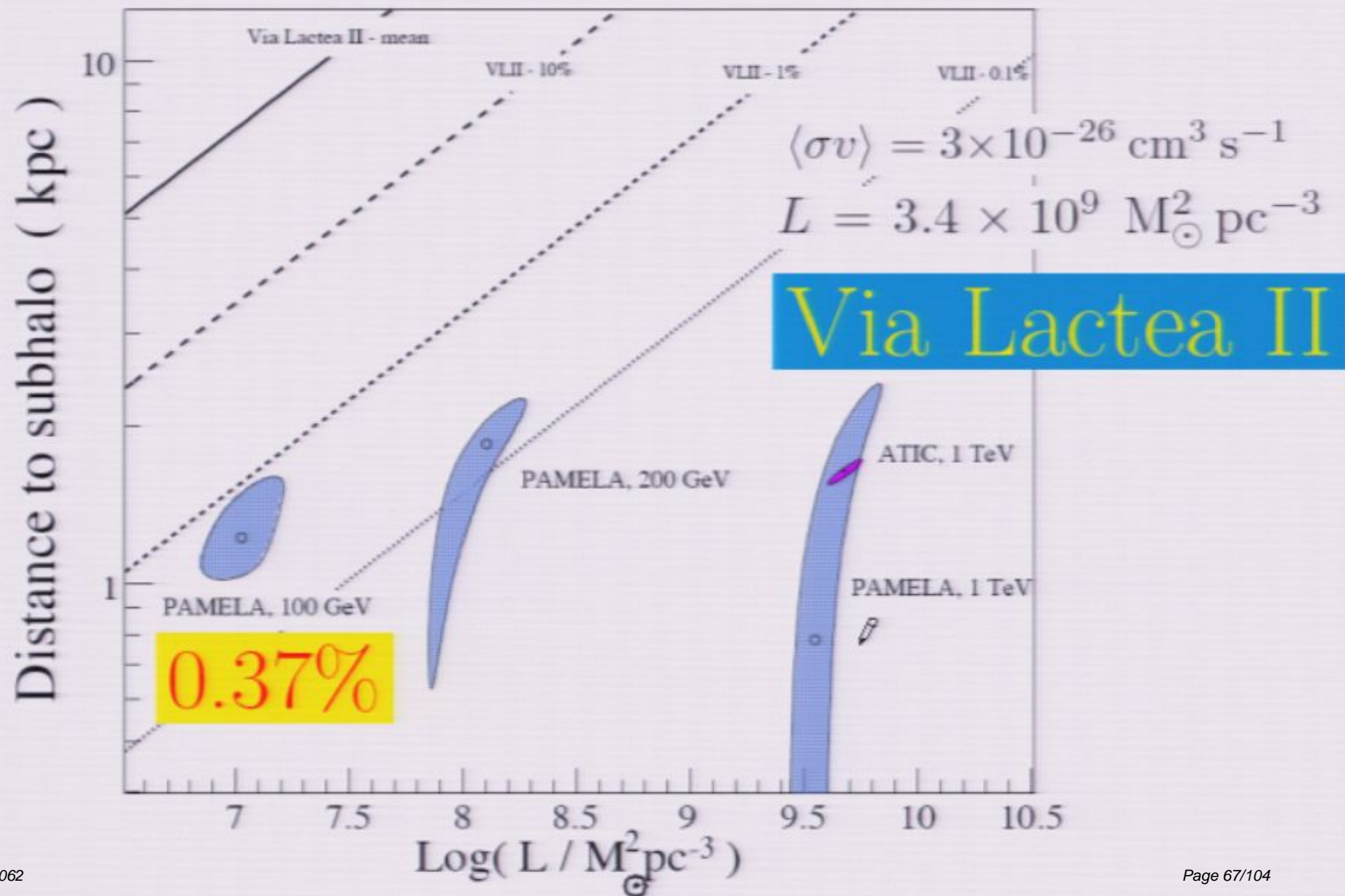
FIG. 1: Best fits to the PAMELA data in the case of a positronic line (see the  $e^+/e^-$  row of Tab. I) (left panel) and fits to the ATIC data (right panel).

	PAMELA		ATIC
$m_\chi$ (GeV)	100	1 000	1 000
$e^+/e^-$	(1.22; $1.07 \cdot 10^7$ )	(0.78; $3.56 \cdot 10^9$ )	(1.64; $4.81 \cdot 10^9$ )
$e^\pm + \mu^\pm + \tau^\pm$	(0.44; $2.51 \cdot 10^7$ )	(0.27; $9.84 \cdot 10^9$ )	(1.45; $9.44 \cdot 10^9$ )

TABLE I: Best fit values of the ( $D; L$ ) couple in units of (kpc;  $M_\odot^2 pc^{-3}$ ) for various DM particle masses and annihilation channels.

# The cosmic ray lepton puzzle in the light of cosmological N-body simulations

P. Brun, T. Delahaye, J. Diemand, S. Profumo & P. Salati, arXiv:0904.0812



# The cosmic ray lepton puzzle in the light of cosmological N-body simulations

P. Brun, T. Delahaye, J. Diemand, S. Profumo & P. Salati, arXiv:0904.0812

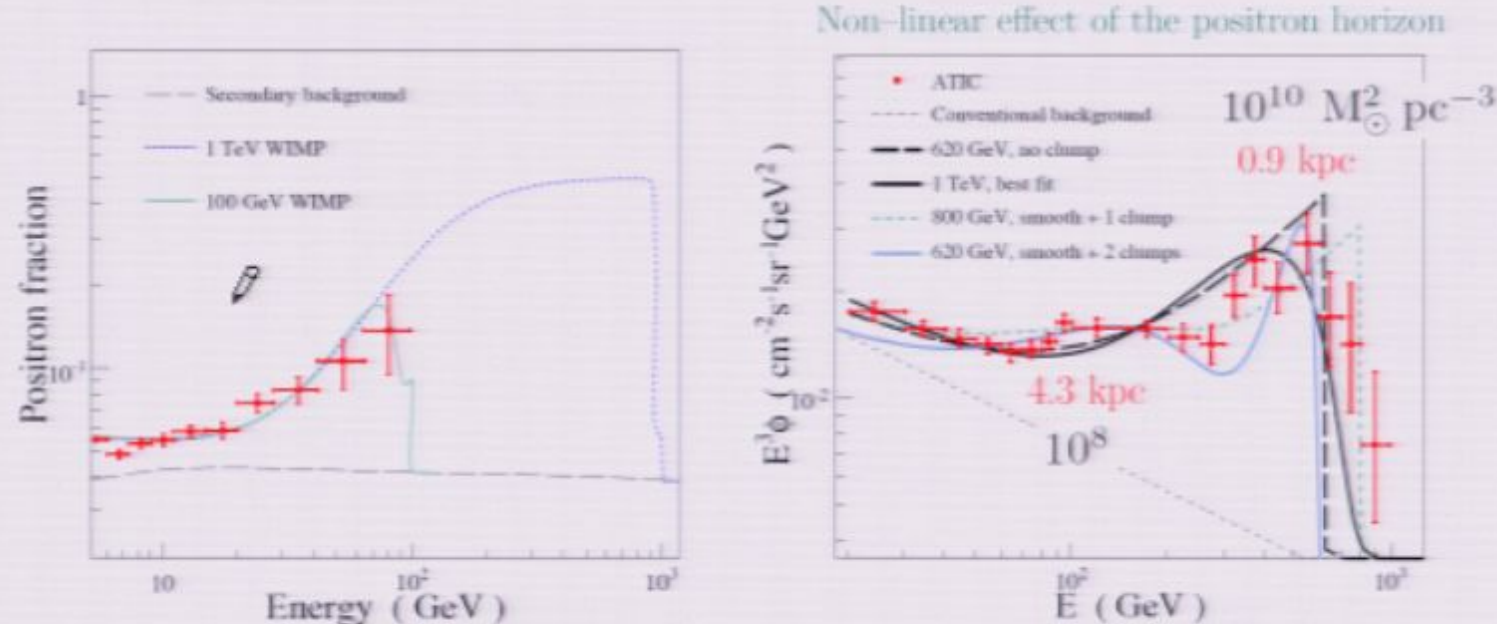


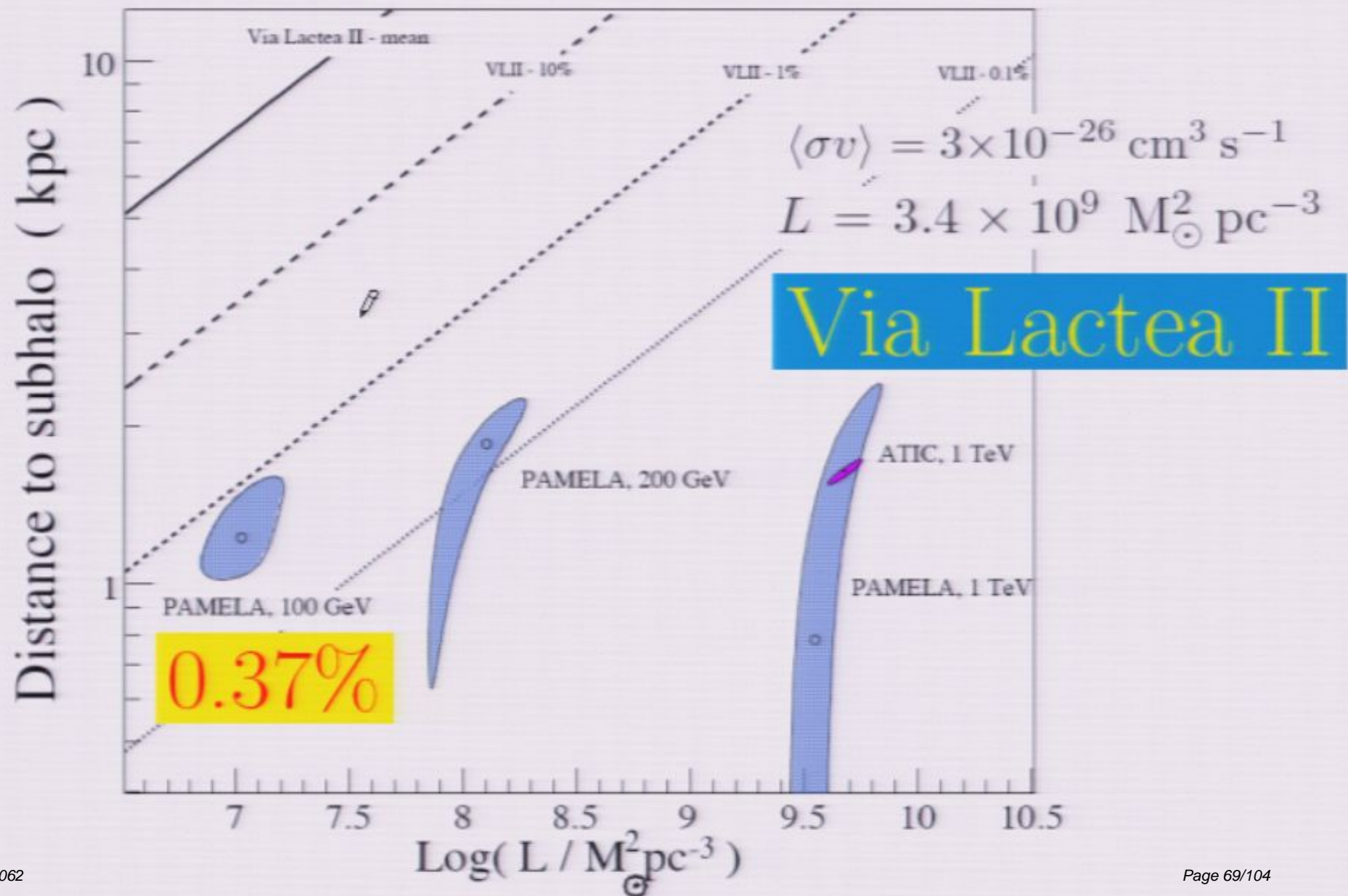
FIG. 1: Best fits to the PAMELA data in the case of a positronic line (see the  $e^+/e^-$  row of Tab. I) (left panel) and fits to the ATIC data (right panel).

	PAMELA		ATIC
$m_\chi$ (GeV)	100	1 000	1 000
$e^+/e^-$	(1.22; $1.07 \cdot 10^7$ )	(0.78; $3.56 \cdot 10^9$ )	(1.64; $4.81 \cdot 10^9$ )
$e^\pm + \mu^\pm + \tau^\pm$	(0.44; $2.51 \cdot 10^7$ )	(0.27; $9.84 \cdot 10^9$ )	(1.45; $9.44 \cdot 10^9$ )

TABLE I: Best fit values of the ( $D; L$ ) couple in units of (kpc;  $M_\odot^2 \text{ pc}^{-3}$ ) for various DM particle masses and annihilation channels.

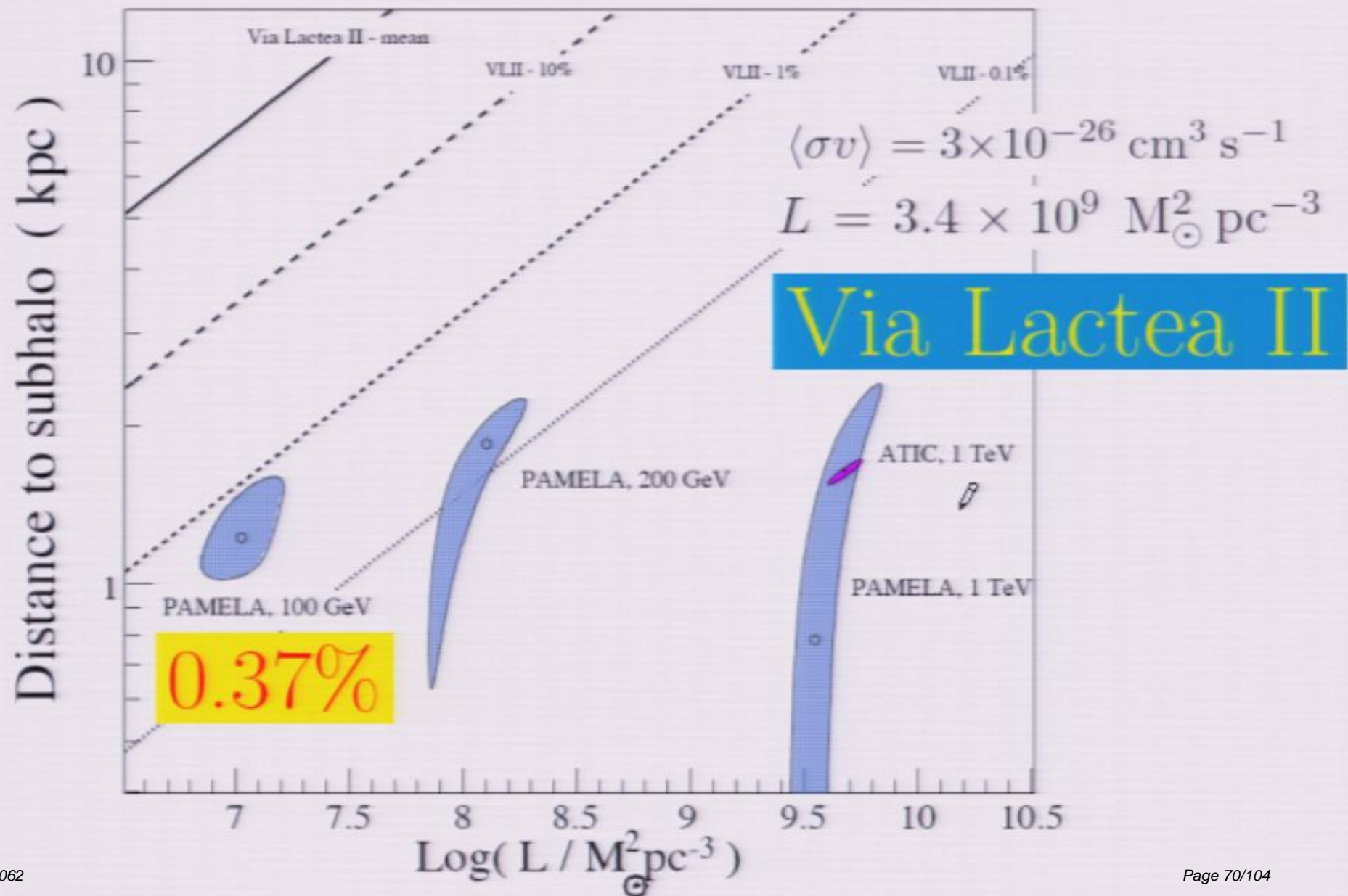
# The cosmic ray lepton puzzle in the light of cosmological N-body simulations

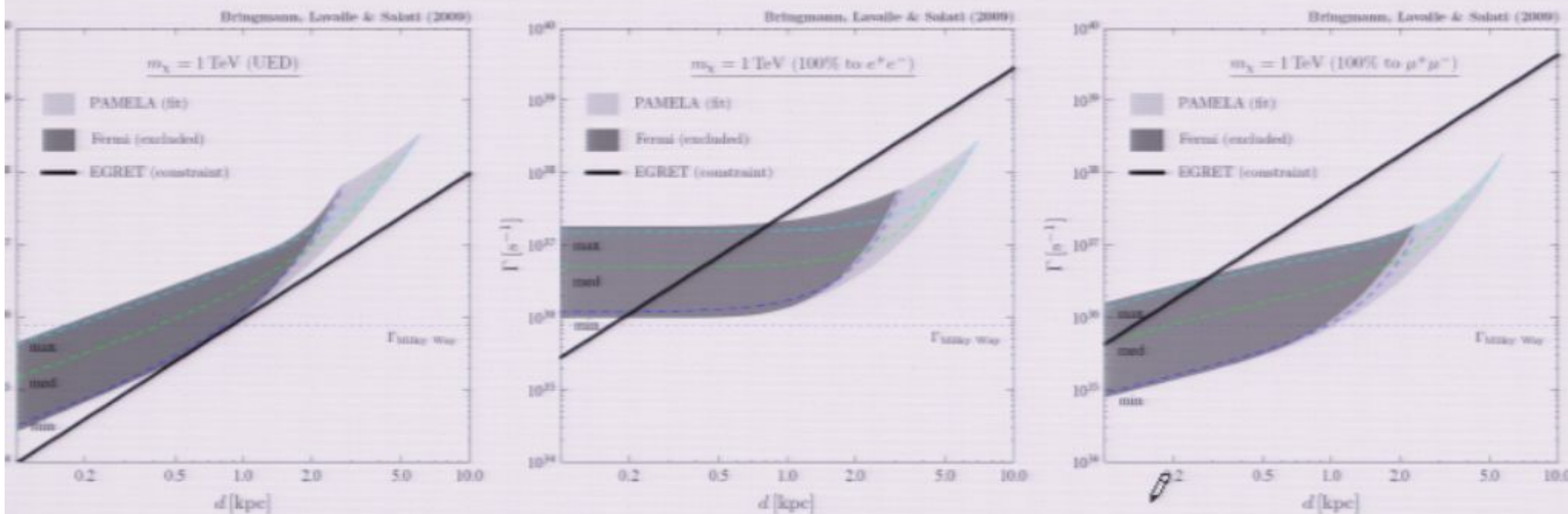
P. Brun, T. Delahaye, J. Diemand, S. Profumo & P. Salati, arXiv:0904.0812



# The cosmic ray lepton puzzle in the light of cosmological N-body simulations

P. Brun, T. Delahaye, J. Diemand, S. Profumo & P. Salati, arXiv:0904.0812



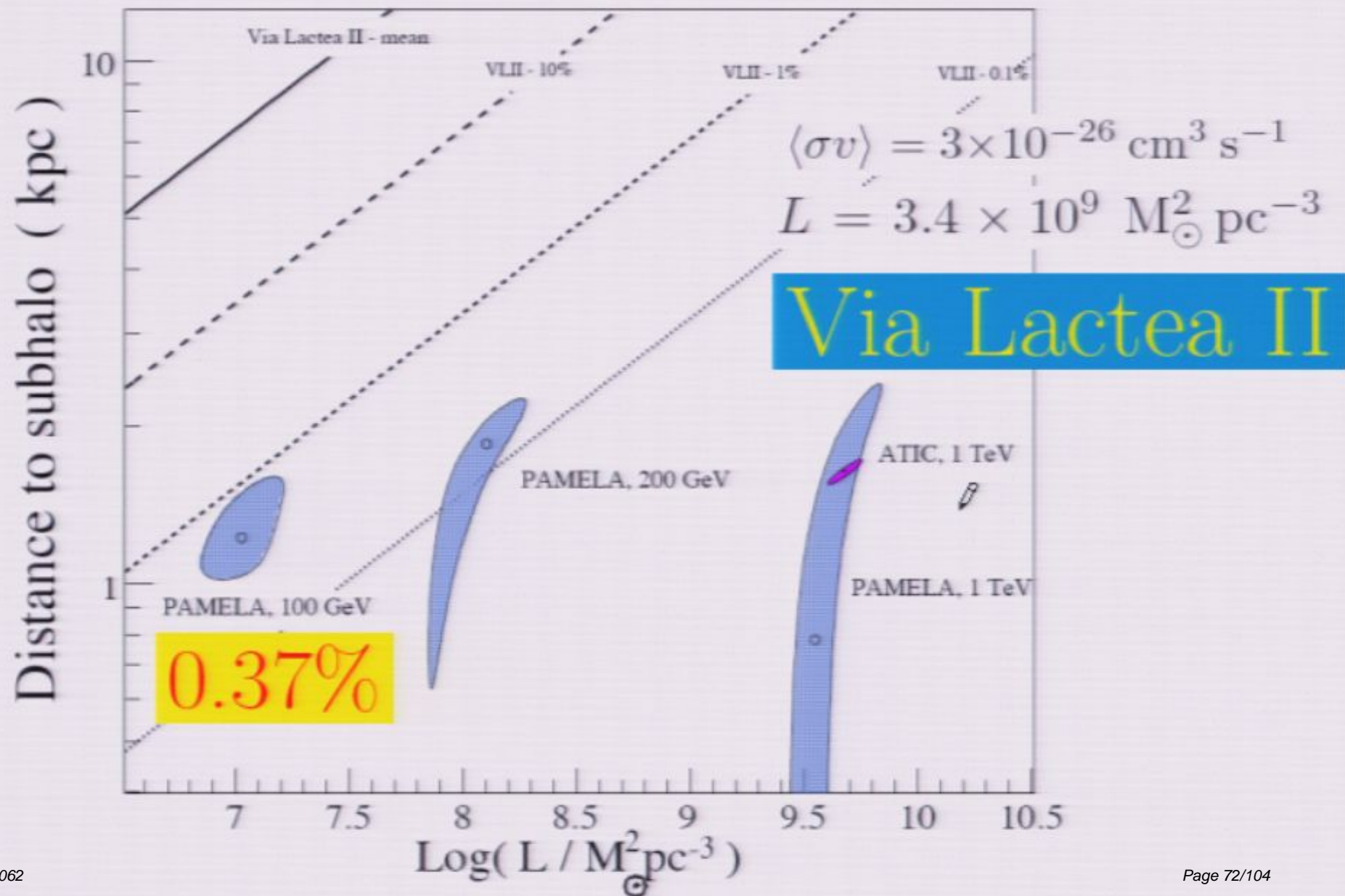


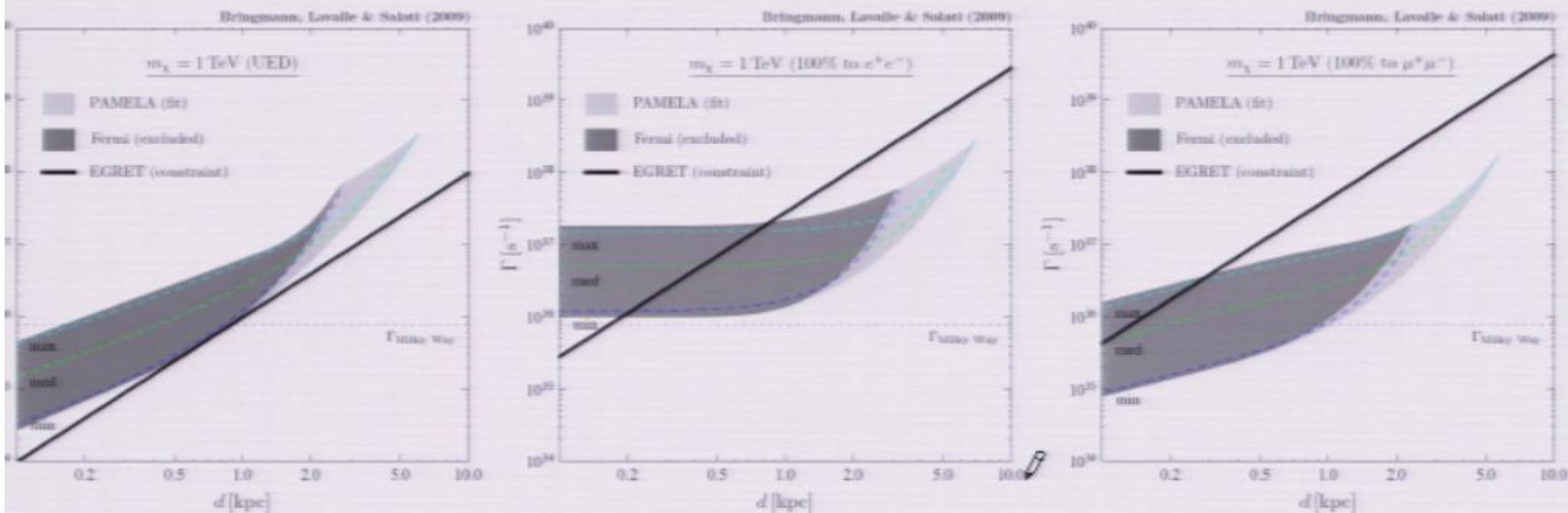
	PAMELA		ATIC
$m_\chi$ (GeV)	100	1 000	1 000
$e^+ / e^-$	$(1.22; 1.07 \cdot 10^7)$	$(0.78; 3.56 \cdot 10^9)$	$(1.64; 4.81 \cdot 10^9)$
$e^\pm + \mu^\pm + \tau^\pm$	$(0.44; 2.51 \cdot 10^7)$	$(0.27; 9.84 \cdot 10^9)$	$(1.45; 9.44 \cdot 10^9)$

TABLE I: Best fit values of the  $(D; L)$  couple in units of  $(\text{kpc}; M_\odot \text{ pc}^{-3})$  for various DM particle masses and annihilation channels.

# The cosmic ray lepton puzzle in the light of cosmological N-body simulations

P. Brun, T. Delahaye, J. Diemand, S. Profumo & P. Salati, arXiv:0904.0812



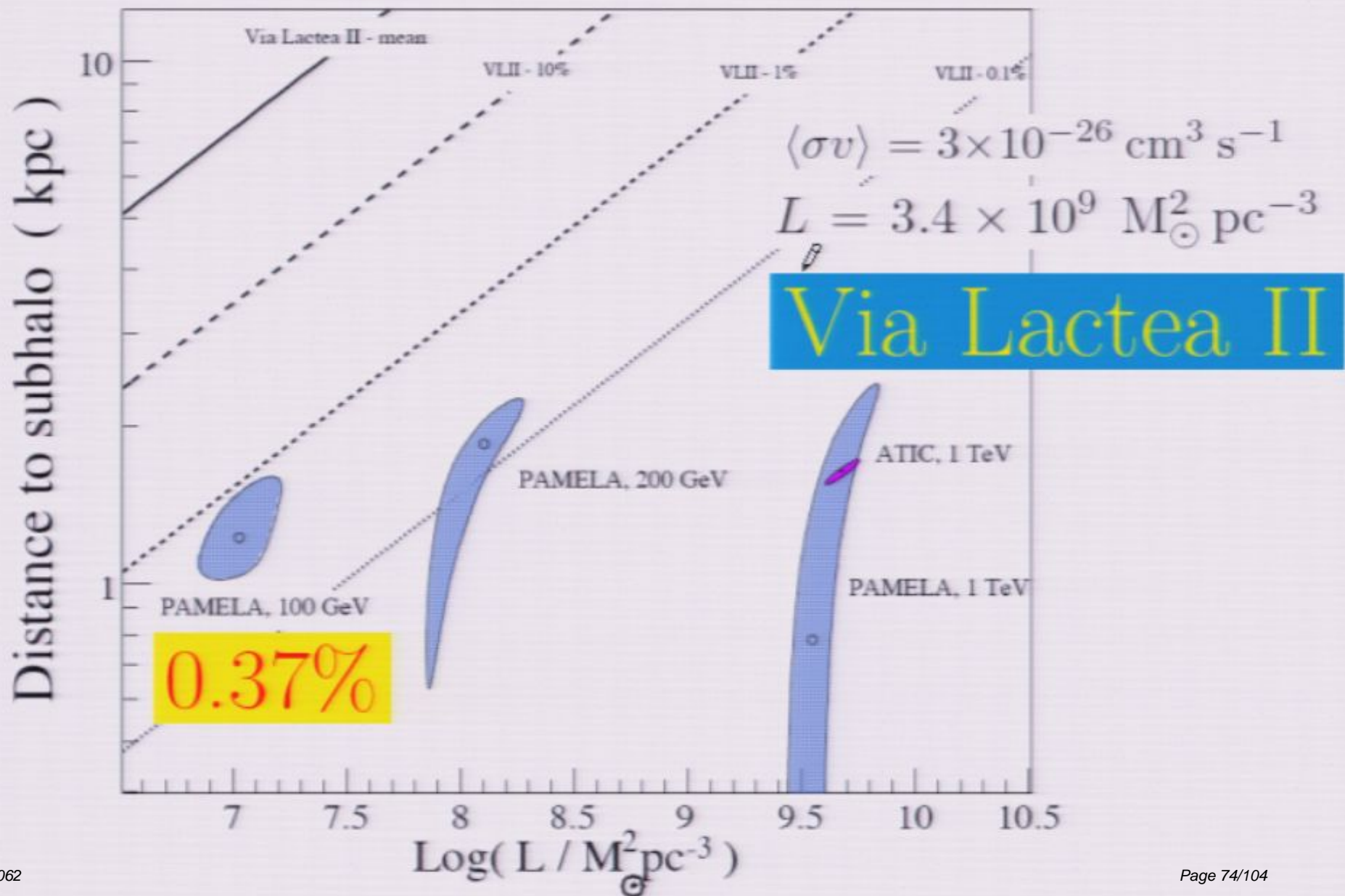


$m_\chi$ (GeV)	PAMELA		ATIC
$e^+ / e^-$	(1.22; $1.07 \cdot 10^7$ )	(0.78; $3.56 \cdot 10^9$ )	(1.64; $4.81 \cdot 10^9$ )
$e^\pm + \mu^\pm + \tau^\pm$	(0.44; $2.51 \cdot 10^7$ )	(0.27; $9.84 \cdot 10^9$ )	(1.45; $9.44 \cdot 10^9$ )

TABLE I: Best fit values of the  $(D; L)$  couple in units of  $(\text{kpc}; M_\odot^2 \text{ pc}^{-3})$  for various DM particle masses and annihilation channels.

# The cosmic ray lepton puzzle in the light of cosmological N-body simulations

P. Brun, T. Delahaye, J. Diemand, S. Profumo & P. Salati, arXiv:0904.0812



# The cosmic ray lepton puzzle in the light of cosmological N-body simulations

P. Brun, T. Delahaye, J. Diemand, S. Profumo & P. Salati, arXiv:0904.0812

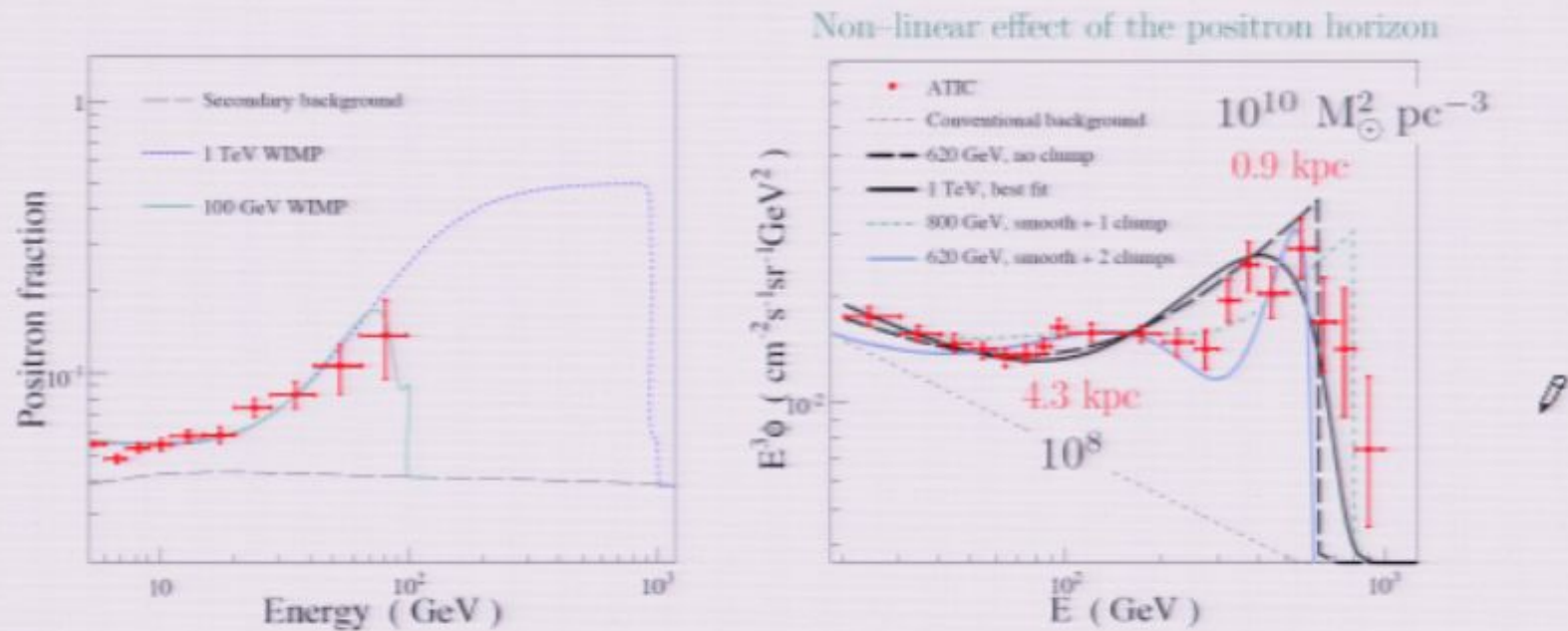
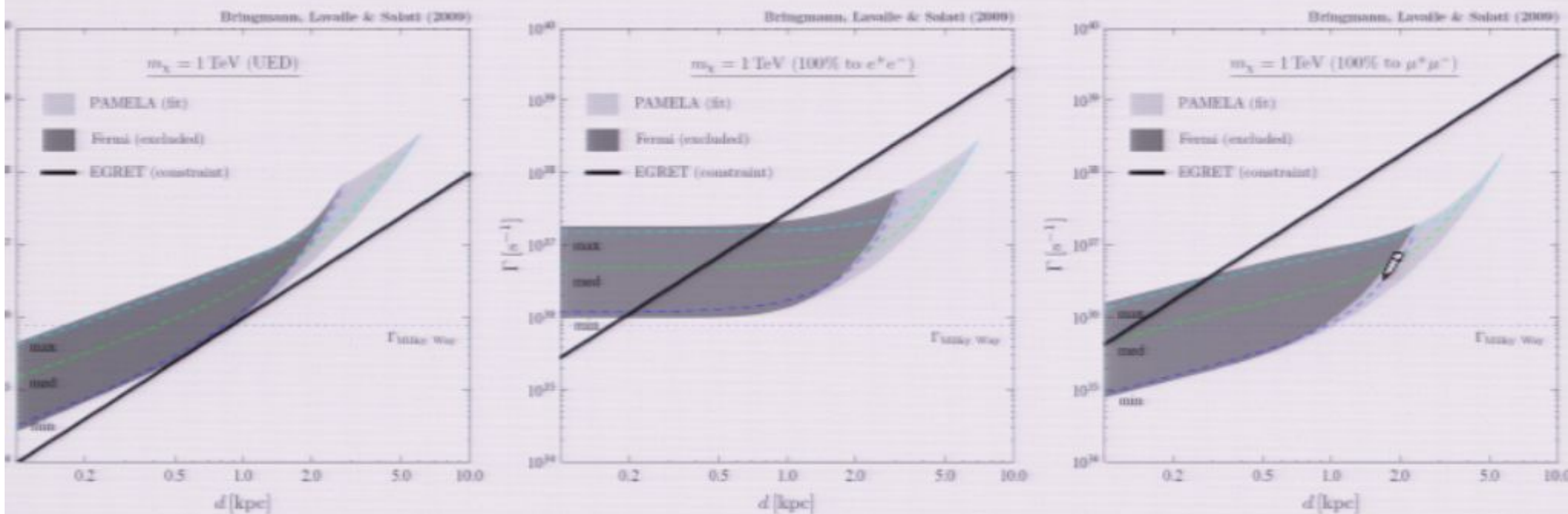


FIG. 1: Best fits to the PAMELA data in the case of a positronic line (see the  $e^+/e^-$  row of Tab. I) (left panel) and fits to the ATIC data (right panel).

	PAMELA		ATIC
$m_\chi$ (GeV)	100	1 000	1 000
$e^+/e^-$	(1.22; $1.07 \cdot 10^7$ )	(0.78; $3.56 \cdot 10^9$ )	(1.64; $4.81 \cdot 10^9$ )
$e^\pm + \mu^\pm + \tau^\pm$	(0.44; $2.51 \cdot 10^7$ )	(0.27; $9.84 \cdot 10^9$ )	(1.45; $9.44 \cdot 10^9$ )

TABLE I: Best fit values of the ( $D; L$ ) couple in units of (kpc;  $M_\odot^2 pc^{-3}$ ) for various DM particle masses and annihilation channels.

# T. Bringmann, J. Lavalle & P. Salati, arXiv:0902.3665



	PAMELA		ATIC
$m_\chi$ (GeV)	100	1 000	1 000
$e^+/e^-$	(1.22; $1.07 \cdot 10^7$ )	(0.78; $3.56 \cdot 10^9$ )	(1.64; $4.81 \cdot 10^9$ )
$e^\pm + \mu^\pm + \tau^\pm$	(0.44; $2.51 \cdot 10^7$ )	(0.27; $9.84 \cdot 10^9$ )	(1.45; $9.44 \cdot 10^9$ )

TABLE I: Best fit values of the ( $D; L$ ) couple in units of (kpc;  $M_\odot^2 \text{ pc}^{-3}$ ) for various DM particle masses and annihilation channels.

# Dark matter mini-spikes around IMBHs

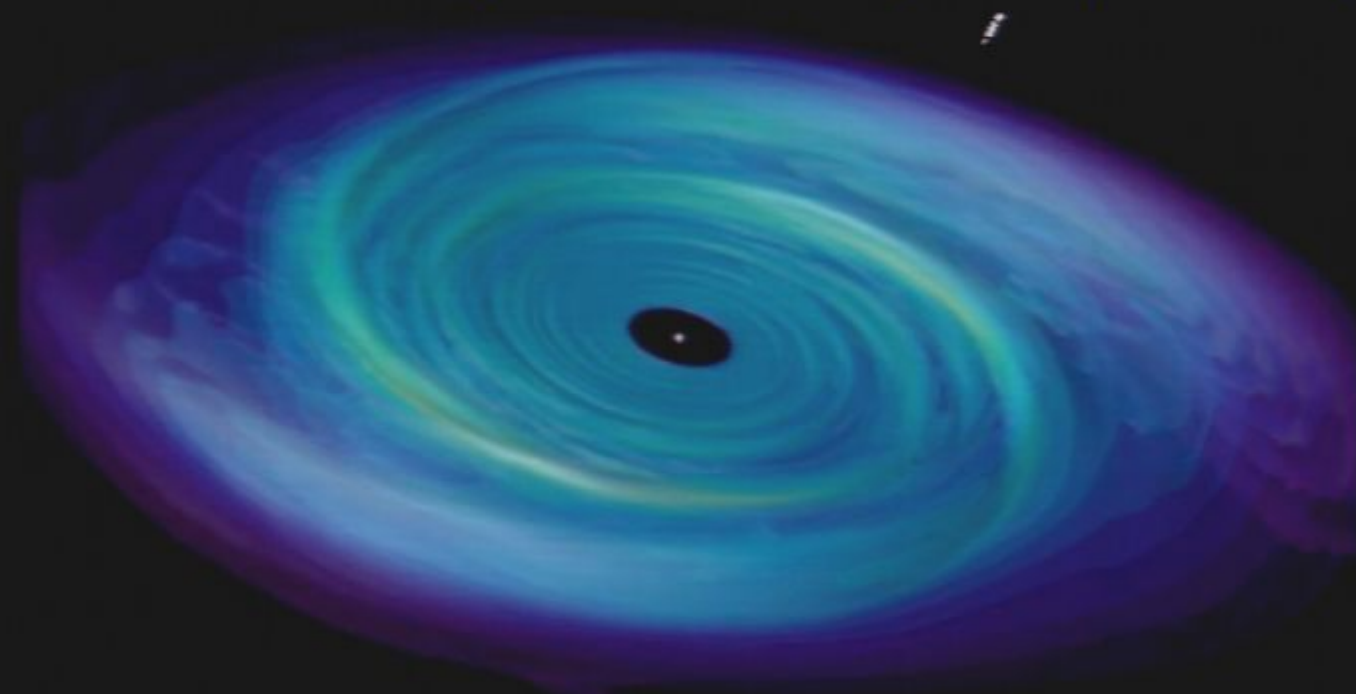
G. Bertone, A.R. Zentner & J. Silk, PRD **72** (2005) 103517



# Dark matter mini-spikes around IMBHs

G. Bertone, A.R. Zentner & J. Silk, PRD **72** (2005) 103517

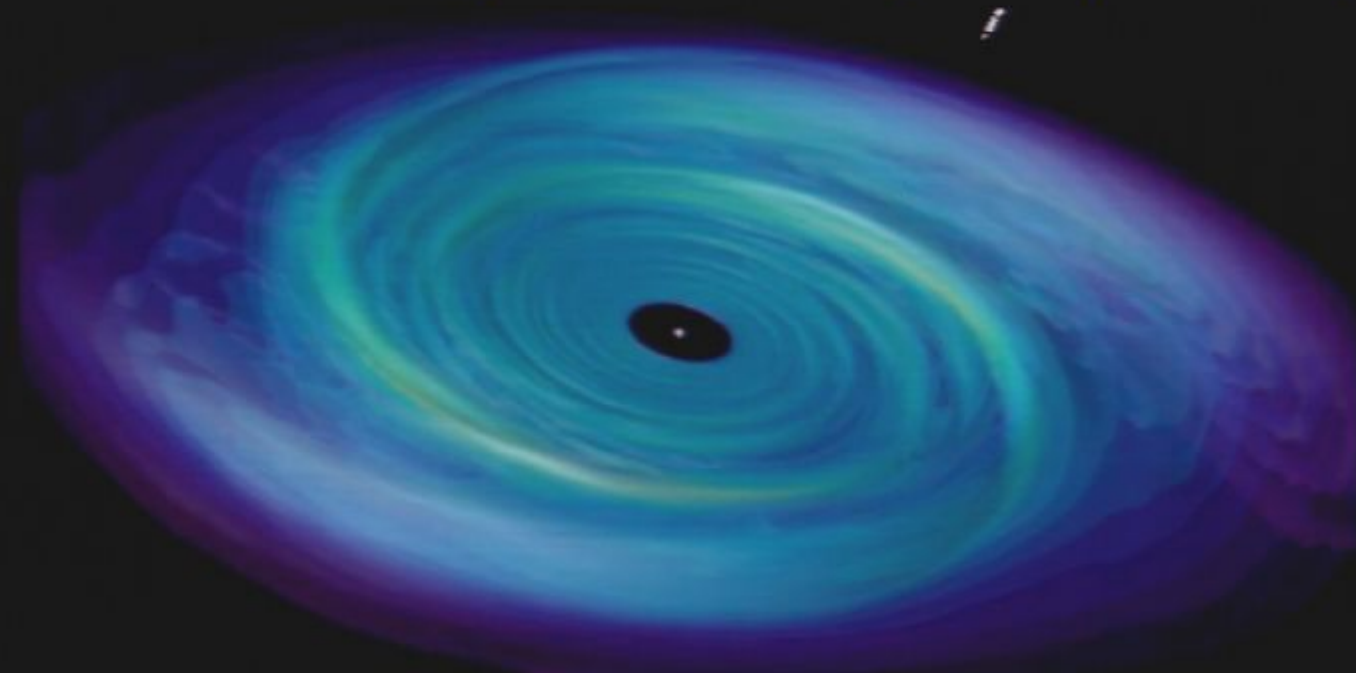
When the first DM halos form, gas cools and collapses as pressure supported disks



# Dark matter mini-spikes around IMBHs

G. Bertone, A.R. Zentner & J. Silk, PRD **72** (2005) 103517

When the first DM halos form, gas cools and collapses as pressure supported disks

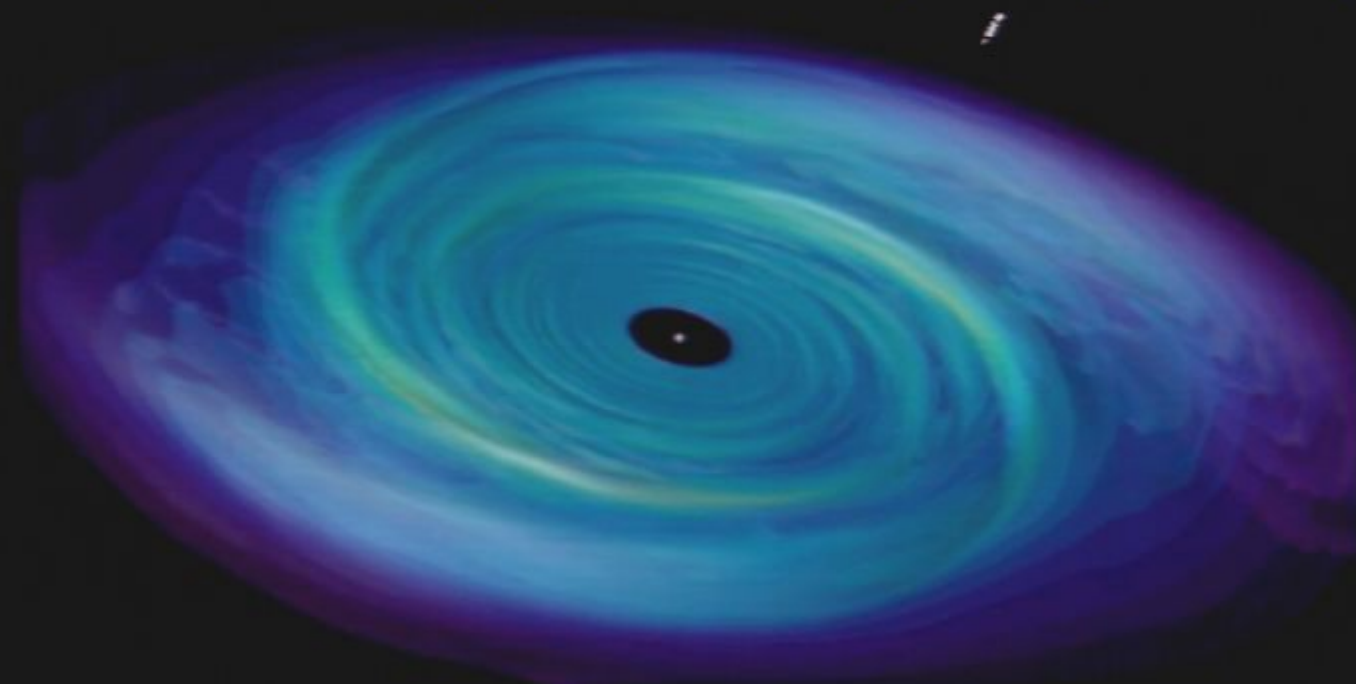


A baryonic mass of  $\sim 10^5 M_\odot$  loses its angular momentum

# Dark matter mini-spikes around IMBHs

G. Bertone, A.R. Zentner & J. Silk, PRD **72** (2005) 103517

When the first DM halos form, gas cools and collapses as pressure supported disks



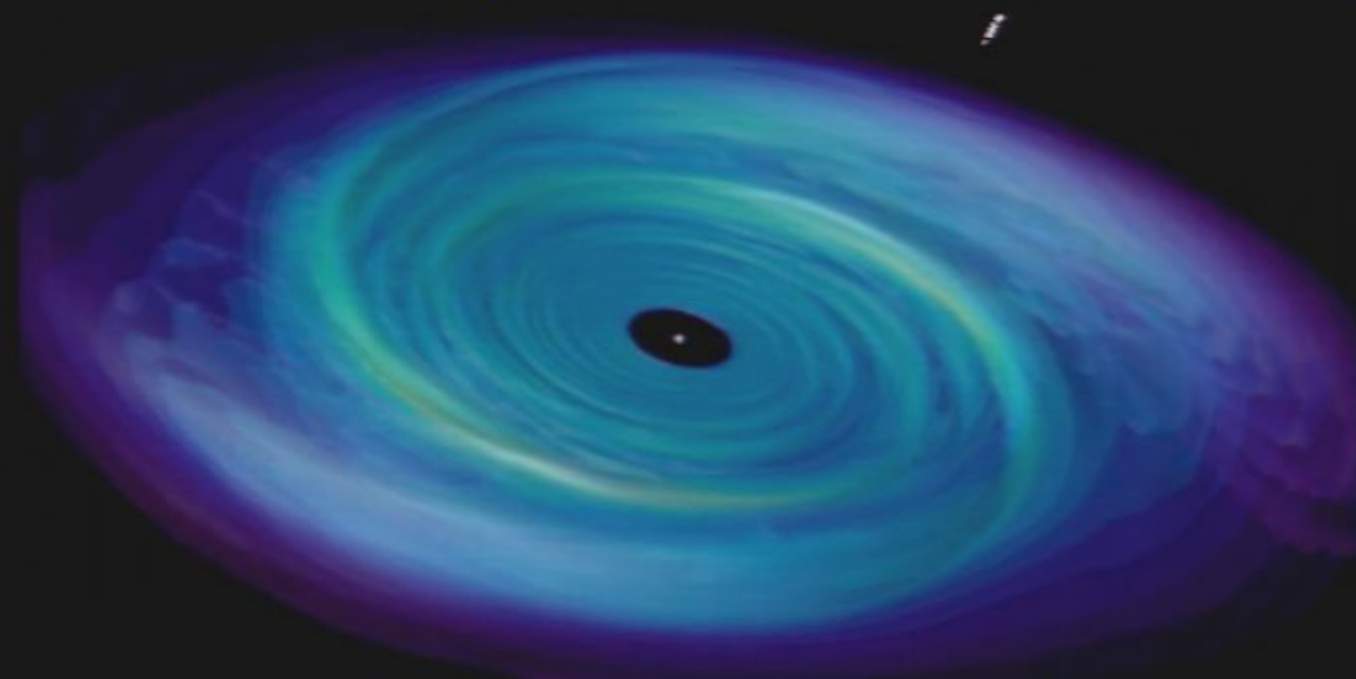
A baryonic mass of  $\sim 10^5 M_\odot$  loses its angular momentum

It is transferred at the center to form an Intermediate Mass Black Hole

# Dark matter mini-spikes around IMBHs

G. Bertone, A.R. Zentner & J. Silk, PRD **72** (2005) 103517

When the first DM halos form, gas cools and collapses as pressure supported disks

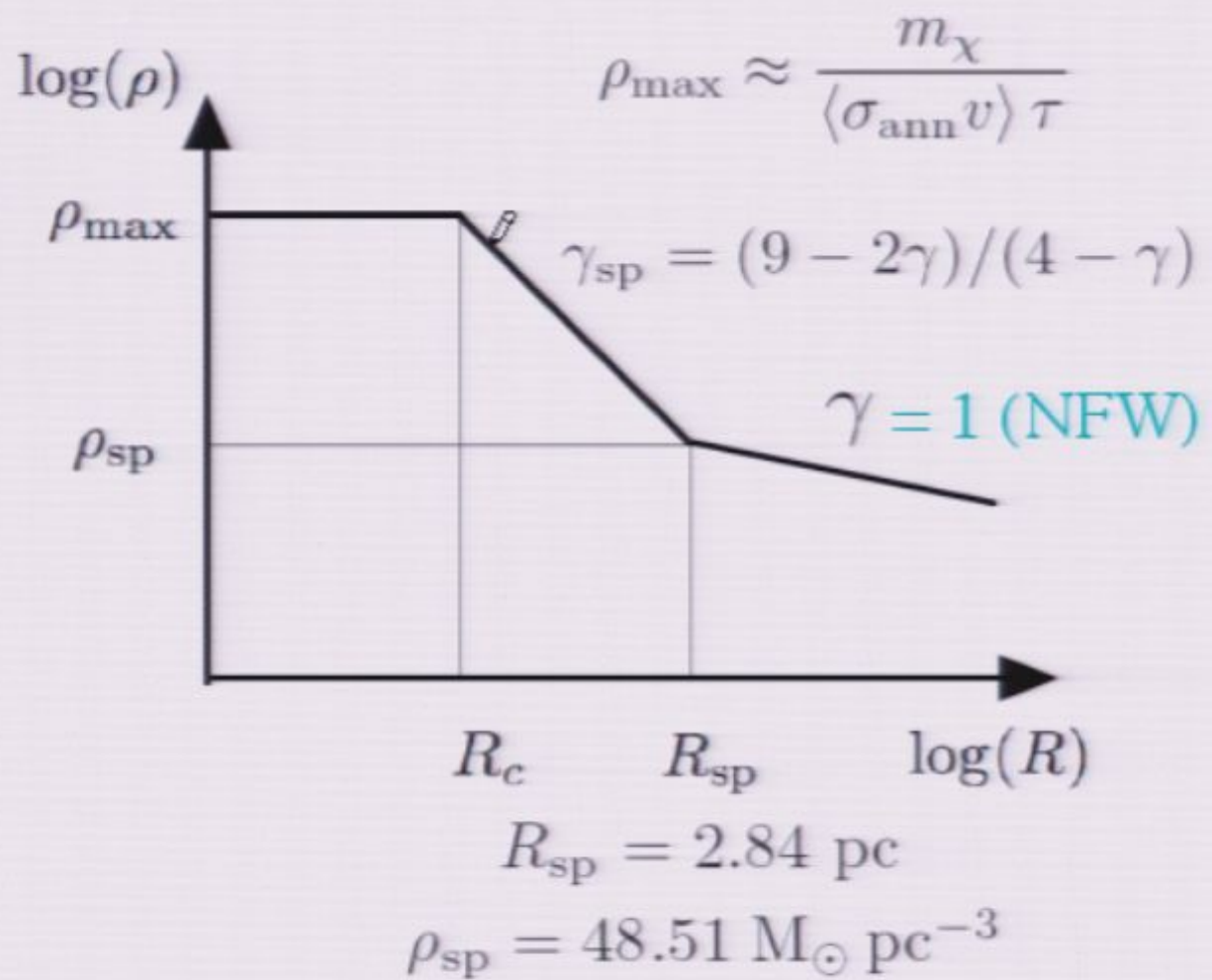
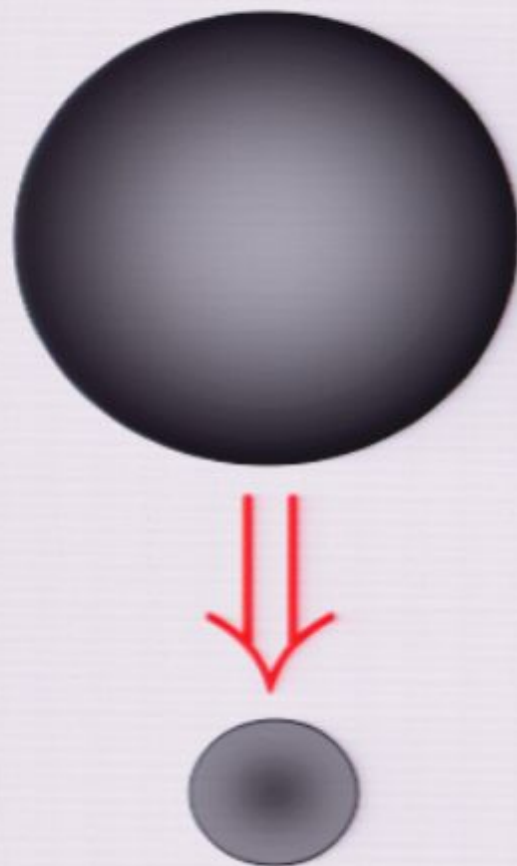


A baryonic mass of  $\sim 10^5 M_\odot$  loses its angular momentum

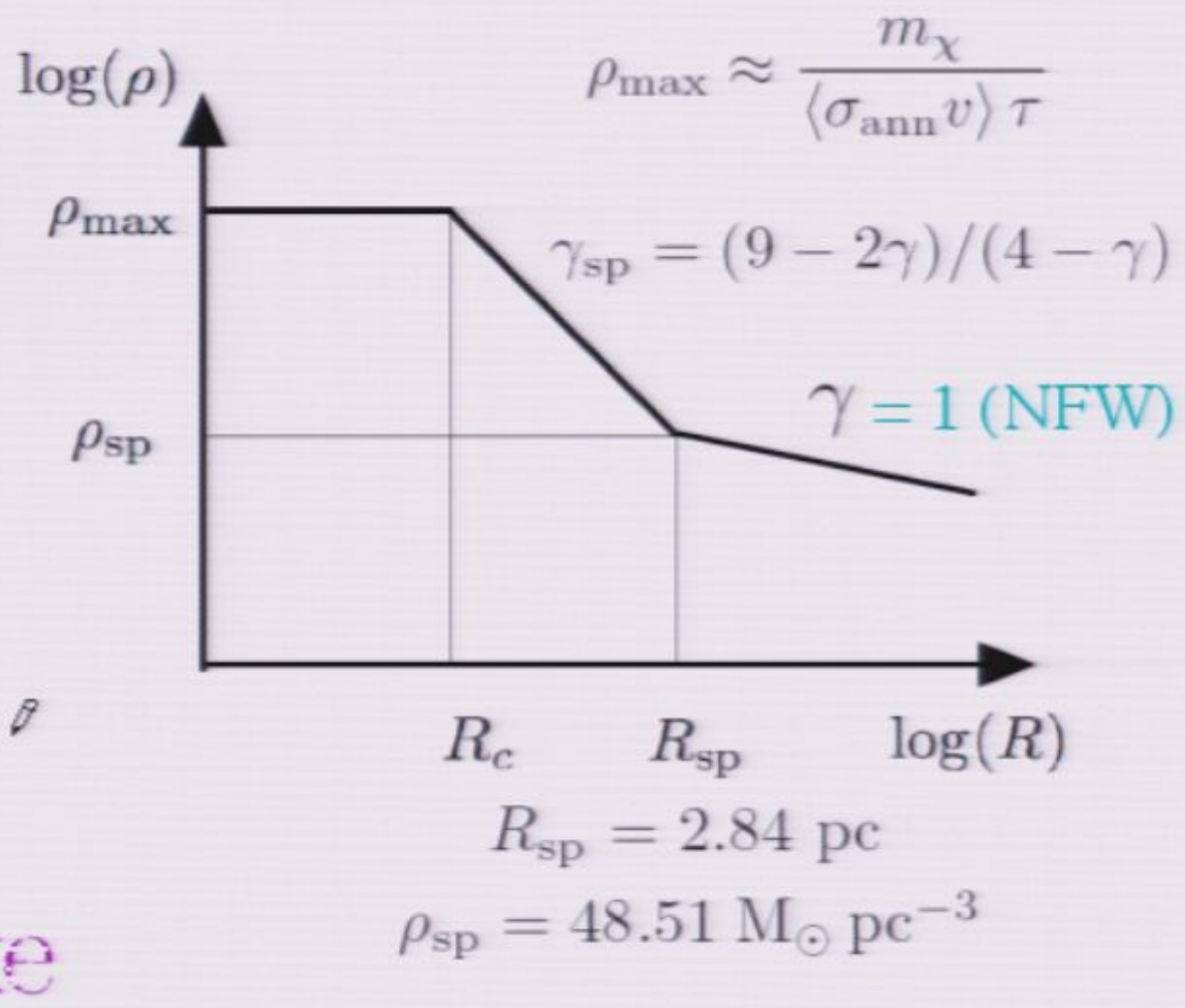
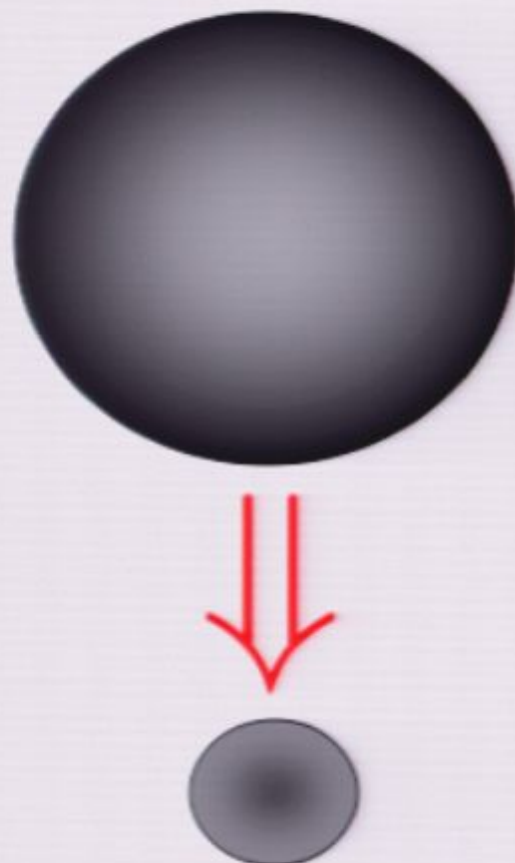
It is transferred at the center to form an Intermediate Mass Black Hole

During the process, DM is adiabatically compressed onto this central object

# Adiabatic DM compression around the IMBH

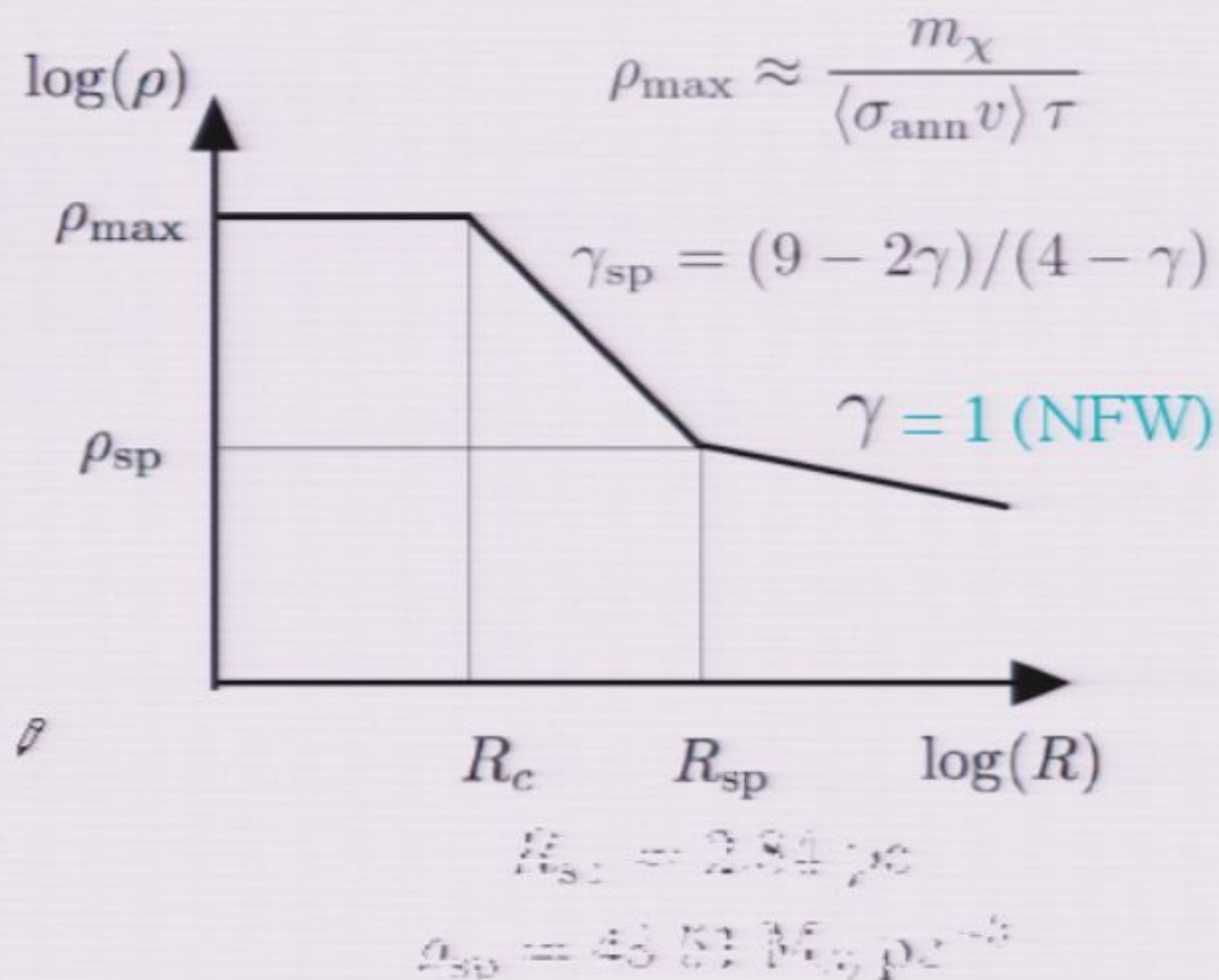
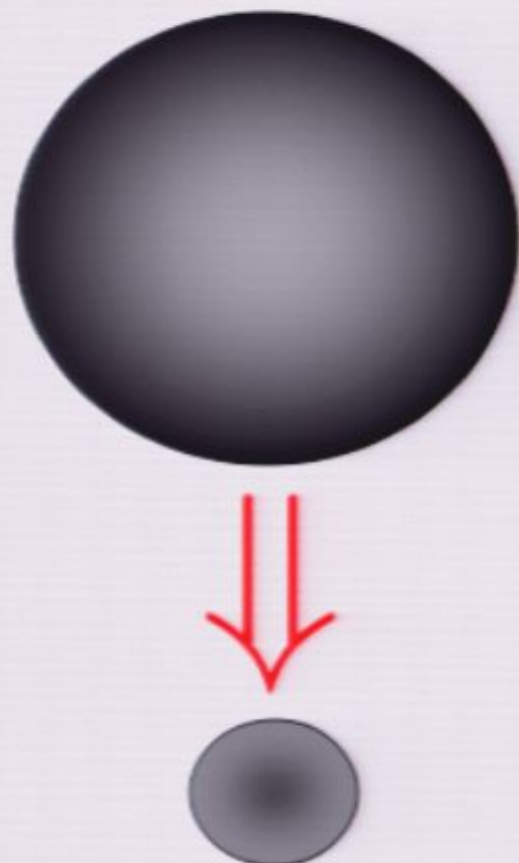


# Adiabatic DM compression around the IMBH

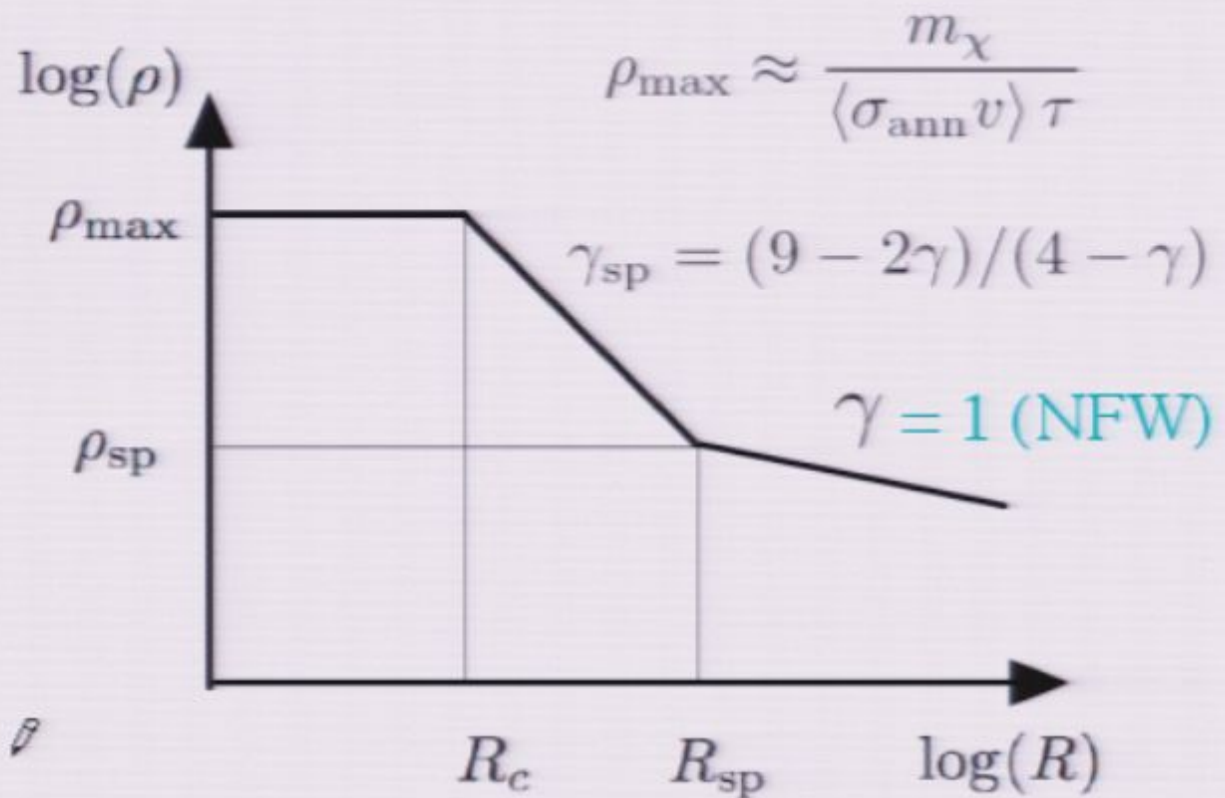
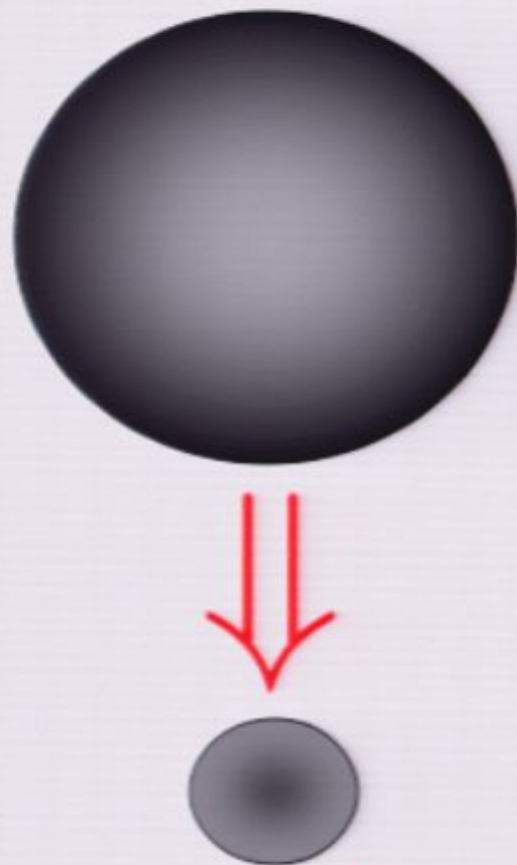


DM mini-spike

# Adiabatic DM compression around the IMBH



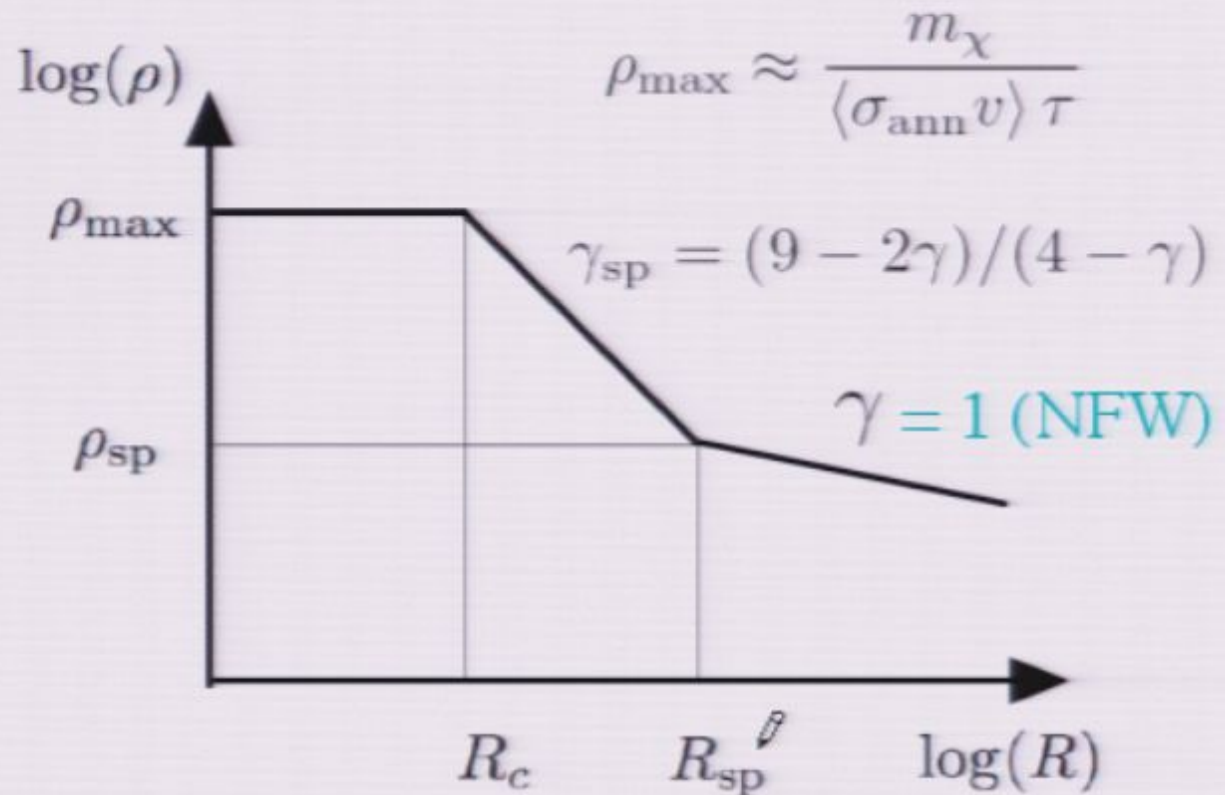
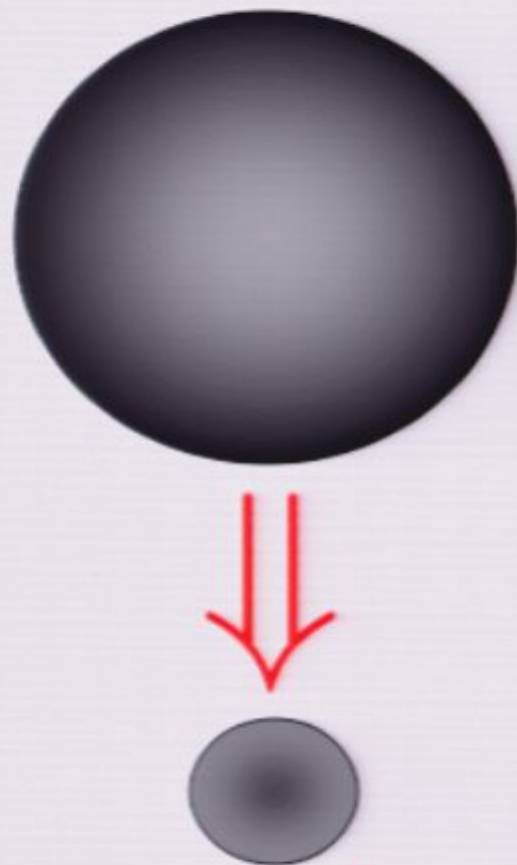
# Adiabatic DM compression around the IMBH



Large annihilation volume

$$\xi = \frac{12}{5} \pi R_{\text{sp}}^3 \left\{ \frac{\rho_{\text{sp}}}{\rho_\odot} \right\}^2 \left\{ \frac{14}{9} \eta^{5/7} - 1 \right\} \text{ where } \frac{R_{\text{sp}}}{R_c} = \left\{ \eta \equiv \frac{\rho_{\max}}{\rho_{\text{sp}}} \right\}^{3/7}$$

# Adiabatic DM compression around the IMBH

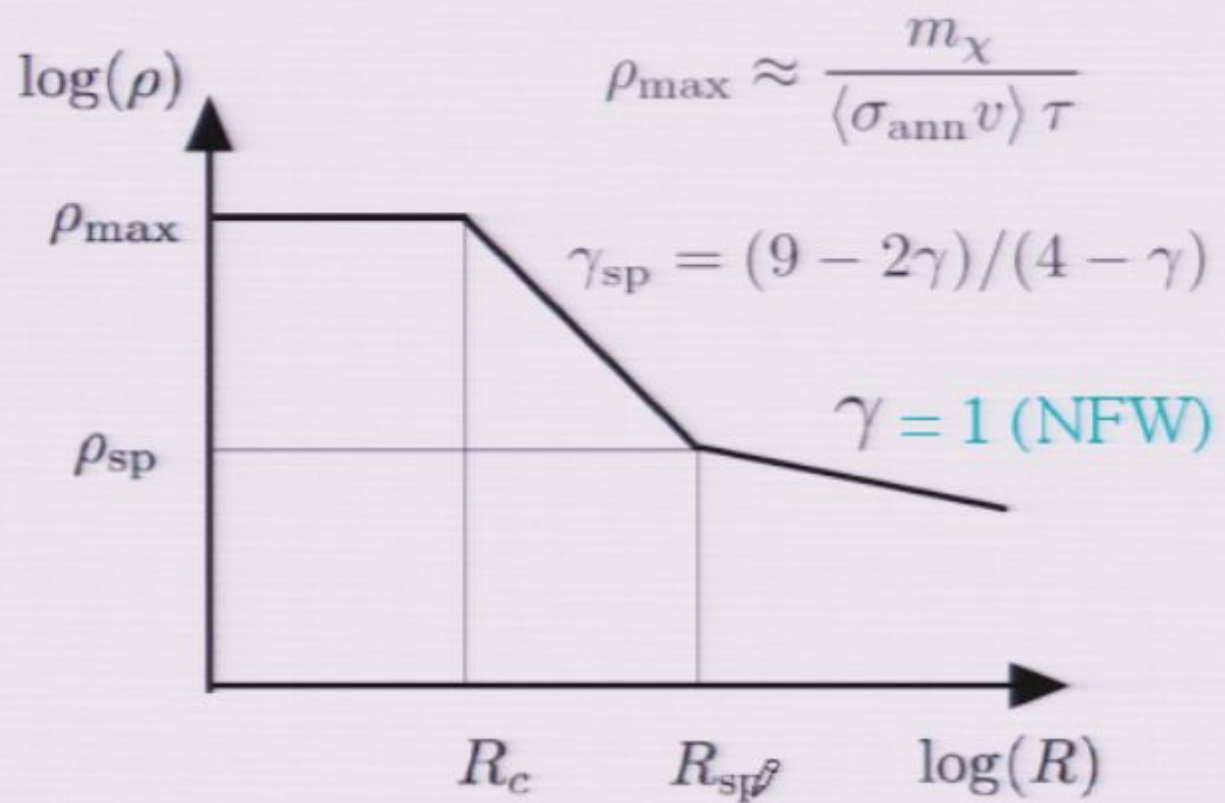
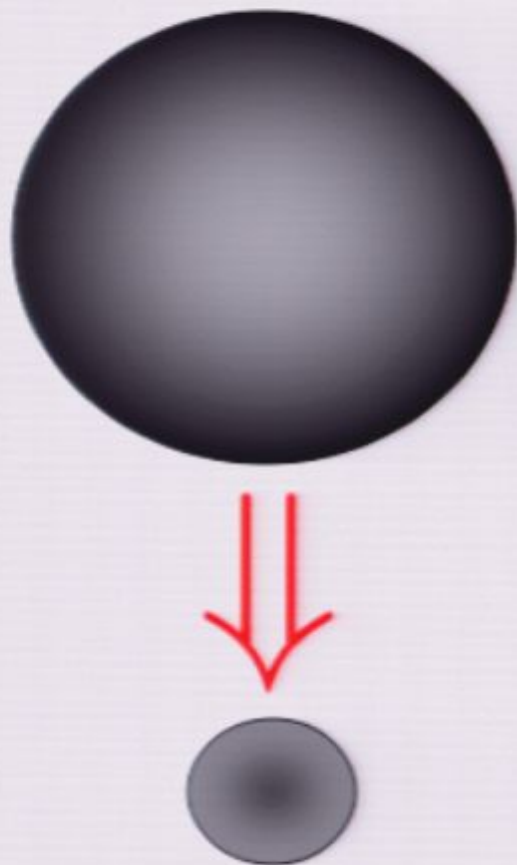


Large annihilation volume

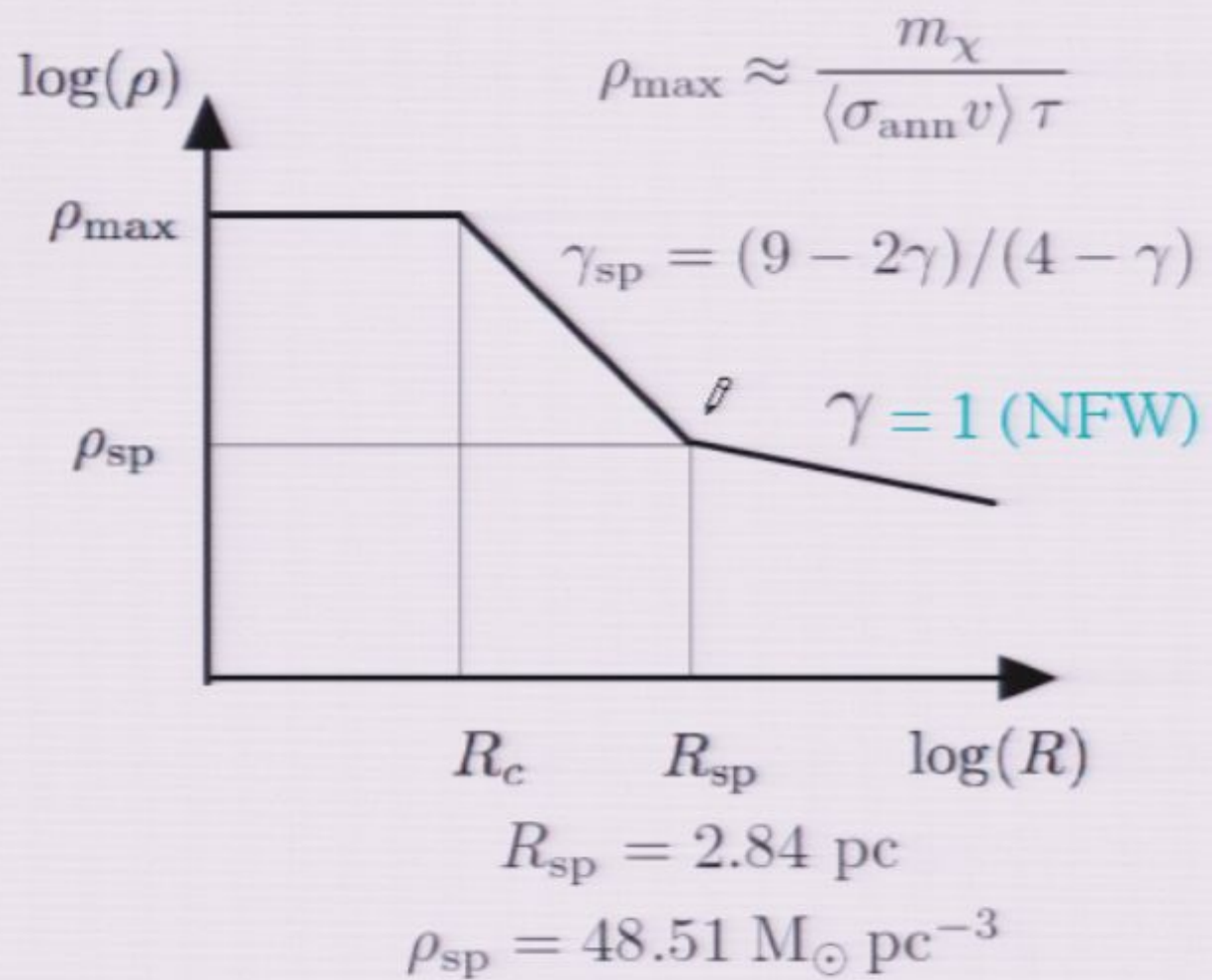
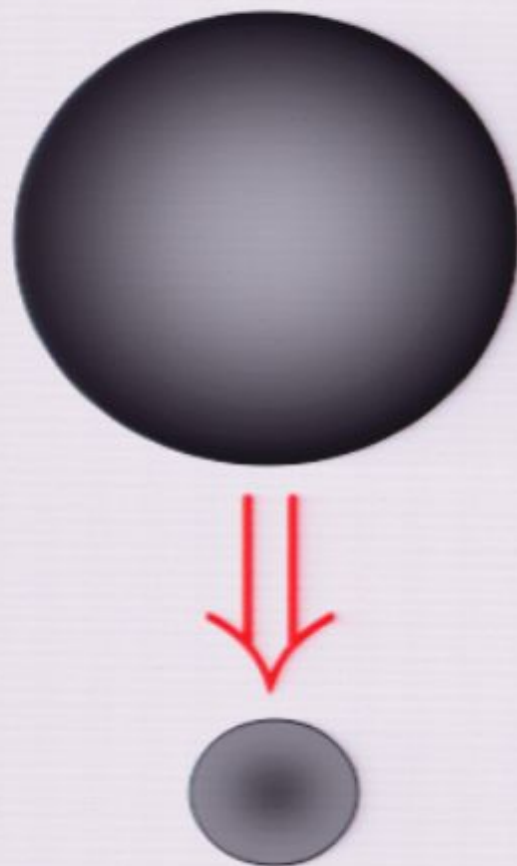
$$\xi = \frac{12}{5} \pi R_{\text{sp}}^3 \left\{ \frac{\rho_{\text{sp}}}{\rho_\odot} \right\}^2 \left\{ \frac{14}{9} \eta^{5/7} - 1 \right\} \text{ where } \frac{R_{\text{sp}}}{R_c} = \left\{ \eta \equiv \frac{\rho_{\max}}{\rho_{\text{sp}}} \right\}^{3/7}$$

$$\xi \sim 3.3 \times 10^6 \text{ kpc}^3 \text{ for } \langle \sigma_{\text{ann}} v \rangle_{26} = 3 \text{ & } m_\chi = 1 \text{ TeV}$$

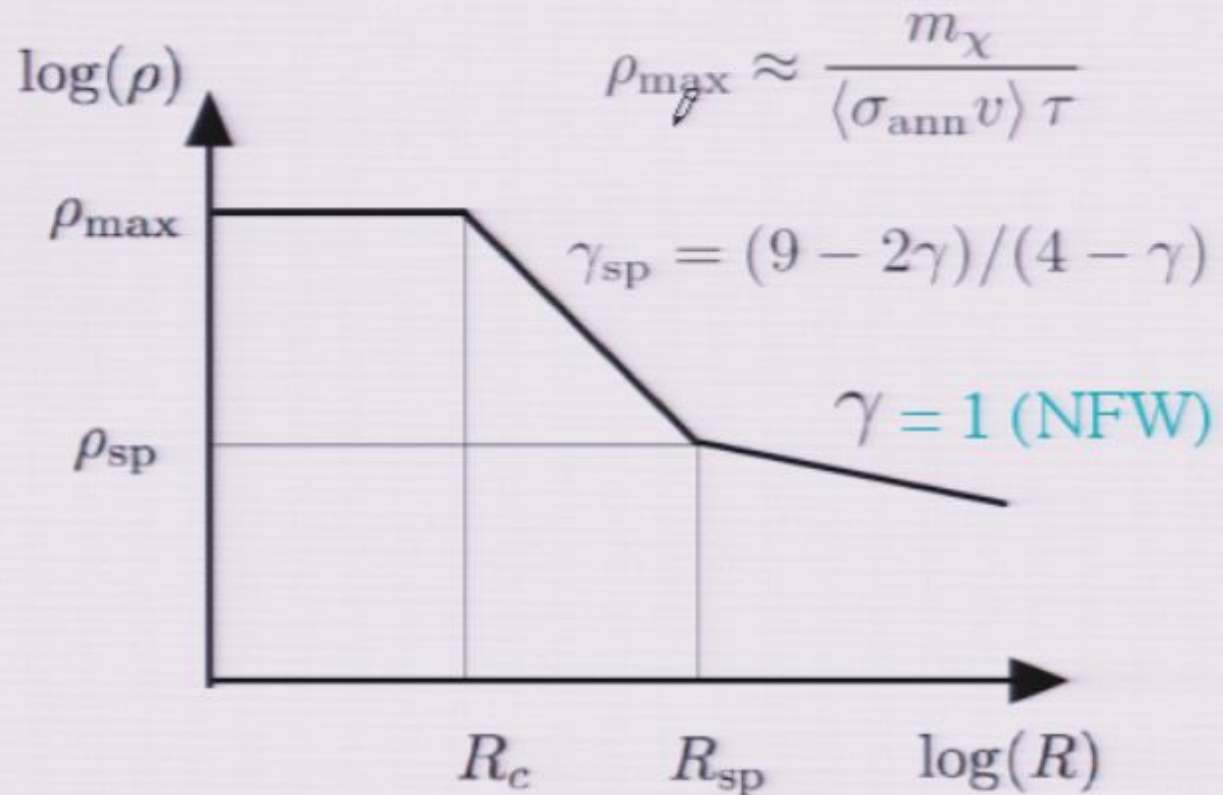
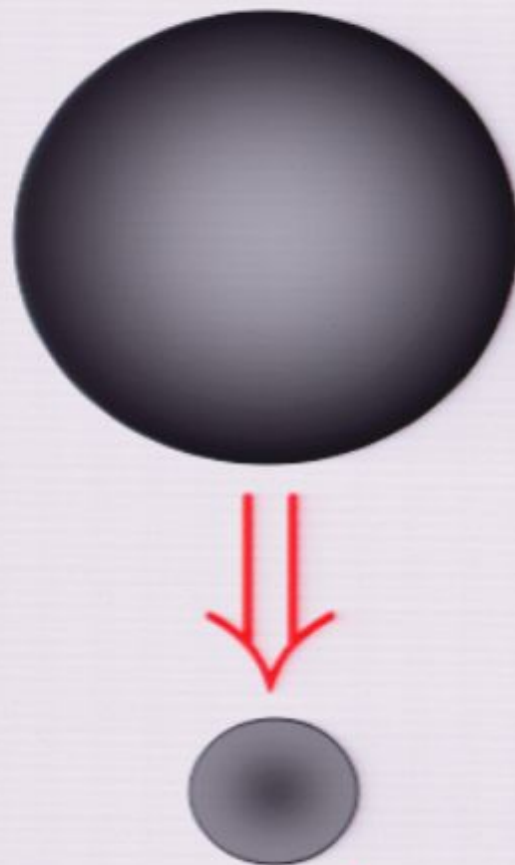
# Adiabatic DM compression around the IMBH



# Adiabatic DM compression around the IMBH



# Adiabatic DM compression around the IMBH



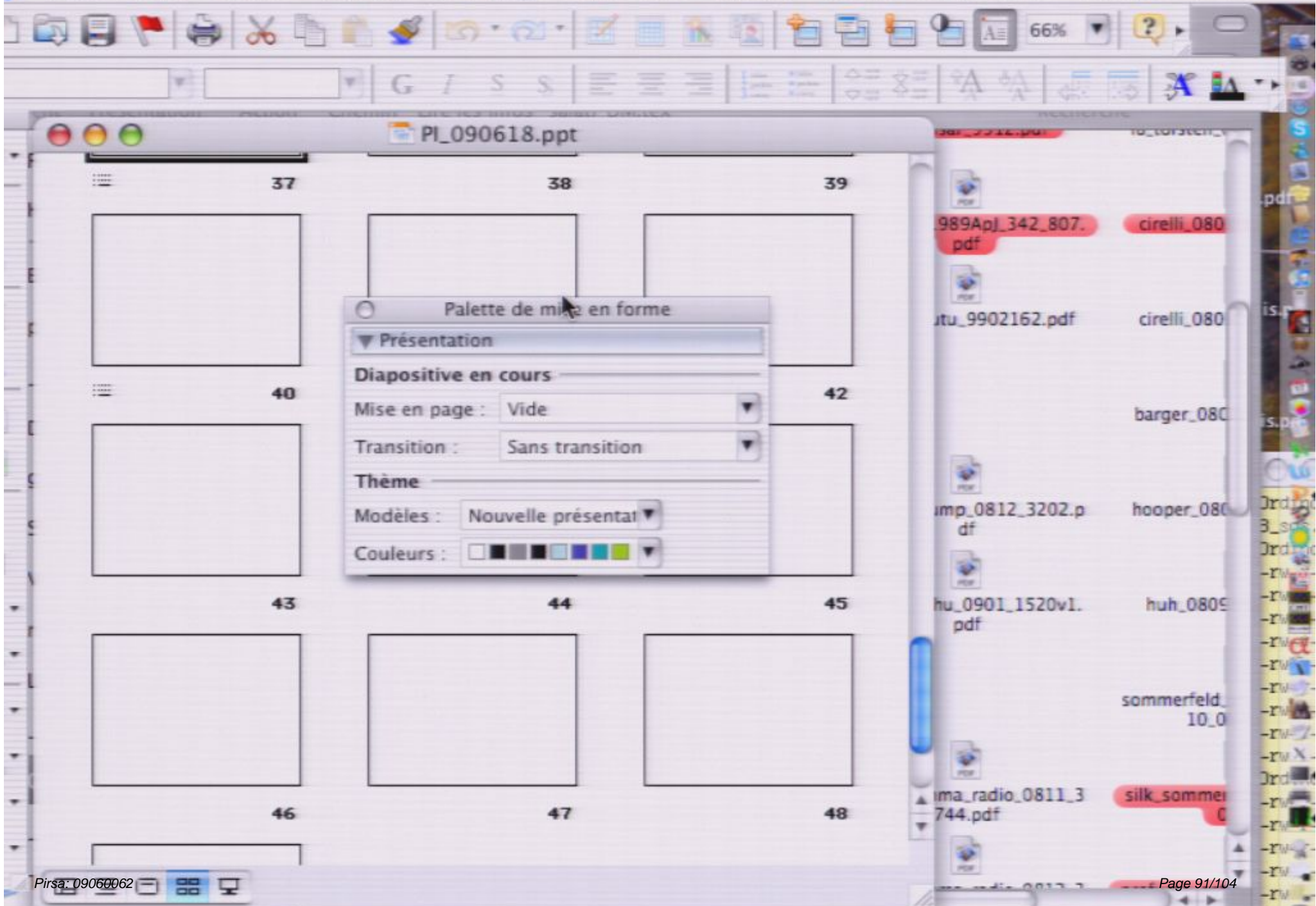
Large annihilation volume

$$\xi = \frac{12}{5} \pi R_{\text{sp}}^3 \left\{ \frac{\rho_{\text{sp}}}{\rho_{\odot}} \right\}^2 \left\{ \frac{14}{9} \eta^{5/7} - 1 \right\} \text{ where } \frac{R_{\text{sp}}}{R_c} = \left\{ \eta \equiv \frac{\rho_{\text{max}}}{\rho_{\text{sp}}} \right\}^{3/7}$$

The screenshot shows a Microsoft PowerPoint window titled "PI\_090618.ppt". The slide contains nine numbered boxes (28, 29, 30, 31, 33, 34, 35, 36, 37, 38, 39) arranged in three rows. A floating "Format" ribbon is visible, containing sections for "Présentation" (Presentation), "Diapositive en cours" (Current Slide), and "Modèles" (Themes). The "Présentation" section includes dropdowns for "Mise en page" (Layout) set to "Vide" and "Transition" (Transition) set to "Sans transition" (No transition). The "Modèles" section shows "Nouvelle présentation" (New presentation) selected. The "Format" ribbon also features a color palette for "Couleurs" (Colors). To the right of the slide, a vertical sidebar displays a list of PDF files:

- 989Apj\_342\_807.pdf (highlighted with a red box)
- itu\_9902162.pdf cirelli\_080
- barger\_080
- imp\_0812\_3202.pdf hooper\_080
- hu\_0901\_1520vl.pdf huh\_0809
- sommerfeld\_10\_0
- ima\_radio\_0811\_3744.pdf silk\_sommer

At the bottom left, there is a status bar with the text "Pirsa: 09060062" and icons for file operations. The bottom right corner shows the page number "Page 90/104".



PI\_090618.ppt

37 38 39

40 41

43 44 45

46 47 48

989Apj\_342\_807.pdf cirelli\_080

Palette de mise en forme

Présentation

Diapositive en cours

Mise en page : Vide

Transition : Sans transition

Thème

Modèles : Nouvelle présentation

Couleurs :

hu\_0901\_1520vl.pdf huh\_0809

sommerfeld\_10\_0

ima\_radio\_0811\_3 744.pdf silk\_sommer

Pirsa: 09060062

Page 92/104

Sans transition

PI\_090618.ppt

Recherche

37

38

39

40

41

42

43

44

45

46

47

48

Palettes de mise en forme

Présentation

Diapositive en cours

Mise en page : Vide

Transition : Sans transition

Thème

Modèles : Nouvelle présentation

Couleurs :

ong\_bo\_hu\_0901\_1520vl.pdf

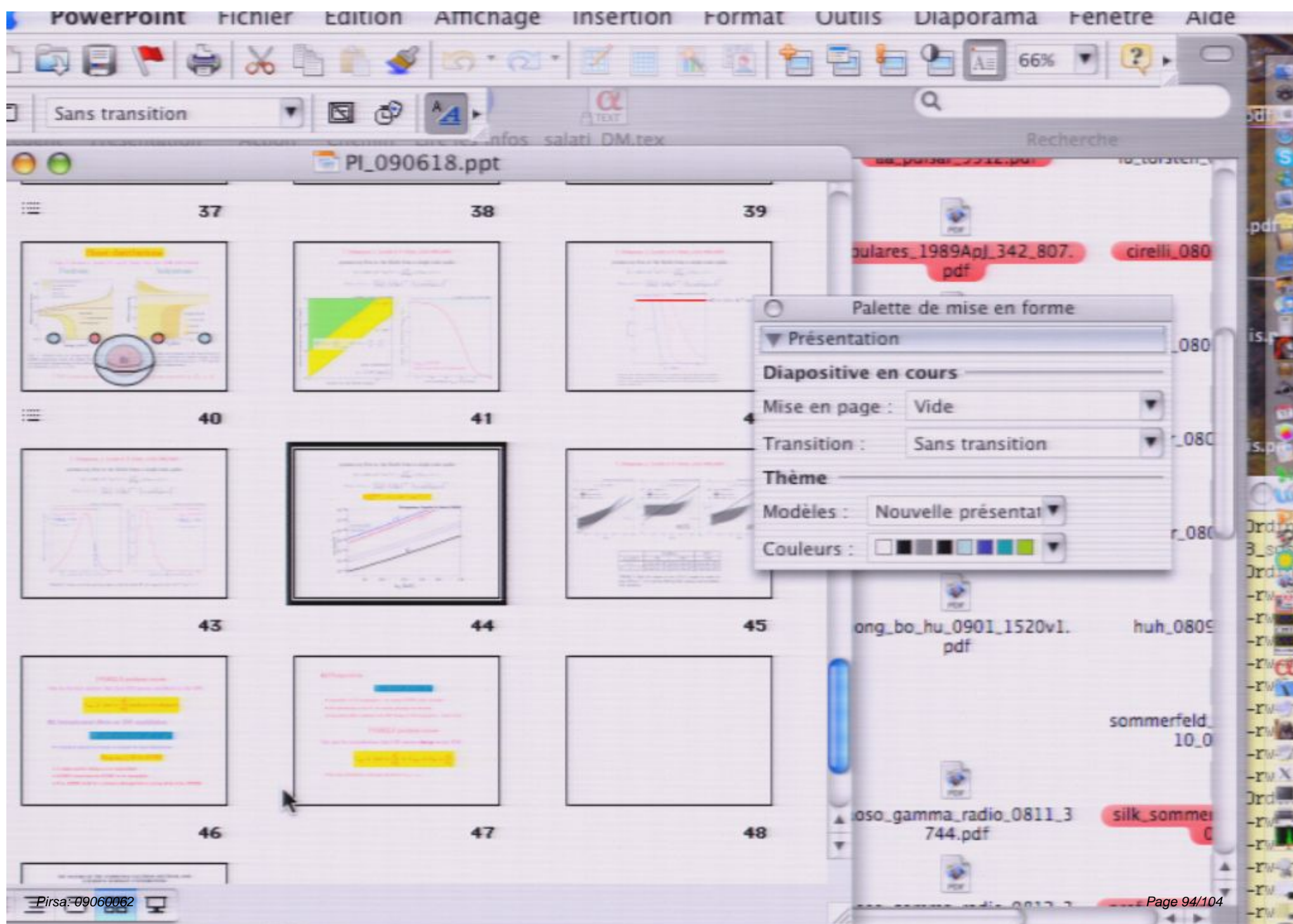
sommerfeld\_10\_0.pdf

oso\_gamma\_radio\_0811\_3744.pdf

silk\_sommerfeld\_0.pdf

Pirsa: 09060062

Page 93/104



Sans transition

PI\_090618.ppt

Recherche

37

38

39

40

41

42

43

44

45

46

47

48

Palette de mise en forme

Présentation

Diapositive en cours

Mise en page : Vide

Transition : Sans transition

Thème

Modèles : Nouvelle présentation

Couleurs :

ong\_bo\_hu\_0901\_1520vl.pdf

sommerfeld\_10\_0

oso\_gamma\_radio\_0811\_3744.pdf

silk\_sommer

Pirsa: 09060062

Diaporama

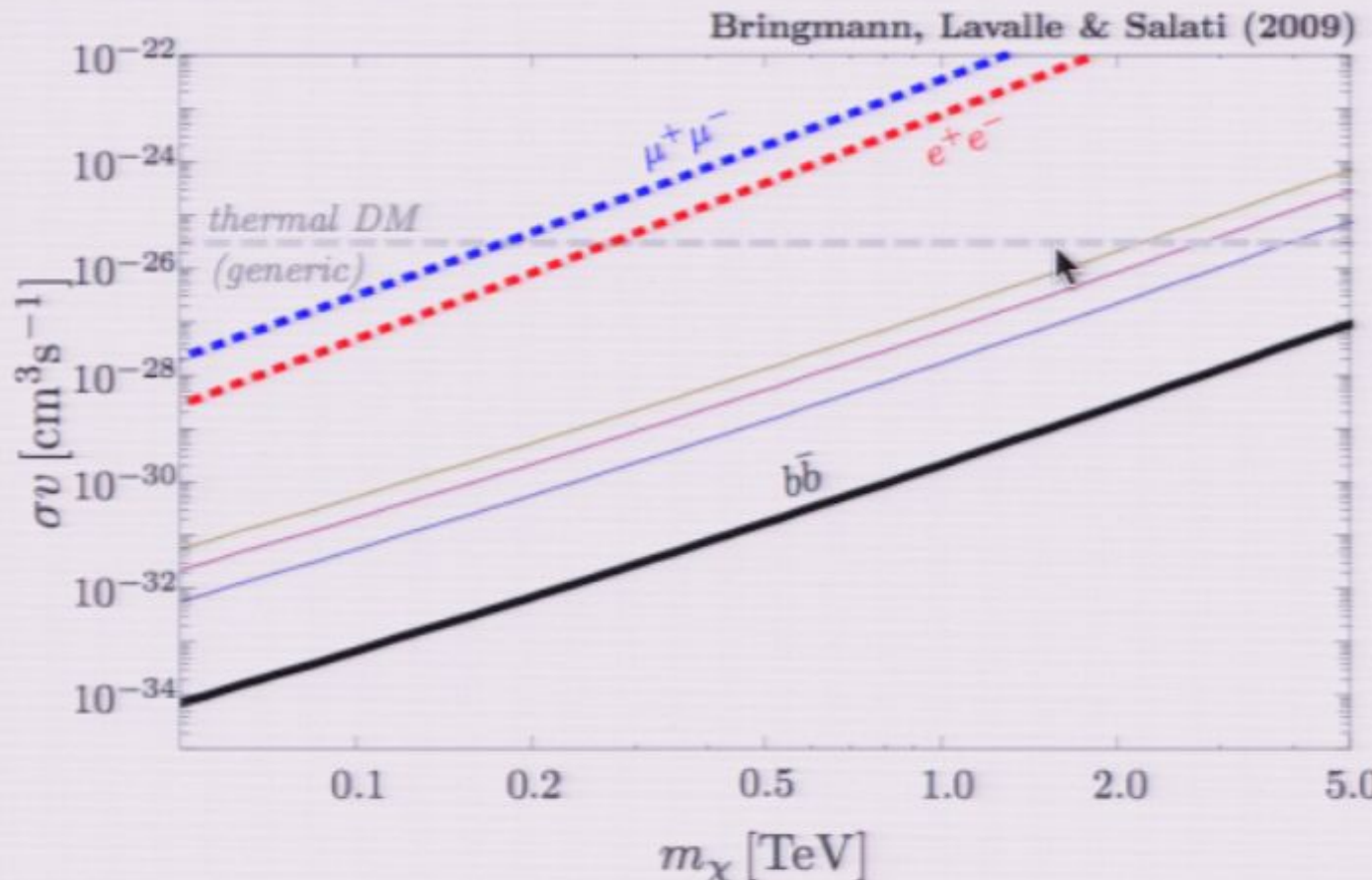
Page 95/104

gamma ray flux at the Earth from a single mini-spike

$$\Phi_\gamma \simeq 3.315 \times 10^{-7} \text{ cm}^{-2} \text{ s}^{-1} \times \frac{\xi/d^2}{10^4 \text{ kpc}} \times \mathcal{F}(m_\chi, <\sigma v>)$$

$$\mathcal{F}(m_\chi, <\sigma v>) = \left\{ \frac{N_\gamma}{100} \right\} \times \left\{ \frac{m_\chi}{1 \text{ TeV}} \right\}^{-9/7} \times \left\{ \frac{<\sigma v>}{3 \times 10^{-26} \text{ cm}^3 \text{ s}^{-1}} \right\}^{2/7}$$

$$\Phi_{\max}^{\text{EGRET}} = 2 \times 10^{-7} \text{ cm}^{-2} \text{ s}^{-1}$$

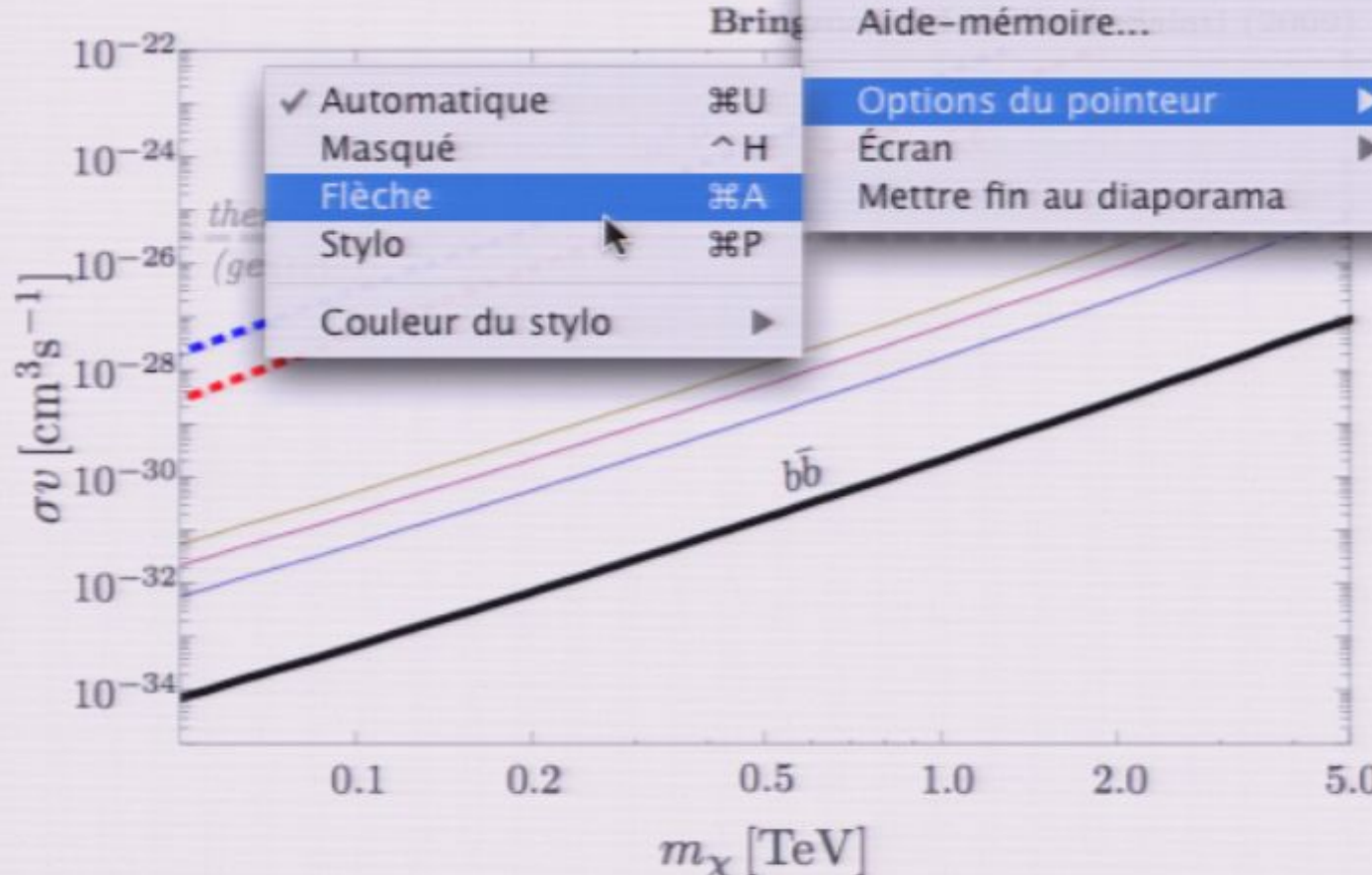


gamma ray flux at the Earth from a single mini-spike

$$\Phi_\gamma \simeq 3.315 \times 10^{-7} \text{ cm}^{-2} \text{ s}^{-1} \times \frac{\xi/d^2}{10^4 \text{ kpc}} \times \mathcal{F}(m_\chi, <\sigma v>)$$

$$\mathcal{F}(m_\chi, <\sigma v>) = \left\{ \frac{N_\gamma}{100} \right\} \times \left\{ \frac{m_\chi}{1 \text{ TeV}} \right\}^{-9/7}$$

$$\Phi_{\max}^{\text{EGRET}} = 2 \times 10^{-7}$$

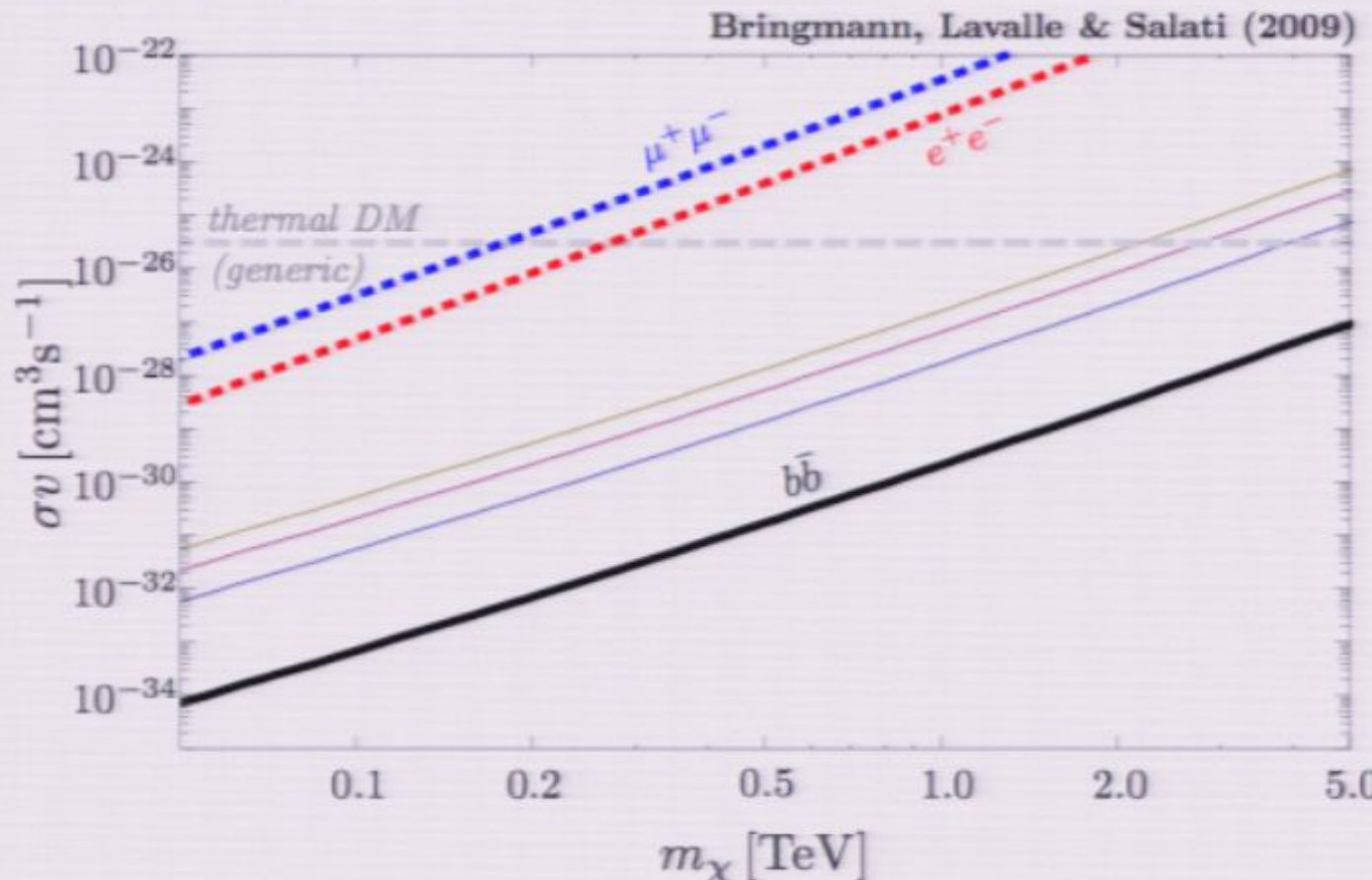


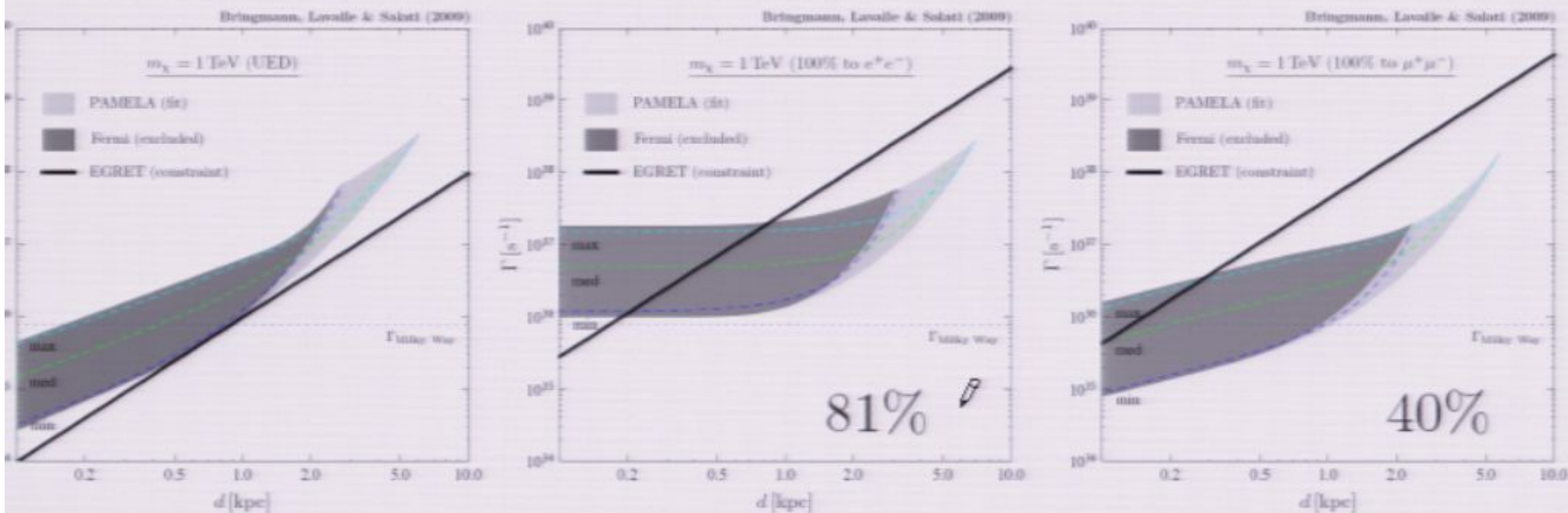
gamma ray flux at the Earth from a single mini-spike

$$\Phi_\gamma \simeq 3.315 \times 10^{-7} \text{ cm}^{-2} \text{ s}^{-1} \times \frac{\xi/d^2}{10^4 \text{ kpc}} \times \mathcal{F}(m_\chi, <\sigma v>) \beta$$

$$\mathcal{F}(m_\chi, <\sigma v>) = \left\{ \frac{N_\gamma}{100} \right\} \times \left\{ \frac{m_\chi}{1 \text{ TeV}} \right\}^{-9/7} \times \left\{ \frac{<\sigma v>}{3 \times 10^{-26} \text{ cm}^3 \text{ s}^{-1}} \right\}^{2/7}$$

$$\Phi_{\max}^{\text{EGRET}} = 2 \times 10^{-7} \text{ cm}^{-2} \text{ s}^{-1}$$





$m_\chi$ (GeV)	PAMELA		ATIC
100	100	1 000	1 000
$e^+/e^-$	$(1.22; 1.07 \cdot 10^7)$	$(0.78; 3.56 \cdot 10^9)$	$(1.64; 4.81 \cdot 10^9)$
$e^\pm + \mu^\pm + \tau^\pm$	$(0.44; 2.51 \cdot 10^7)$	$(0.27; 9.84 \cdot 10^9)$	$(1.45; 9.44 \cdot 10^9)$

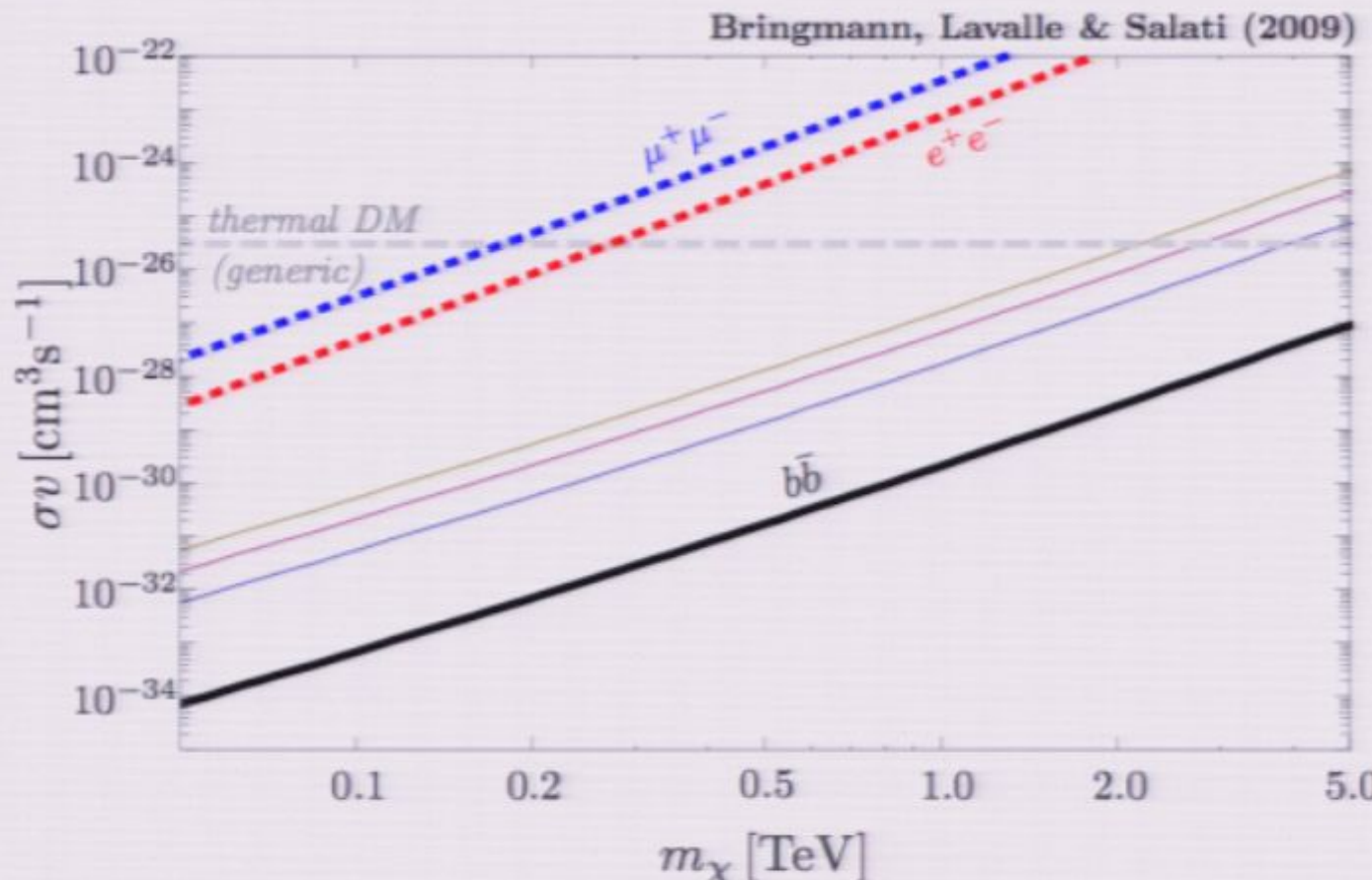
TABLE I: Best fit values of the  $(D; L)$  couple in units of  $(\text{kpc}; M_\odot^2 \text{ pc}^{-3})$  for various DM particle masses and annihilation channels.

gamma ray flux at the Earth from a single mini-spike

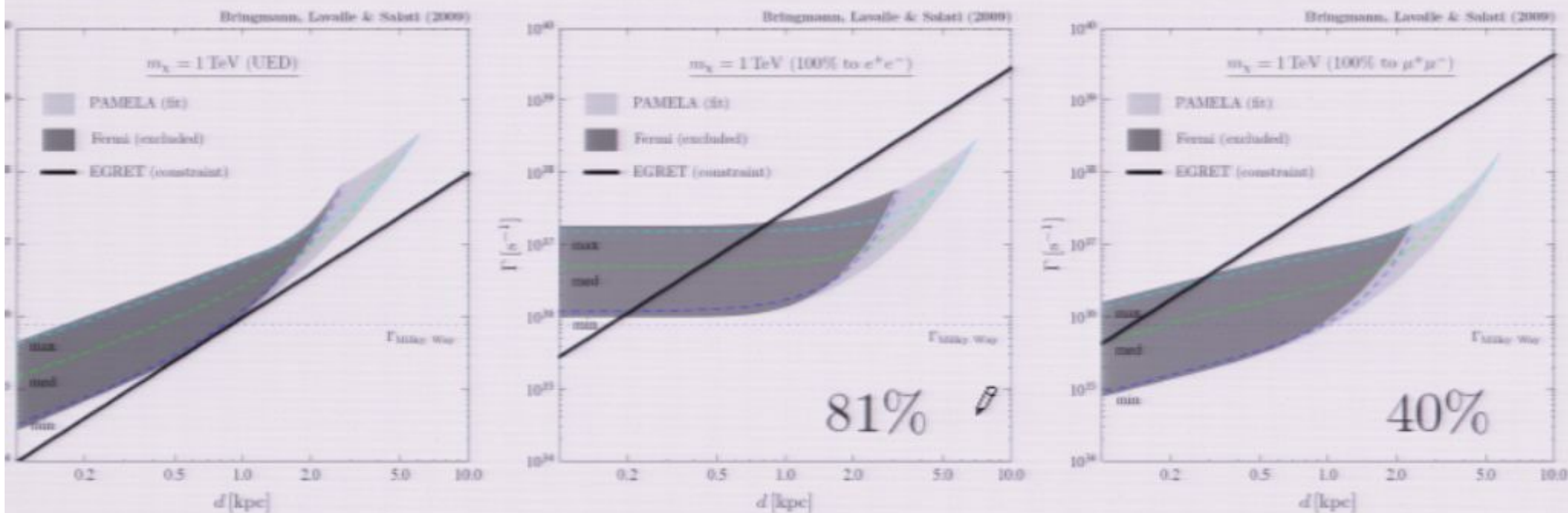
$$\Phi_{\gamma} \simeq 3.315 \times 10^{-7} \text{ cm}^{-2} \text{ s}^{-1} \times \frac{\xi/d^2}{10^4 \text{ kpc}} \times \mathcal{F}(m_{\chi}, <\sigma v>)$$

$$\mathcal{F}(m_{\chi}, <\sigma v>) = \left\{ \frac{N_{\gamma}}{100} \right\} \times \left\{ \frac{m_{\chi}}{1 \text{ TeV}} \right\}^{-9/7} \times \left\{ \frac{<\sigma v>}{3 \times 10^{-26} \text{ cm}^3 \text{ s}^{-1}} \right\}^{2/7}$$

$$\Phi_{\max}^{\text{EGRET}} = 2 \times 10^{-7} \text{ cm}^{-2} \text{ s}^{-1}$$



# T. Bringmann, J. Lavalle & P. Salati, arXiv:0902.3665



	PAMELA		ATIC
$m_\chi$ (GeV)	100	1 000	1 000
$e^+ / e^-$	$(1.22; 1.07 \cdot 10^7)$	$(0.78; 3.56 \cdot 10^9)$	$(1.64; 4.81 \cdot 10^9)$
$e^\pm + \mu^\pm + \tau^\pm$	$(0.44; 2.51 \cdot 10^7)$	$(0.27; 9.84 \cdot 10^9)$	$(1.45; 9.44 \cdot 10^9)$

TABLE I: Best fit values of the ( $D; L$ ) couple in units of ( $\text{kpc} \cdot M_\odot^2 \text{ pc}^{-3}$ ) for various DM particle masses and annihilation channels.

## PAMELA positron excess

May be the first indirect hint that DM species annihilate in the MW.

$$\Gamma_{\text{ann}} \equiv \langle \sigma v \rangle \times \frac{\rho_\chi^2}{m_\chi^2} \text{ needs to be enhanced}$$

### 3) Astrophysical effects on DM annihilation



DM substructures have  $\langle \rho^2 \rangle \geq \langle \rho \rangle^2$ .

- A statistical analysis is necessary to compute the signal enhancement.

$$B_{\text{Milky Way}} \leq 20 \text{ in } \Lambda\text{CDM}$$

- A single nearby clump is very improbable.
- EGRET constrains the WIMP to be leptophilic.
- If so, IMBH could be a solution although future strong limits from FERMI.

## 4) Perspectives

No coherent picture yet !

- Leptophilic vs CR propagation : are normal WIMPs really excluded ?
- DM distribution at the GC not known although concentrated.
- Sommerfeld effect combined with DM clumps & CR propagation – under study.

### PAMELA positron excess

May also be an indication that DM species **decay** in the MW.

$$\Gamma_{\text{ann}} \equiv \langle \sigma v \rangle \times \frac{\rho_\chi^2}{m_\chi^2} \Rightarrow \Gamma_{\text{ann}} \equiv \Gamma_{\text{dec}} \times \frac{\rho_\chi}{m_\chi}$$

- Decaying DM species could pass the tests as  $\Gamma_{\text{ann}} \propto \rho_\chi$ .



gamma ray flux at the Earth from a single mini-spike

$$\Phi_\gamma \simeq 3.315 \times 10^{-7} \text{ cm}^{-2} \text{ s}^{-1} \times \frac{\xi/d^2}{10^4 \text{ kpc}} \times \mathcal{F}(m_\chi, <\sigma v>)$$

$$\mathcal{F}(m_\chi, <\sigma v>) = \left\{ \frac{N_7}{100} \right\} \times \left\{ \frac{m_\chi}{1 \text{ TeV}} \right\}^{-9/7} \times \left\{ \frac{<\sigma v>}{3 \times 10^{-26} \text{ cm}^3 \text{ s}^{-1}} \right\}^{2/7}$$

$$\Phi_{\max}^{\text{EGRET}} = 2 \times 10^{-7} \text{ cm}^{-2} \text{ s}^{-1}$$

